ESA/SRE(2013)5
December 2013

PLATO

Revealing habitable worlds around solar-like stars

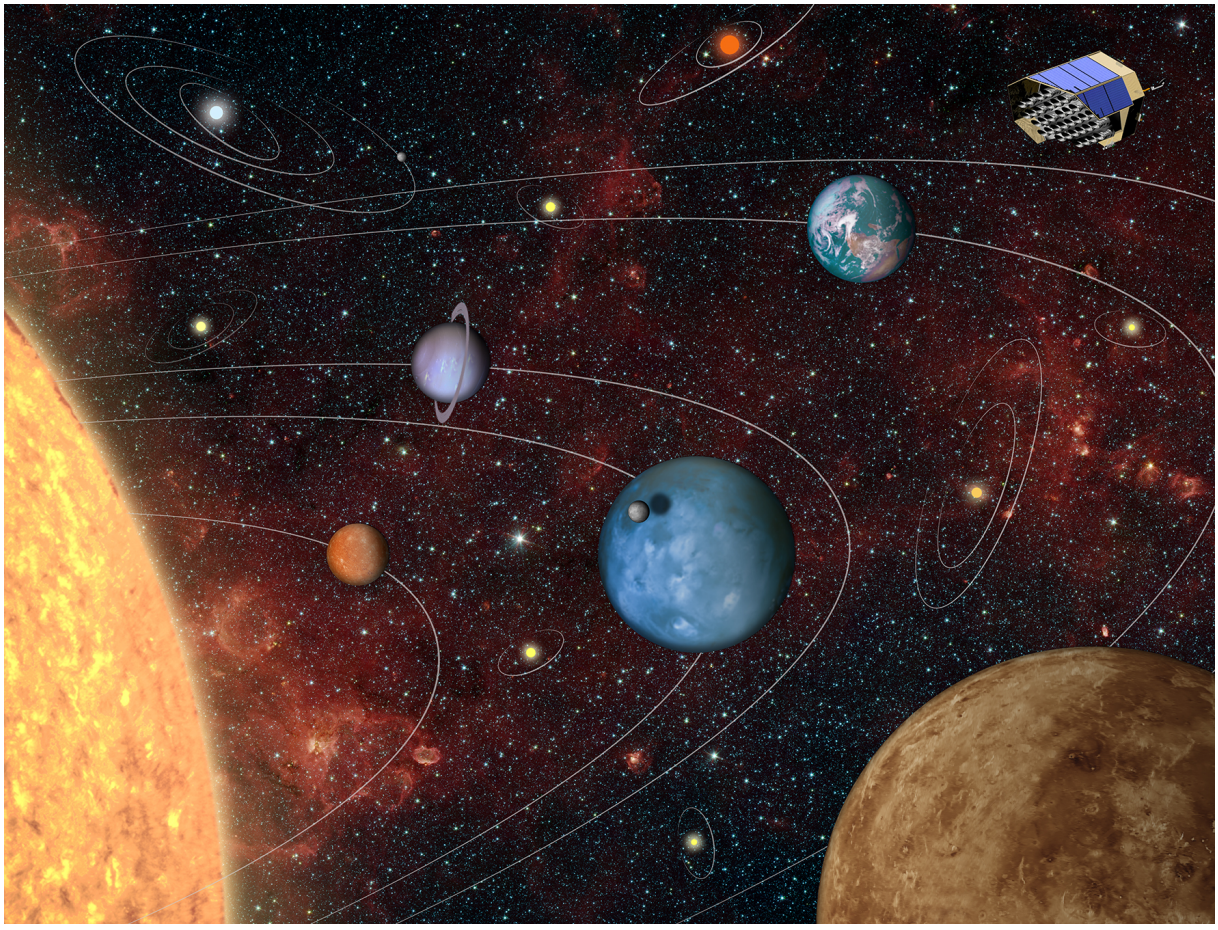

Assessment Study Report

European Space Agency

The front page shows an artist’s impression of planetary systems viewed by PLATO (©DLR).

PLATO Assessment Study – Mission Summary	
Key scientific goals	Detection of terrestrial exoplanets in the habitable zone of solar-type stars and characterisation of their bulk properties needed to determine their habitability. Characterisation of thousands of rocky (including Earth twins), icy or giant planets, including the architecture of their planetary system, to fundamentally enhance our understanding of the formation and the evolution of planetary systems. These goals will be achieved through: 1) planet detection and radius determination (2% precision) from photometric transits; 2) determination of planet masses (better than 10% precision) from ground-based radial velocity follow-up, 3) determination of accurate stellar masses, radii, and ages (10% precision) from asteroseismology, and 4) identification of bright targets for atmospheric spectroscopy.
Observational concept	Ultra-high precision, long (up to several years), uninterrupted photometric monitoring in the visible band of very large samples of bright ($m_V \leq 11$) stars.
Primary data product	Very accurate optical light curves of large numbers of bright stars.
Payload	
Payload concept	• Set of 32 normal cameras organised in 4 groups resulting in many wide-field co-aligned telescopes, each telescope with its own CCD-based focal plane array; • Set of 2 fast cameras for bright stars, colour requirements, and fine guidance and navigation.
Optical system	6 lenses per telescope (1 aspheric)
Focal planes	136 CCDs (4 CCDs per camera) with 4510×4510 18 µm pixels
Instantaneous field of view	~ 2250 deg^2
Overall mission profile	
Observing plan	Two long monitoring phases (two years each) single field monitored. Two years additional "step-and-stare" phase with several successive fields monitored for a few months each.
Duty cycle	$\geq 95\%$
Launcher	Launch by Soyuz-Fregat2-1b from Kourou in 2022/2024
Orbit	Transfer to L2, then large amplitude libration orbit around L2
Description of Spacecraft	
Stabilisation	3-axis
Telemetry band	X-band (10 MHz maximum bandwidth)
Average downlink capacity	109 Gb per day (Assumption: ground station contact for 4 hours per day, 3.5 hours for data downlink with a rate of 8.7 Mbps)
Pointing stability	0.2 arcsec rms over 14 hours
Pointing strategy	A 90° rotation around the line of sight every 3 months

… for had we never seen the stars, and the sun, and the heaven, none of the words which we have spoken about the universe would ever have been uttered. But now the sight of day and night, and the months and the revolutions of the years, have created number, and have given us a conception of time, and the power of enquiring about the nature of the universe…

Plato, in Timaeus

Foreword

The PLATO mission was proposed in 2007 as a medium class candidate in response to the first call for missions of the Cosmic Vision 2015-2025 program for a launch in 2017−2018. The proposal was submitted by Dr. Claude Catala (Observatoire de Paris) on behalf of a large consortium of scientists from laboratories all across Europe. Following favourable reviews by ESA's scientific Advisory structure, PLATO was selected in 2007 as one of the missions for which an ESA assessment study was carried out in 2008 and 2009. The PLATO mission was subsequently selected for a definition study, starting in February 2010. The definition study involved two concurrent industrial contracts for the definition of the mission profile, the satellite, and parts of the payload module. The PLATO Mission Consortium, involving more than 350 scientists and engineers in virtually all ESA Member States, as well as a few members from the US and Brazil, carried out the study of the instrument and their contributions to the science ground segment. A specific industrial contract for the study of the CCDs procurement was issued by ESA.

Following the non-selection of PLATO in October 2011 for the M1 or M2 launch opportunities, the ESA Science Programme Committee endorsed the solicitation of a proposal to the PLATO Mission Consortium to be a candidate for the M3 launch opportunity in 2022−2024. This had considered the positive recommendation by ESA's Advisory structure concerning the PLATO mission scientific competitiveness with the missions selected in response to the Cosmic Vision 2010 Call (the "M3 candidates"). The PLATO Mission Consortium responded with a proposal for the provision of the payload and science ground segment components formulated in the M3 mission framework. A major change was the transfer of the lead activities from France to Germany, with Prof. Heike Rauer (DLR) as new PLATO Mission Consortium lead. Subsequent to ESA's review, PLATO has been a candidate for the M3 launch opportunity since March 2013.

Whereas the technical solution for the spacecraft, payload and operations has remained unchanged, the organisational, programmatic and cost aspects of the mission have been updated taking into account the M3 reference schedule. The science case for the mission has been significantly reworked and elaborated, to account for the large developments in exoplanetology and asteroseismology of the last two years, and to describe the high relevance of PLATO in the scientific context of the next decade.

This report describes the outcome of the current assessment study, which is based on the definition study carried out in 2010 and 2011. It covers the scientific, technical, and as well as managerial aspects. This report results from a vast team effort, involving several parties (ESA, the PLATO Mission Consortium, Astrium/EADS, and Thales Alenia Space) under the general supervision by the PLATO Science Study Team and the ESA Study Team.

The PLATO Study Team

Authorship, acknowledgements

This report was prepared by:

ESA Science Study Team (SST)		
Name	*Affiliation*	*City, Country*
Heike Rauer	Inst. of Planetary Research, DLR	Berlin, Germany
Don Pollacco	University of Warwick	Coventry, UK
Marie-Jo Goupil	Observatoire de Paris-Meudon	Paris, France
Giampaolo Piotto	Università di Padova	Padova, Italy
Stéphane Udry	Université de Genève	Genève, Switzerland
PLATO Study Data Processing Manager		
Laurent Gizon	MPI for Solar System Research	Göttingen, Germany

The ESA Team supporting the activities is composed by:

ESA Study Team		
Philippe Gondoin Osvaldo Piersanti (Study Managers)	ESA	Noordwjik, The Netherlands
Ana M. Heras Malcolm Fridlund (Study Scientists)	ESA	Noordwjik, The Netherlands
Anamarija Stankov (Payload Manager)	ESA	Noordwjik, The Netherlands
Mark Baldesarra (System Engineer)	ESA	Noordwjik, The Netherlands
Laurence O'Rourke (Science Ops)	ESA	Madrid, Spain
ESA Coordinator		
Arvind Parmar	ESA	Noordwjik, The Netherlands

Contributions to this Assessment Study have been made by the PLATO Team, and part of its text has been submitted to Experimental Astronomy (arXiv:1310.0696). Contributors to these activities are acknowledged in the Annex.

The PLATO Team gratefully thanks William J. Borucki, Kepler PI, for his letter of support (link to letter).

Table of contents

1 Executive summary

The PLATO space mission (PLAnetary Transits and Oscillation of stars) will detect terrestrial exoplanets in the habitable zone of solar-type stars and characterise their bulk properties. PLATO will provide the key information (planet radii, mean densities, stellar irradiation, and architecture of planetary systems) needed to determine the habitability of these unexpectedly diverse new worlds. The PLATO legacy database will provide a unique resource that will be crucial to test our models of planetary and stellar evolution. PLATO capitalises on tremendous developments in high-precision photometry from space and ultra-stable ground-based spectroscopy techniques that have largely been led by Europe over the last 20 years. PLATO will answer the profound and captivating question**: how common are worlds like ours and are they suitable for the development of life?** PLATO is the only mission either approved or in advanced planning that will be able to address these questions.

Understanding planet habitability is a true multi-disciplinary endeavour. It requires knowledge of the planetary composition, to distinguish terrestrial planets from non-habitable gaseous mini-Neptunes, and of the atmospheric properties of planets. PLATO will be leading this effort by combining: 1) planet detection and radius determination from photometric transits, 2) determination of planet masses from ground-based radial velocity follow-up, 3) determination of accurate stellar masses, radii, and ages from asteroseismology, and 4) identification of bright targets for atmospheric spectroscopy. The mission will characterise thousands of rocky (including Earth twins), icy or giant planets by providing exquisite measurements of their radii (2% precision), masses (better than 10% precision) and ages (10% precision). This will revolutionise our understanding of planet formation and the evolution of planetary systems. **PLATO will assemble the first catalogue of confirmed and characterised planets in habitable zones with known mean densities, compositions, and evolutionary ages/stages.** This resource will be extremely valuable as these Earth-like planets will be the targets of future ESA missions that will be designed to characterise and probe their atmospheres.

PLATO is designed to address the following fundamental science questions:

- How do planetary systems form and evolve?
- What makes a planet habitable?
- Is the Earth unique or has life also developed elsewhere?

To reach these aims PLATO data will be used to drive forward our knowledge of the following important areas:

The Uniqueness of our Solar System: While the structure and mass distributions of bodies in our Solar System are well known, we only have indirect and partial knowledge of its formation and evolution. To place our system in context we must look to other systems and study their architectures and composition. From current observations, it has become obvious that the bulk compositions of exoplanets can differ substantially from those of solar system planets and this must be indicative of the formation process. Thanks to PLATO, the density and composition of exoplanets will be obtained from the measured mass and the radius. In addition, important properties of host stars, such as chemical composition and stellar activity will be measured by PLATO and the associated ground-based follow-up for a large sample of systems. Extending the bulk characterisation towards cool terrestrial Earth-sized planets on Earth-like orbits will be unique to PLATO and key to answering the question: how unique is our Solar System?

Interiors of terrestrial and gas planets: Many confirmed exoplanets fall into new classes unknown from our Solar System, for example “hot Jupiters”, “mini-Neptunes”, or “super-Earths” (rocky planets with masses below 10 M_E). It came as a surprise that gaseous planets can be as small (or light) as a few Earth radii (or masses). As a result, many of the smallest (or lightest) exoplanets known today cannot be classified as either rocky (required for habitability) or gaseous, because their mean densities remain unknown for lack of

mass or radius measurements. PLATO is the only mission able to provide vital constraints for planetary interior models.

Planets around different types of stars: Most planets today are detected around solar-like and cool M-dwarf stars. We have taken the first steps in our theoretical predictions of how stellar type and stellar activity influence the habitability of orbiting planets. Planets have also been observed around binary and multi-stellar systems. PLATO will primarily focus on small planets around solar-like stars to cover the planet parameter range not tackled by previous missions. In addition, PLATO will offer the possibility to study the evolution of planetary systems around evolved stars: sub-giant, giant, and post-RGB stars.

Evolution of planetary systems: Planets and their host stars evolve. Giant gas planets cool and contract, a process which can last up to several billion years: this process will be studied by PLATO through accurate measurements of stellar ages. Using accurate radius and mass measurements, we will determine how planets form and evolve by observationally building evolutionary tracks for gaseous exoplanets as functions of stellar properties. Over time, terrestrial planets lose their primary hydrogen atmospheres, develop secondary atmospheres, and may develop life. PLATO will provide key data on terrestrial planets at intermediate orbital distances, including in the habitable zones of solar-like stars with different ages, allowing us to study Earth-like planets at different epochs. Furthermore, the architecture of planetary systems is shaped through physical and dynamical processes on time scales accessible to PLATO asteroseismic dating.

Planetary atmospheres and star-planet interactions: Planets discovered around the bright PLATO stars ($4 \leq m_V \leq 11$) will be prime targets for spectroscopic transit follow-up observations of their atmospheres (using, e.g., JWST, E-ELT). Small planets with low mean density are particularly interesting as they are likely to have a primordial hydrogen atmosphere. Small planets with high densities are likely to be terrestrial planets with secondary atmospheres. The PLATO catalogue will therefore play a key role in identifying small planet targets of interest at intermediate orbital distances. It will also provide information on planetary albedos and the stratification of planetary atmospheres. Finally, the close-in planets found around stars of different types and ages will provide a huge sample to study the interaction between stars and planets due to, e.g., stellar winds or tides.

Rings, moons, trojans and comets: The sensitivity of PLATO will allow us to detect not only planets, but also their rings and moons, trojans (objects that share an orbit with a larger planet), as well as large comets. Moons and trojans can be used to constrain models of planet formation but are also themselves potentially habitable objects. Rings can influence measurements of planetary radii and are thus important to improving the precision of these measurements.

Stellar structure and evolution: Asteroseismology of PLATO's bright targets will allow us to tightly constrain and test new stellar models of a variety of stars in different evolutionary stages drawn from different populations. These constraints will improve the descriptions of physical processes used in stellar models, including rotation, additional mixing, and convective heat transport. Improvements in the models will in turn reduce the systematic uncertainties in the derived stellar parameters and, consequently, even better characterise the observed planets and their hosts.

Structure and evolution of the Milky Way: The intrinsic luminosity of red giant stars allows us to probe distances up to 10 kpc in our Galaxy and determine accurate ages from asteroseismology. Red giants can thus be efficiently used to map and date the Galactic disc. These data will complement the information on distances and chemical composition obtained by the Gaia mission. In addition, asteroseismic ages provided for PLATO targets can be compared to age determinations by other means, for example to calibrate gyrochronology.

The long-term legacy: The PLATO catalogue will consist of thousands of characterised planets, 85,000 stars with accurately known ages and masses, and 1,000,000 high-precision stellar light curves. PLATO will thus provide a huge long-lasting legacy for generations of astronomers to come that will not be limited to the realm of exoplanet and stellar science, but extend into many other fields in astronomy.

PLATO will consist of a spacecraft module and a payload module. The spacecraft module was studied by two industrial contractors, while the instrument will be provided by the PLATO Mission Consortium. The instrument consists of 32 "normal" telescopes with CCD based focal planes, operating in white light and providing a very wide field of view (FoV). They will be read out with a cadence of 25 s and will monitor stars with $m_V > 8$. Two additional "fast" cameras with high read-out cadence (2.5 s) will be used for stars

with m_V ~4–8. The paucity of bright stars necessitates a wide FoV, while the science drivers dictate the required sensitivity (numbers of cameras). Hence, the unusual multi-telescope design allows for a large photometric dynamic range of $4 \leq m_V \leq 16$ ($4 \leq m_V \leq 11$ for the prime targets) and an extremely wide field. The ensemble of instruments is mounted on an optical bench. The cameras are based on a fully dioptric design with 6 lenses. Each camera has an 1100 deg^2 FoV and a pupil diameter of 120 mm and is equipped with a focal plane array of 4 CCDs each with 4510² pixels of 18 μm size, working in full frame mode for the "normal" camera and in frame transfer mode for the "fast" cameras.

The "normal" cameras are arranged in four groups of eight. Each group has the same FoV but is offset by a 9.2° angle from the PLM+Z axis, allowing us to survey a total field of ~2250 deg^2 per pointing, but with different sensitivities over the field. This strategy optimises both the number of targets observed at a given noise level and the number of bright targets. The satellite will rotate around the mean line of sight by 90° every 3 months, enabling a continuous survey of the same region of the sky.

The current baseline observing plan consists of a combination of two long-term target fields lasting 2–3 years each, with a step-and-stare phase where a large number of different fields are observed for up to 5 months per field within the 6 years of total mission lifetime. The mission will be able to cover about 50% of the sky during the nominal observing time.

The prime PLATO data product will be a large sample of high precision stellar light curves, obtained over time intervals of months to several years with a high duty cycle (> 95%). PLATO will provide planetary radii, masses and ages from high accuracy stellar parameters and dedicated radial velocity follow-up spectroscopy within the main planet hunting target range of the mission, $4 \leq m_V \leq 11$. Stellar radii will also be available from the Gaia mission, and the stellar masses and ages will be tightly constrained by the unique and systematic use by PLATO of asteroseismology for about 85,000 stars. Planetary radii will be constrained with 2% precision, and masses with 10% precision or better. For the first time, the ages of planet host stars will be known to 10% for solar-like stars. PLATO will in addition detect terrestrial planets down to m_V ~13 (1,000,000 stars, tens of thousands of small-size planet candidates). Larger planets will be detected down to m_V ~ 16, which will be important for statistical studies or to discover golden *Rosetta stone* systems. PLATO will carry out an unbiased, magnitude-limited survey that will observe stars throughout the Hertzsprung-Russell Diagram, including main-sequence F, G, K stars and the brightest M dwarfs.

The PLATO Ground Segment consists of four main elements:

- An ESA provided Mission Operations Centre (MOC), in charge of satellite operations.
- An ESA provided Science Operations Centre (SOC), in charge of the scientific mission planning and the generation, validation, and distribution of the light and centroid curves. The SOC will also develop and operate the archives used to store and distribute all PLATO mission products to the science community.
- A PLATO Data Centre (PDC), provided by the Member States, which will process the light curves at six Data Processing Centres across Europe and generate the final scientific data products for archival and distribution by the SOC.
- A PLATO Science Preparatory Management team (PSPM), which will carry out scientific preparatory and operational activities, as well as support ESA in public relations and outreach activities. The PSPM provides the scientific specification of the PDC software.

For the benefit of the extremely rapidly evolving science related to exoplanets, the validated PLATO data will immediately be made public. A small number of light curves (< 1%) from targets selected prior to launch will remain the property of the PLATO scientists directly involved in the mission for one year.

The search for planets similar to our Earth, potentially suitable for the development of life, is one of the greatest scientific, technological, and philosophical undertakings of our time, which is captivating public interest. The PLATO results will have a profound influence on our understanding of the Universe and our place in the *Cosmos*. PLATO will accurately measure the radii, masses, and ages of Earth-like planets in the habitable zones of stars similar to our own. This is unique to PLATO and will lay the foundations for exoplanetary research in the following decades.

2 Scientific objectives

2.1 Science Goals I: Planetary Science

2.1.1 Planet detection and characterisation of bulk parameters

Today, about 1000 extrasolar planets have been discovered and confirmed as planets. For most of these planets we could determine only one of their fundamental parameters directly: radius or mass. In those cases where planets have been observed with both the transit and radial velocity (RV) methods, their mass, radius, and thus mean density have been measured. This has led to exciting discoveries, including new classes of intermediate planets called "super-Earths" and "mini-Neptunes". In addition to the confirmed planets, NASA's Kepler mission has published results on several thousands of planet candidates. Together with RV and microlensing survey detections, these results show that small planets are very numerous. Even though the precise frequency of planets in the Galaxy is a matter of debate, the community presently agrees that planets, in particular rocky planets like our Earth, are very common around solar-type stars (FGK and M dwarfs, see e.g., Udry & Santos 2007; Mayor et al. 2011; Howard et al. 2012; Cassan et al. 2012; Bonfils et al. 2013). This idea is fully supported by state-of-the-art planet formation models based on the core-accretion paradigm, which predict small rocky planets to greatly outnumber their Jovian or Neptune-like counterparts (e.g., Ida & Lin 2004; Mordasini et al. 2009, 2012a).

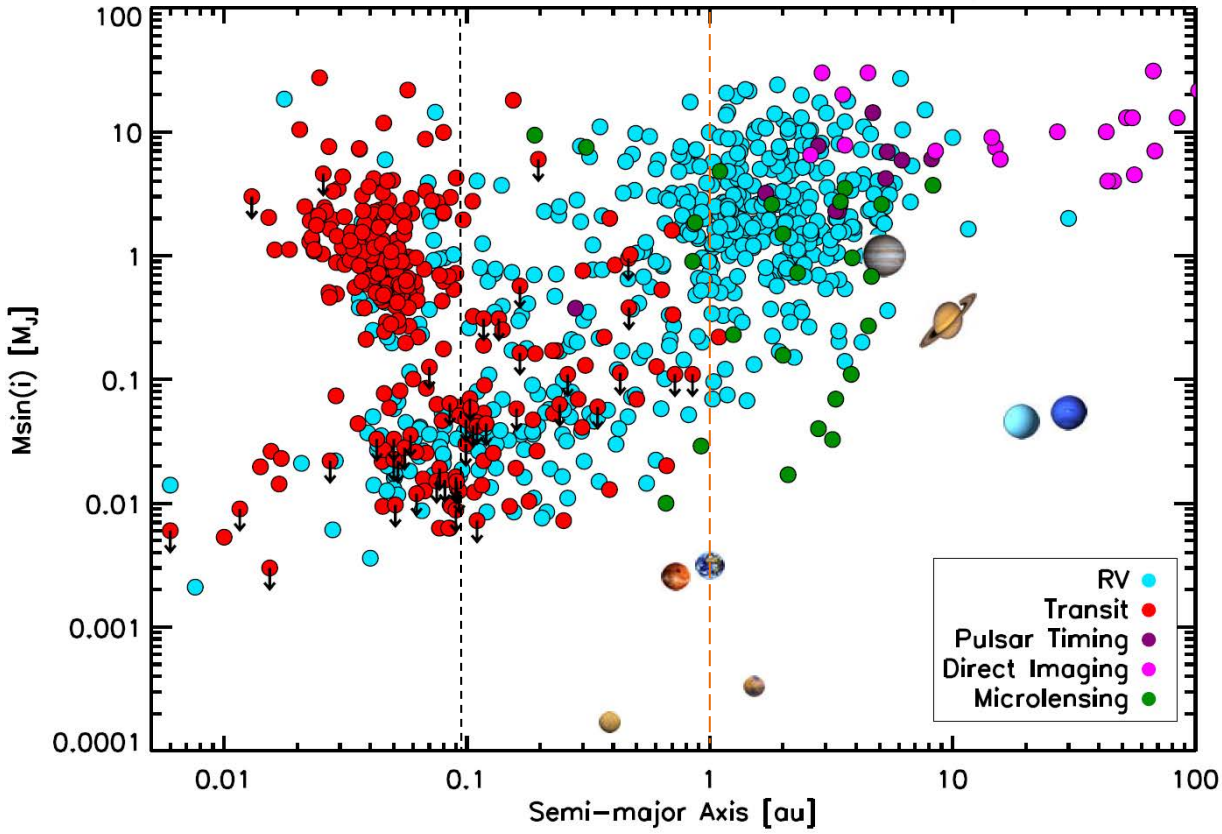

Figure 2.1: Current status of planet detections. Blue dots indicate RV detections with m sin i limits. Red dots are transit detections with known radii and masses. Red dots with downward arrows indicate transit detections with only upper mass limits available (update from Rauer et al. 2013). The vertical black dashed black line indicates the orbit of the most distant transiting planet detected from ground today (HAT-P-15b (Kovacs et al. 2010)). The orange dashed line shows the envisaged distance limit for PLATO detections and characterisation of super-Earths.

Figure 2.1 provides an overview of the confirmed exoplanet detections today. Jupiter-sized planets are well represented out to several au. Detections beyond ~0.1 au are dominated by the radial velocity technique which provides lower mass (*m* sin *i*) limits (blue dots). Masses and radii are known mainly for close-in planets, where data from both transits and RV are available (red dots). Transit detections beyond about 0.1

au are very difficult from the ground due to the limited duty cycle of observations caused by the Earth's rotation (the most distant ground-based transit detection is HAT-P-15b at 0.095 au (Kovacs et al. 2010)). The known transits at intermediate orbital separations result from CoRoT and Kepler, showing that transit detections of planets at larger orbital separations are feasible from space. However, Kepler did not provide us with planet bulk parameters for the vast majority of its discoveries since most Kepler targets are too faint to allow for the direct RV measurement of terrestrial planet masses. We point out that the range of terrestrial planets as found in our Solar System, with masses from Earth- down to Mercury-sized objects beyond 0.3 au, is still basically unexplored today.

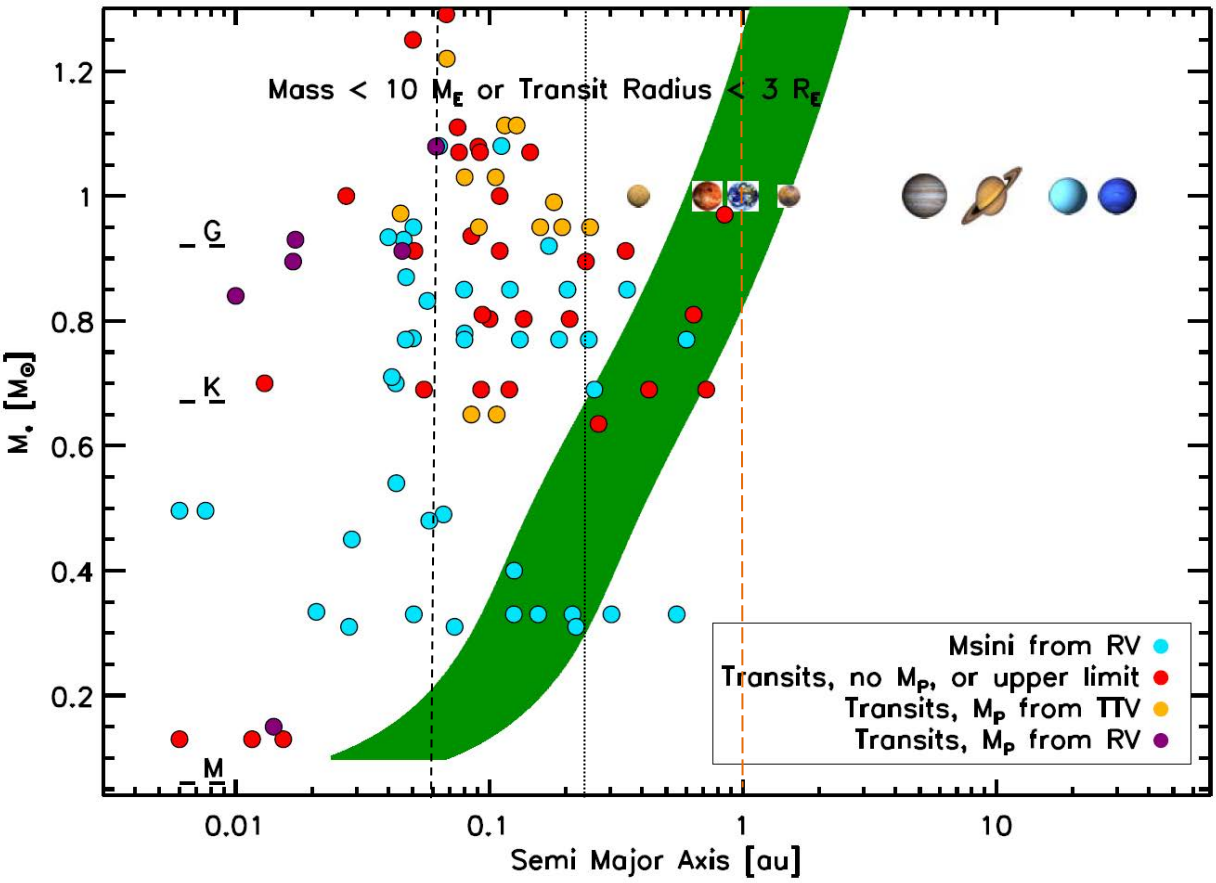

Figure 2.2: Super-Earth exoplanets ($1 < m \leq 10\ M_E$ or $r_p \leq 3\ R_E$) for different host star masses in comparison to the position of the habitable zone (green). Black dashed line: current max. distance of super-Earths with RV and transit measurements; Dotted line: most distant planet with transits and TTVs. Orange dashed line: distance goal of PLATO for fully characterised (transit+RV) super-Earths.

Figure 2.2 shows the current status of Super-Earth planet detections in comparison to the position of the HZ, defined as the region around a star where liquid water can exist on a planetary surface (scaling based on Kasting et al. 1993). Most super-Earths have been found at orbital distances to the star closer than the HZ. Detections in the HZ have been made by RV or transit measurements (red and blue dots). However, only a small number of super-Earths have both mass and radius determined (purple dots), and these do not lie in the HZ. A recent example is the system around Kepler-62 with two planets orbiting in the HZ; no masses could be derived due to the faintness of the host star (Borucki et al. 2013). The black dashed line indicates the most distant super-Earths for which radii and masses could be directly measured by transits and RVs. Transit Time Variations (TTV) are capable expanding the distance limit (dotted line) for which masses of transiting planets are available, but we recall that TTV determinations of masses can have relatively large uncertainties, unless we observe co-planar transiting systems. The goal of PLATO therefore focuses on providing terrestrial planets in the HZ of solar-like stars (up to about 1 au, orange dashed line) with accurately determined bulk parameters, which necessitates direct transit and RV measurements.

PLATO will not only study the frequency of terrestrial planet occurrence, but ask about their nature: their bulk properties, atmospheres, and ultimately whether they could harbour life. These questions require detailed follow-up observations at high signal-to-noise ratios. To address these science questions, we need to

- detect planets around bright stars ($m_V \leq 11$) to determine accurate mean densities and ages and allow for follow-up spectroscopy of planetary atmospheres;
- detect and characterise terrestrial planets at intermediate orbital distances up to the habitable zone around solar-like stars to place our Solar System in context; and
- detect and characterise planets in statistically significant numbers for a broad range of planet and planetary system classes to constrain planet formation scenarios.

These requirements are at the core of the design of PLATO and its observation strategy.

Figure 2.3 shows that past and existing transit surveys, including CoRoT and Kepler, have target stars that are too faint to fully characterise most detected planets. PLATO's main detection range is however $m_V \leq 11$ and will provide large numbers of targets for follow-up spectral characterisation.

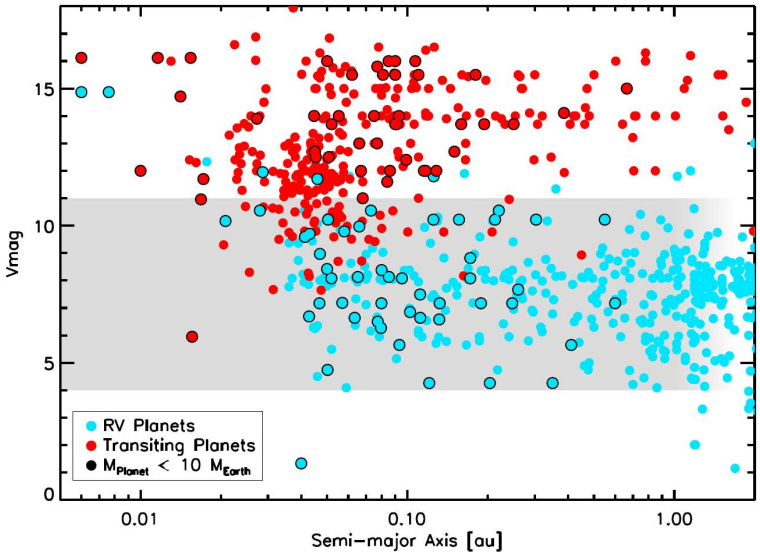

Figure 2.3: Magnitude of known planet hosting stars versus planet orbital distance. The grey shaded band indicates the prime detection range of PLATO (4-11 mag) for accurate bulk planet parameters and astero-seismology down to Earth-sized planets. Detection of Earth-sized planets is still possible down to 13 mag, and of larger planets down to 16 mag, but with lower bulk parameter accuracy.

PLATO goes beyond already selected future space missions

Recent space missions, e.g. CoRoT (Baglin et al. 2006) and Kepler (NASA, Koch et al. 2010), have provided about 100 planets *with known radii and masses*, from hot gas giants to a few hot super-Earths. Kepler furthermore provides planet frequency (or number of planet candidates per star). For the cool terrestrial planets it will, however, not provide accurate planet parameters due to the faintness of the target stars. This also applies to transiting planets expected from Gaia mission photometry (Dzigan & Zucker 2012) that will be mainly below 11mag, whereas astrometric detections are made for large planets (Lattanzi & Sozzetti 2010). ESA's selected Small Mission CHEOPS (Broeg et al. 2013) is the first significant step forward to a better characterisation of exoplanets (launch in 2017), since it will provide bulk properties for a number of previously detected planets around bright stars. NASA's selected mission TESS (launch 2017) will search over the whole sky for short-period planets around bright stars. TESS is expected to detect about 1000 small planets, including about hundreds of Earths to super-Earth's. However, TESS will focus mainly on planets in short periods (up to about 20 days) because of its pointing strategy, which covers most fields for 27 days only. Its yield on small long-period planets is expected to be small, since only the ecliptic poles, about 2% of the sky, will be covered for a whole year and provide some potential for the detection of longer period planets. TESS will have a large impact concerning the detection of the first small planets around stars close to our Solar System. It will, however, not address the science case of characterising rocky planets at intermediate distances (a > 0.3 au) around solar-like stars, which remains unique for PLATO. On the other

hand, TESS, being the first all-sky survey, will identify interesting short-period targets defining science cases that PLATO could address in detail during its step-and-stare phase.

Searches for small planets in the habitable zone of solar-like stars by radial velocity (RV) techniques, e.g., via the ESPRESSO project (ESO) will help to unveil the presence of Earth-like planets orbiting other Suns, however not in large numbers and the geometrical probability for them to show transits will be low.

It is thus unclear whether our Solar System is typical or special, and this will remain so until we can reliably detect and characterise Earth-like planets in Earth-like orbits around all kinds of bright host stars. Detecting these planets and accurately determining their bulk parameters, hence radius, mass, density and age, is the primary objective of PLATO and remains unique to this mission for the next decades.

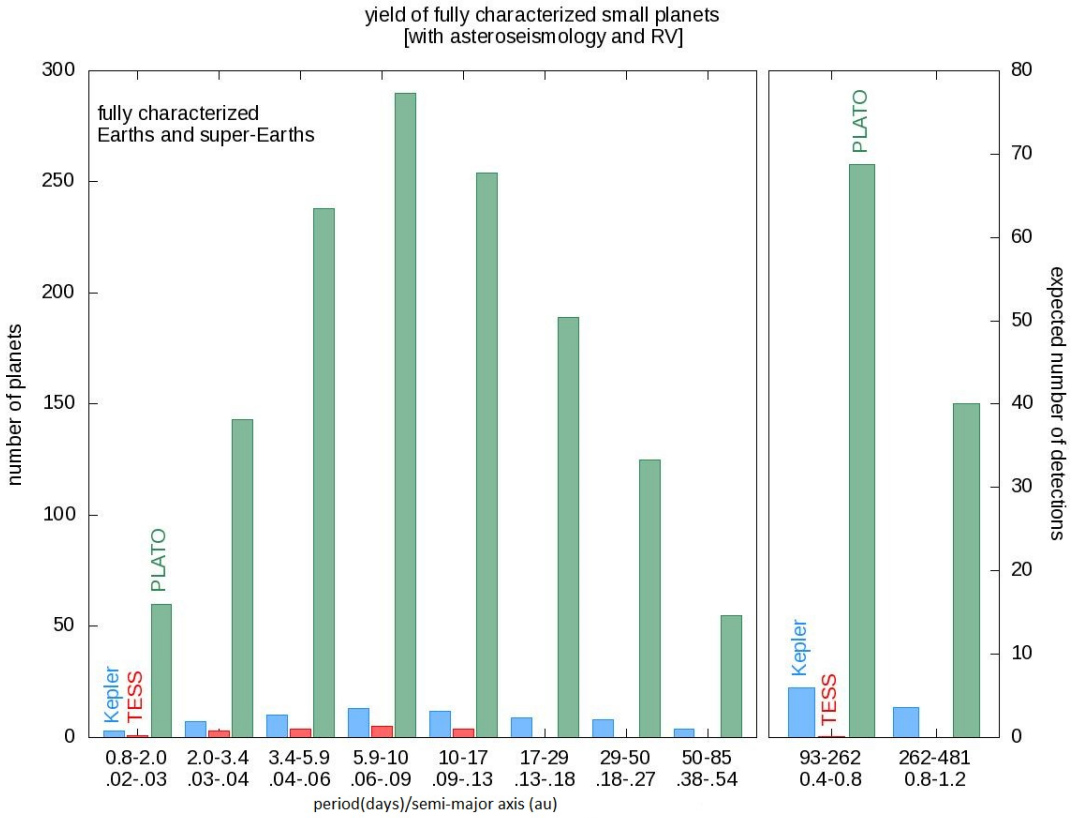

Figure 2.4: PLATO transit signal detection performance for super-Earth planets (≤ 2 R_E) for stars $m_V \leq 11$, hence with RV follow-up and host star asteroseismology possible. For comparison, Kepler results (Fressin et al. 2013) and expected yield at long periods are shown. In addition, expected yields for TESS assuming 27 day observing coverage per field and 2% of the sky observed for 1 year (see Rauer et al. 2013).

Figure 2.4 shows a performance comparison for the paramaters of PLATO's main targets: "super-Earths", hence planets with radii ≤ 2 R_E, which allow for RV follow-up spectroscopy and asteroseismology of the host stars. RV follow-up with reasonable telescope resources for a large number of targets is limited to about $m_V = 11$. The Kepler mission performed asteroseismology for stars up to about $m_V = 12$ (Huber et al. 2013), and PLATO will do so for stars up to $m_V = 11$. For the all-sky survey by TESS, little has been published on its asteroseismology performance yet. However, from the much smaller aperture per star (10 cm) it is expected that asteroseismology should be limited to stars brighter than about $m_V = 7$. Thus, for Kepler and PLATO, full characterisation is limited by RV follow-up to stars $m_V \leq 11$. For TESS, asteroseismology limits fully characterised planets to host stars brighter than about $m_V = 7$. With these magnitude constraints for fully characterised planets, we can estimate the number of suitable target stars within the fields surveyed. For PLATO we use the baseline observing strategy, as outlined below. *As seen in Figure 2.4, PLATO will outnumber the detection of small, characterised planets by 1–3 orders of magnitude compared to Kepler and TESS.*

PLATO will detect hundreds of small/low-mass planets in the habitable zones of bright solar-like stars for which accurate radii, masses, mean densities, and ages can be derived. This goal is unique to PLATO. A complete and unbiased picture of the planet bulk parameters requires data covering the full parameter space that only PLATO will provide. The case for PLATO gets even stronger when we consider transiting planets located in the habitable zones of solar-like stars and orbiting around targets bright enough for atmosphere follow-up spectroscopy. Without PLATO, no other instruments planned, on the ground or in space, will provide the required information.

2.1.2 Constraints on planet formation from statistics

A prime goal of PLATO will be to detect a large number of planets, in size down to the terrestrial regime, and with well-determined masses, radii and hence mean densities with unprecedented accuracy. Bulk density is a testable quantity from theoretical planet formation models and is the key parameter to evaluate simulated planet population distributions and their input physics. Better understanding of the relevant input physics into these models will, however, require a large statistical sample covering the complete parameter space.

Figure 2.5 shows the mean density of planets versus planetary mass (top: for all planets; bottom: planets with P > 50 days). We point out that planet candidates cannot be considered here, since it is impossible to derive reliable mean densities for these objects. In the figure, we note again that no exoplanets in the mass range of Earth, Venus and below with measured densities and masses are available to date. Generally the mass range below 0.1 M_J is sparsely populated. This is the highest priority detection space for PLATO. The PLATO mission can uniquely provide thousands of rocky and icy planets with well-known radii (2%), masses (10%) and ages (10%) around $m_V \leq 11$ stars, filling the left branch of Figure 2.5 with a high number of planets.

Dashed lines in Figure 2.5 indicate modelled densities for planets with different bulk compositions (following Wagner et al. 2012). The right branch in each figure contains gas giant planets that follow roughly the green dashed line computed for planets with a Jupiter-like H-He bulk composition. The left branch of the roughly V-shaped density- mass distribution in Figure 2.5 is composed of planets with bulk densities from silicate to ice, some with extended atmospheres.

The formation of planets is presently believed to result from two different scenarios, which may or may not be mutually exclusive. In the core-accretion scenario, a planetary core is first formed by the accretion of solids that mutually collide. During this phase, the growing planet is in quasi-static equilibrium, the energy loss at the surface of the planet being compensated for by the energy resulting from the accretion of planetesimals. When the mass of the core reaches a so called critical mass however, this compensation is no longer possible, and the planet envelope starts to contract, the contraction energy being radiated away at the surface. This contraction triggers a very rapid accretion of gas, which is rapidly limited by the amount of gas that can be delivered by the protoplanetary disk surrounding the forming planet. This scenario has been studied by many authors, accounting for different physical effects, like protoplanet migration (Alibert et al. 2004, 2005), opacity reduction in the planetary envelope (e.g., Hubickyj et al., 2005), excitation of accreted planetesimals by forming planets (e.g., Fortier et al. 2007, 2013), competition between different planets (e.g., Guilera et al. 2011) to cite only some of them.

In the second scenario, the disk instability model, the formation of a giant planet is the result of the presence of a gravitational instability in a cold and massive protoplanetary disk (e.g., Boss 1995; Mayer et al. 2005; Boley et al. 2010). After its formation, a giant planet clump is believed to cool and contract, and eventually accrete some planetesimals, forming a planetary core (e.g., Helled and Bodenheimer 2011; Vazan and Helled 2012).

In the framework of the core-accretion model one of the central issues is the possibility to build a core larger than the critical mass. The critical mass, in turn, depends on a number of processes that are poorly known. It depends strongly on the core luminosity (which results mainly from the accretion of planetesimals), and decreases for low luminosity (e.g., Ikoma et al. 2000). Moreover the critical mass depends on the opacity inside the planet envelope. Indeed, low opacity envelopes lead to a reduced critical mass, and a larger

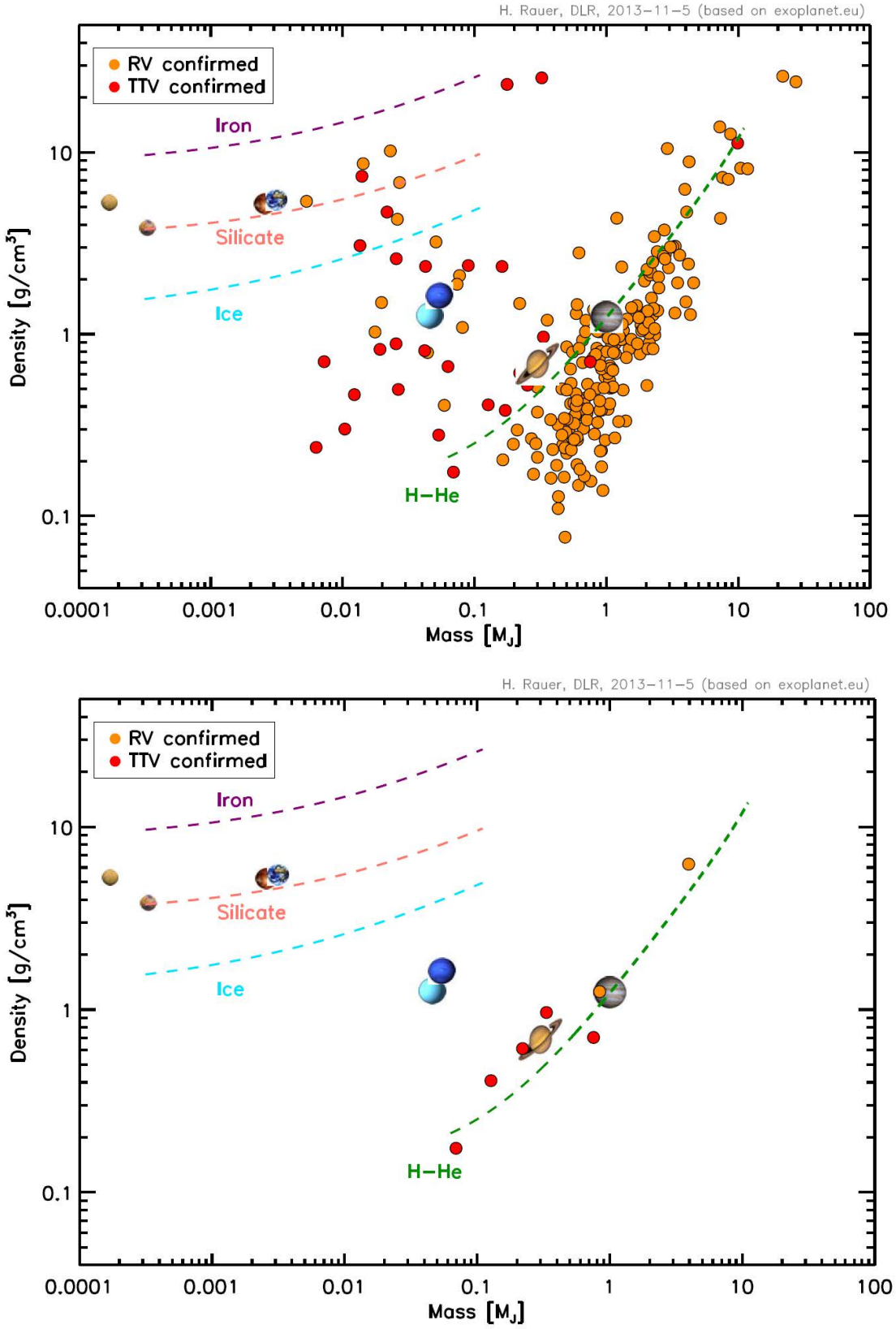

Figure 2.5: Mean planet density versus mass with density lines for different bulk compositions. Top: All currently known planets with measured radius and mass (hence mean density). Bottom: only planets with orbital period >50 days.

envelope mass (for a given core mass). Finally, the critical mass depends on the mean molecular weight inside the planetary envelope, which again depends on the planetesimals´ characteristics (size, strength, composition, see e.g., Hori and Ikoma 2011).

Determining observationally the critical core mass as a function of distance to the star, stellar metallicity, and other parameters would therefore place constraints on the characteristics of planetesimals (e.g., mass function, excitation state, internal strength). It would moreover determine up to which mass planets may be potentially habitable, since the presence of a massive H_2-He envelope in a super-critical planet probably prevents any habitability.

The core accretion model scenario can be tested in particular by increasing the statistics of the high density, low-mass rocky exoplanets, since those planets define the critical mass limit beyond which efficient gas accretion starts. This is likely the reason why basically no planets appear at high densities in the (approximately V-shaped) density-mass distribution in Figure 2.5. For example, following the silicate composition line with increasing mass in Figure 2.5, we find no planets beyond about 0.03 M_J (about 6-9 M_E). This is consistent with the core accretion scenario where higher-mass silicate planets would quickly accrete significant H-He envelopes and end up as high mass but lower density planets in Figure 2.5, e.g. in the ice planet regime or even growing to gas giant planets.

Peculiar observations, however, such as two mass-rich planets (around Saturn's mass, 0.2-0.3 M_J) with almost iron-like bulk density (> 20 g cm^{-3}), hence no or weakly accreted gas envelopes (see Figure 2.5), challenge commonly accepted planet formation models. How can such planets form? Are they formed after the gaseous disc disappeared? These planets, Kepler 24b and c, belong to the same planetary system and were detected by Transit-Timing Variations in Kepler data (Fabrycky et al. 2012; Ford et al. 2012). Hence their masses have not been measured directly by RV but inferred from gravitational perturbations, leading to potentially large mass uncertainties. This example illustrates that well determined bulk densities are mandatory to securely identify exciting new planet types that potentially challenge formation theories. This will be of increasing importance for low mass, but high-density planets, which are of central interest. We emphasize that PLATO will not only discover such planets, but will also deliver accurate measurements of their radius, mass, and density. This is only possible because the PLATO asteroseismic measurements will obtain accurate stellar parameters, and because the targets are bright and more amenable to Doppler measurements. Multi-planet, co-planar systems can be supplemented by TTV measurements. All of these discoveries will be facilitated by the large number of planets detected around bright stars which will on one hand allow us to obtain sufficient objects for statistics, and on the other hand allow finding 'Rosetta Stone' objects with the potential to resolve some of the outstanding key questions.

We also note a wide range of densities (more than an order-of-magnitude) for the low-mass planets in Figure 2.5. Planets at low masses and densities below the pure ice (blue) line are indicative for planet with large H-atmosphere envelopes. By filling the parameter space in Figure 2.5, PLATO will identify a large sample of low-mass planets that are likely to have H envelopes, around different types of stars with different ages. Planet population synthesis models (e.g., Mordasini et al. 2012b) predict a large number of low-mass planets (super-Earths and below) with large hydrogen envelopes. Such predictions can be validated by PLATO observations, testifying our planet formation theories. The situation becomes even more interesting if one considers also atmospheric loss processes that can remove a primordial H-atmosphere over time. These processes will be stronger closer to the host star, and they reduce the planetary envelope with time. It will be interesting to observationally study these effects by correlating planetary mass and mean density of low-mass objects with e.g. orbital distance and age of the system. We also expect the lowest-mass planets to lose their H atmospheres completely (e.g., like Earth, Venus, Mars). PLATO will determine for which planets primordial atmospheres are unlikely to exist after a certain lifetime of their system, and it will determine which planets have likely developed a secondary atmosphere resulting in smaller scale heights, hence apparent radii and higher mean densities.

Figure 2.5 shows the current situation for planet bulk characterisation for planets with orbital periods >50 days. Only two exoplanets with measured transits and RV signals are currently known in this parameter range (orange dots), and an additional five (red dots) arise from TTV mass determinations. Furthermore, only few additional planets are expected to fill this diagram from the already selected/built future ground- and space-based surveys. Thus, while we will be able to compare planet population synthesis models with data for planets at small orbital distances, the picture we will get at least until the end of this decade will be

very limited for planets on larger orbits, i.e. orbits undisturbed by their host star and with potentially temperate surface conditions. PLATO will be crucial to probe these orbital distances.

PLATO will be the first mission to cover the parameter range of small, characterised planets with sufficiently large detection statistics to provide the direct observational constraints to formation models and their predictions, as well as the dynamical evolution of young planetary systems.

PLATO will answer fundamental questions about planetary formation such as:

- What is the bulk density distribution of low-mass, terrestrial planets?
- What is the observed critical core mass for giant planet formation?
- Can super-massive rocky planets exist and how are they formed?
- When and where do planets stop accreting gas?
- Which planets likely have extended, primordial H-envelopes?
- How do these parameters depend on orbital distances, stellar type, metallicity, chemical composition or age?

These questions can only be addressed with a sufficiently large sample of planets of all sizes, from rocky to giant, with well determined masses, radii and bulk densities, around stars of different types and ages.

2.1.3 Terrestrial planets

This section discusses in more detail what can be learned from accurate radii and masses of terrestrial exoplanets, despite the limitations in observables for such distant planetary systems compared to our Solar System.

Terrestrial exoplanets up to about ten Earth masses are thought to have similar interior structures and bulk compositions as the terrestrial bodies in the Solar System. Their interiors are thought to be composed of rock-forming elements and metals such as iron, the latter evenly distributed or concentrated in central cores (Elkins-Tanton & Seager 2008). Gravitational and magnetic field measurements indicate that terrestrial planet interiors are strongly differentiated and subdivided into distinct layers. The composition of the layers varies with depth in such a way that the heaviest materials are concentrated in the center (core). An example of a differentiated terrestrial planet is the Earth which is divided into a partly or entirely liquid metallic core, a silicate mantle, and an outermost magmatic crust derived from partial melting of the mantle below. Unlike for the Solar System inner planets, there are fewer constraints than unknowns in the case of solid terrestrial extrasolar planets, and even basic interior structure models that would involve only two or three chemically homogeneous layers of constant density suffer from inherent non-uniqueness (e.g., Sohl & Schubert 2007, and references therein). To address these degeneracies, assumptions are usually made about their composition and its depth dependence.

Numerical models of planetary interiors using laboratory data on material properties aim at improving the general understanding of their origin, internal evolution, and present thermal states. In the case of the rocky planets within the Solar System, the resulting radial profiles are required to be consistent with geophysical observations and cosmochemical evidence for the compositions of crust, mantle and core (e.g., Sohl & Schubert 2007, and references therein). For rocky exoplanets, the numerical models have to be consistent with the observed planetary masses and radii. Such models have been used to derive mass-radius relationships for exoplanets assuming a range of different mineralogical compositions to gain insight into the interior structure and possible bulk compositions of these planets (Valencia et al. 2006; Fortney et al. 2007; Seager et al. 2007; Sotin et al. 2007; Valencia et al. 2007; Grasset et al. 2009; Figueira et al. 2009; Wagner et al. 2011; Swift et al. 2012). The principal uncertainties mainly arise from the extrapolation of an equation-of-state to high pressures owing to the lack of reliable experimental data in the pressure range of 200 GPa to 10 TPa, whereas the surface temperature and internal thermal state of a massive rocky exoplanet are less important for its radial density distribution (e.g., Seager et al. 2007). Nevertheless, the latter are expected to have severe consequences for geodynamical processes. Furthermore, scaling laws for key physical and chemical properties have been obtained (e.g., Wagner et al. 2012, and references therein), which are essential

for a better understanding of the global planetary processes controlling the general evolution of a planetary body and its astrobiological potential to be life-sustaining.

Figure 2.6 shows modeled mass-radius relationships in comparison to the relatively large (1 sigma) error bars obtained for low-mass planets to date. For the smallest planets, radii are better constrained than masses. These planets are usually detected by space missions (CoRoT and Kepler) providing photometrically accurate light curves, and hence radii, but the target objects are too faint to permit an accurate mass determination. In many cases, even a rocky or icy nature cannot be distinguished within the 1 sigma error bars shown. There is a need to reduce the error bars, as planned for PLATO, by providing highly accurate radii and masses with corresponding uncertainties of merely a few percent.

The knowledge of mean planet density is foremost dependent on the quality of the stellar mass and radius determinations that feed into the determinations of planetary mass and radius. One of the main goals of PLATO is therefore to provide highly precise and accurate measurements of the planet host stars' characteristics, in particular their radii, masses and ages. Typical current uncertainties for radius and mass determinations of small planets are around ±6% and ±20%, respectively, leading to uncertainties of 30 to 50% in mean density. The observational accuracy envisaged for PLATO will reduce the uncertainty in mean density to about 10%.

Provided the solid planet interior is fully differentiated into an iron core and silicate mantle, Figure 2.7 illustrates that the present detection limits are not sufficient to determine satisfactory the interior structure of an Earth-like planet (after Noack et al. 2013). Figure 2.7 (left) shows the iron core size for a radius of 1 Earth radius with 1σ uncertainty of ±6%, while the planet mass is taken constant at 1 Earth mass. To satisfy mass balance constraints, a larger planet radius is then compensated by a smaller iron core size. The dark-shaded band indicates the expected improvement in core size determination using PLATO (radius ±2%). Figure 2.7 (right) shows the possible interior structure if the mass is determined as 1 Earth mass ±20% and the planet radius is held fixed at 1 Earth radius. The dark-shaded band again shows the improvement owing to the enhanced PLATO accuracy. In summary, within the present observational limits, it is difficult to distinguish between an almost coreless planet and a Mercury-like planet interior with a large iron core. This will significantly improve with PLATO accuracies.

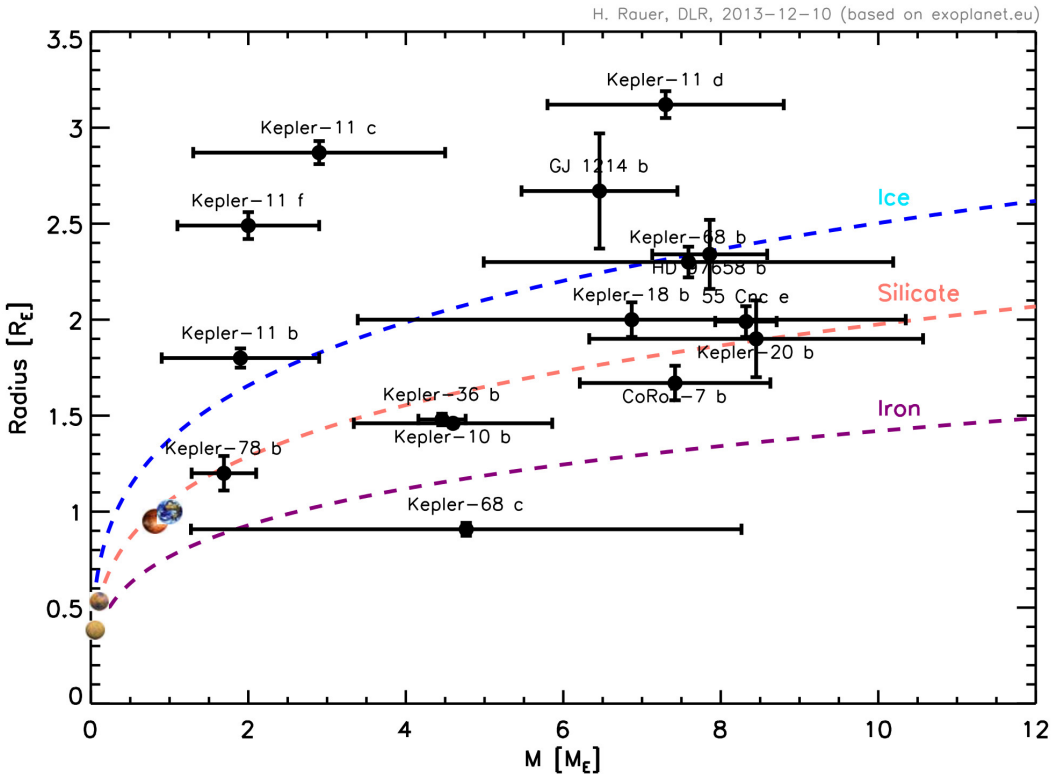

Figure 2.6: Mass-radius diagram for planets with different bulk composition. Water ice (blue), silicate rock (pink), iron (purple) (see Wagner et al. 2011, for details) are compared to known low-mass planets (with 1-σ error bars).

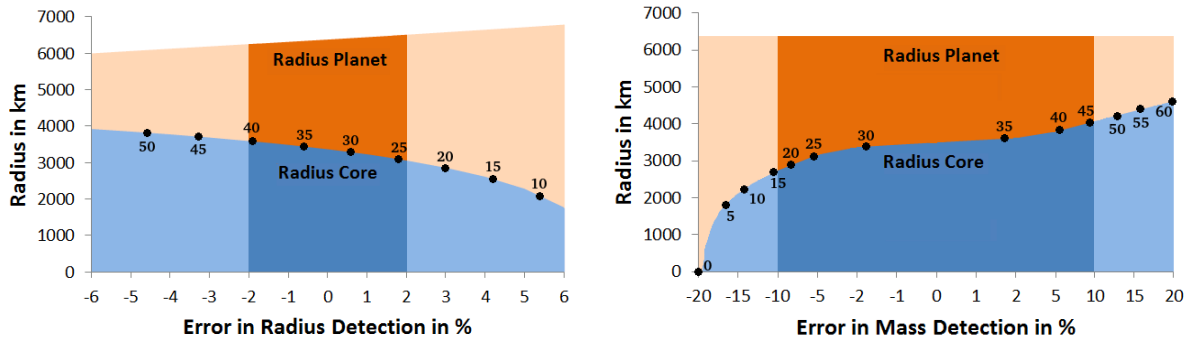

Figure 2.7: Left: Radius of planet and its core depending on the uncertainty in radius R_{planet} or Right: planetary mass M_{planet}. Left, we assume a planet of 1 Earth-mass and vary the radius (0 corresponds to 1 R_E) within current uncertainties (±6% in radius). Right: same, but keeping the radius fixed at 1 R_E and vary the planet mass within current uncertainties (±20%). Numbers at black dots provide the core mass fraction as percentage of total mass. The dark shaded regions illustrate the expected PLATO accuracy (±2% and ±10% in radius and mass, respectively).

The ratio of core radius to planet radius is important for understanding the interior evolution of a terrestrial planet, which can also influence its surface habitability. For example, the volume of the silicate mantle and the hydrostatic pressure in the upper mantle both influence the amount of partial melting and hence the rate of volcanism at the surface. Greenhouse gases are trapped in the uprising melt and are released at the surface feeding the atmosphere. In view of the large uncertainties involved in the underlying exchange processes, important bounds on the present models must be expected from a large and diverse population of well-characterised low-mass planets. Accurate determinations of both mass and radius are therefore important to impose bounds on interior-surface-atmosphere interactions with possible consequences for surface habitability (e.g., Noack et al. 2013).

Current detection limits have prevented the discovery of more than a few rocky exoplanets, although low-mass planets around other stars are most likely abundant. PLATO will provide masses and radii of a large number of solid planets up to 1 au from their host stars. Studying planets at large orbital separations allows us to address the architecture of planetary systems and the connection to proto-planetary disk properties, and finally to study the relationship of interiors to atmospheres in planets up to the habitable zone. These will be complemented by the detection of giant planets at larger orbital separations expected from the Gaia mission.

Constraining the mean composition and bulk interior structure of small planets, PLATO will enable us to answer the following questions:

- Is there another planetary system including a terrestrial planet like Earth?
- What is the typical mean density distribution (and mass function) in planetary systems?
- How is the planet mean density distribution correlated with stellar parameters (e.g., metallicity, mass, age, etc.)?

2.1.4 Gas giants and icy planets

Giant planets are planetary bodies primarily consisting of hydrogen and helium as well as a small fraction of heavy elements (i.e., rocks, ices). The Solar System gas giants, Jupiter and Saturn, orbit the Sun at distances of 5.2 and 9.6 au, respectively. The composition of giant planets and its depth dependence are calculated by interior models, which are constrained by the observational properties of the planet, such as its mass, radius, rotation rate and gravitational field coefficients. For Jupiter and Saturn these physical parameters are well known from space missions.

There is still uncertainty in the bulk composition of Jupiter and Saturn, in particular, the amount of high atomic number (Z > 2) material and the presence of a central core. The sources of uncertainty in giant planet interior models reflect mainly the uncertainty in the equations of state (EOSs) and model parameters and assumptions such as the number of layers, the distribution of the heavy elements within the planet, and the rotation profile/state.

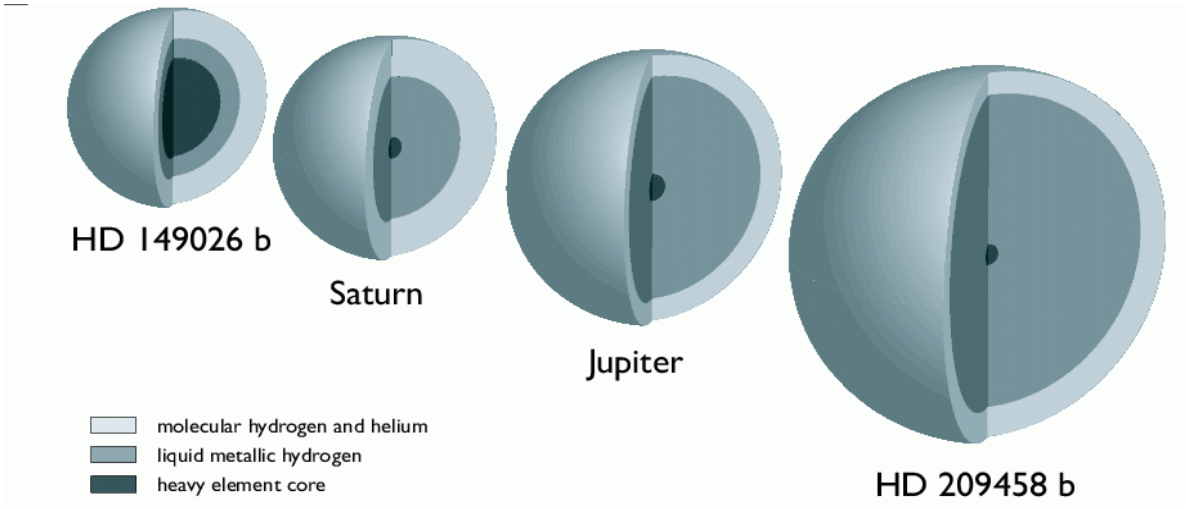

Figure 2.8: Illustration of the interior structure of HD149026b and HD209458b in comparison to Jupiter and Saturn (from Charbonneau et al. 2007). Illustration of the interior structure of HD149026b and HD209458b in comparison to Jupiter and Saturn (from Charbonneau et al. 2007).

Internal models of Jupiter and Saturn using EOSs of hydrogen, helium, and heavier elements suggest that Jupiter's core mass ranges between 0 and 10 M_E and that the high-Z material mass in the envelope is about 30 M_E. The total mass of heavy elements in Jupiter ranges from ~10 to ~30 M_E (see e.g., Saumon & Guillot 2004; Nettelmann et al. 2008). Recently, Militzer et al. (2008) suggested that Jupiter's interior consists of a core of about 14 to 18 M_E surrounded by a homogenous envelope composed mainly of hydrogen and helium. Saturn's total enrichment in heavy elements typically ranges from ~10 to ~30 M_E, with core masses between ~0−15 M_E (e.g., Saumon & Guillot 2004; Fortney & Nettelmann 2010; Helled & Guillot 2013).

The icy planets of the Solar System are Uranus and Neptune, and standard interior models suggest that they consist of three main layers: 1) an inner rocky core; 2) a water-rich envelope; 3) a thin atmosphere composed mostly of hydrogen and helium with some heavier elements (e.g., Podolak et al. 1995; Marley et al. 1995; Fortney & Nettelmann 2010). However, it should be noted that due to the uncertainties of the measurements it is still unclear whether Uranus and Neptune are truly 'icy planets', as their names suggest, or planetary bodies, which primarily consist of silicates, with hydrogen and helium envelopes (e.g., Helled et al. 2011). In addition, calculations of Uranus' evolution (cooling history) imply that the planet contracts "too slowly", i.e., simulations find that Uranus cannot cool to its measured intrinsic luminosity by the age of the Solar System assuming an adiabatic interior. This suggests that Uranus' interior may not be fully convective, and/or that it contains an additional energy source (e.g., compositional gradients) besides its gravitational contraction (e.g., Fortney & Nettelmann 2010). Neptune too, likely has a significant internal energy source. Another important open question regarding these planets is their formation process. It is still unclear what conditions and physical mechanisms lead to the formation of these fairly low-mass objects, especially at the large radial distances we find them today in the Solar System (e.g., Dodson-Robinson & Bodenheimer 2010).

The compositions and internal structures of extrasolar giant and Neptune-sized planets are less constrained than the planets in the Solar System, but they offer the opportunity to study giant planets as a class. The diversity of gas giant and 'icy' exoplanets is much larger than expected from our Solar System, thus expanding the parameter range that can be studied.

Current technology still limits the detection of transits to planets that orbit fairly close to their host stars. Although the majority of transiting giant planets are composed mostly of hydrogen and helium (e.g., Guillot et al. 2006, Miller & Fortney 2011), their internal constitution is not necessarily similar to that of the gas giants in our Solar System. In fact, exoplanets show a large diversity of masses and radii, yet to be explained. Extrasolar giant planets can differ significantly from Jupiter and Saturn (e.g., Figure 2.8) since they formed in different environments. In addition, giant planets close to their parent stars are exposed to an intense stellar radiation that prevents their atmospheres from cooling and therefore affects the contraction of their interiors. Although our understanding of "hot Jupiters" is still incomplete, substantial progress in studying these objects has been made. Interior models including the effects of irradiation have been computed (e.g.,

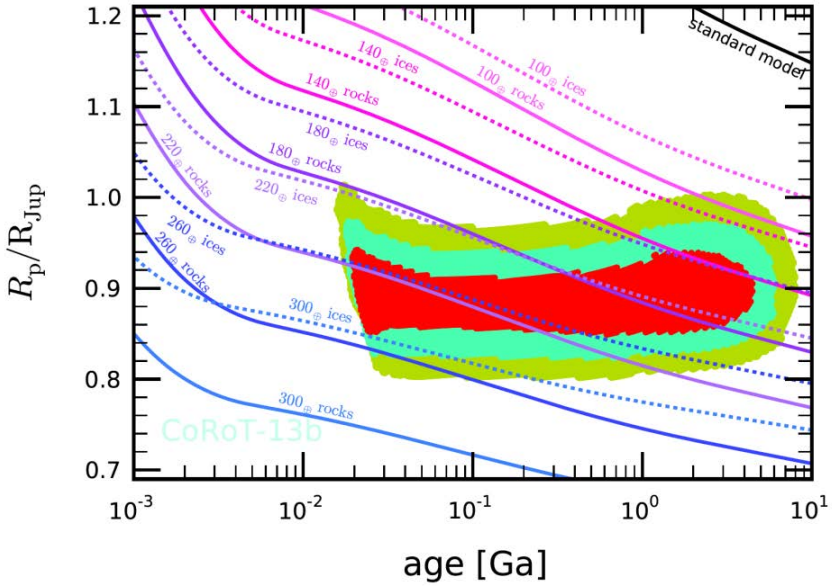

Figure 2.9: CoRoT-13b radius development over age (Cabrera et al. 2010a and references therein). The coloured areas provide the uncertainty in planet radius and in stellar age derived from stellar evolution models matching the stellar density and effective temperature (within 1 (red) to 3 (green) sigma uncertainty). The curves show evolution tracks for CoRoT-13b (assuming M = 1.308 M_J, T_{eq} =1700 K) for different amounts of heavy elements concentrated in a central core, surrounded by a solar-composition envelope.

Guillot et al. 1996; Bodenheimer et al. 2003, Batygin et al. 2011) and detailed models of the giant planets' atmospheres are now available. In addition, detailed studies of interior structure of extrasolar giant planets suggest that these objects typically consist of cores of at least 10 M_E (Guillot et al. 2006, Miller & Fortney 2011), and that the heavy element mass is proportional to stellar metallicity ([Fe/H]) while the planetary enrichment is inversely proportional to the planetary mass (Miller & Fortney 2011). Recently, a class of planets has emerged having a large fraction of rocky material in their cores, with CoRoT-13b (Cabrera et al. 2010a) as an example (Figure 2.9).

The compositions of gas giant planets can reveal important information on giant planet formation. Currently, there are two leading theories for giant planet formation: core accretion, the standard model, and disk instability. In the core accretion model the formation of giant planets begin with planetesimal coagulation and core formation followed by accretion of a gaseous envelope (e.g., Pollack et al., 1996). The disk instability model (e.g., Boss 1998; Mayer 2002) hypothesises that under the right conditions a gravitational instability can form in the protoplanetary disk surrounding a young star. Such instability can lead to the creation of a self-gravitating clump of gas and dust that evolves to become a gaseous planet. While both formation scenarios can lead to a large range of compositions and internal structures the core accretion model typically predicts a non-solar composition for giant planets, while giant planets formed by gravitational disk instability can have different compositions, depending on stellar metallicity, planetary mass, the efficiency of planetesimal accretion etc. (Helled & Schubert 2008). Clearly, a more accurate determination of the bulk composition of giant extrasolar planets that are not strongly irradiated, as is expected from PLATO, can provide valuable constraints on giant planet formation and evolutionary models.

PLATO will improve our understanding of the composition and evolution of gas giant and Neptune-sized planets. The planets discovered by PLATO around bright stars will have 3 times better radius determinations and 5 times better mass determinations than currently known. This will allow us to classify detected planets as rocky, icy, or gas giants with high accuracy, and to constrain their core masses. Constraints on the amount of heavy elements in gas planets from radius, mass and age measurements will help to understand planet formation and evolution. We will be able to determine how ice planets and gas giants contract, which planets can develop atmospheres and retain them, and study atmospheric compositional changes.

With its precise determination of planet radii, PLATO will also significantly contribute to understanding the mechanisms responsible for the inflation of gas giants. Indeed, it has been shown by Schneider et al. (2011) and confirmed by Demory et al. (2011b) that the inflation decreases with the planet illumination by the parent star. PLATO will provide a better statistics of this correlation, and the influence of the stellar wind.

In summary, key questions addressed on gas and ice planets are:

- Up to which orbital distance do we find inflated gas giant planets?
- How does this correlate with stellar parameters (e.g., type, activity, age)?
- Are gas giants with massive cores frequent and how does their distribution depend on orbital distance and stellar type?
- How do gas giants with massive cores form?

2.1.5 Planets around Sub-giant and Giant Stars

Several ground-based Doppler planet searches target sub-giant and giant stars instead of main-sequences stars. The number of planets known to orbit giant stars (~ 50) is still small compared to those known to orbit main-sequence stars, but their number has dramatically increased in recent years and is expected to do so in the near future. The discovery and characterisation of planets orbiting sub-giant and giant stars is of particular importance for the following reasons:

- Confirmation of a planet orbiting a giant star is almost impossible based on radial velocities alone, since an RV signal of an orbiting planet is hard to disentangle from the RV signature of radial and non-radial pulsations. Thus, independent confirmation of planets orbiting giant stars are most useful.
- Sub-giants and giant stars are more massive than solar-like main-sequence stars, so by finding more planets around more massive stars one can disentangle the influence of the host star's mass and its disk on the forming planets and their properties.
- Sub-giants and giant stars have undergone significant stellar evolution, which affected planetary orbits. Studying the planet population around sub-giant and giant stars offers the opportunity to investigate the influence of stellar evolution on the properties of the planetary population.

Unfortunately, few planets have been found to transit a giant star yet, although it would be extremely interesting to study those planets and to derive additional information such as radius and density of the planet. Due to the much larger stellar disk of a giant star compared to the stellar disk of a main-sequence star, the transit probability is much higher for a planet orbiting a giant star than for a planet orbiting a main-sequence star. On the other hand, the transit depth is much smaller for the same reason (much smaller percentage of the stellar disk blocked by the planet), so that it is harder to detect. The photometric precision of CoRot and Kepler was not sufficient to detect transits around giant stars in large numbers, if any. PLATO is in a better position than these two missions to find such planets. The depth of a transit of a Jupiter-sized planet in front of a giant star with a radius of 10 solar units is 100 ppm, which is within the reach of PLATO. The planets found by RV surveys around this type of star have typically periods of several hundred of days. For example, at 400 days orbital period, the transit probability is 3% and the transit duration almost 4 days. Its detection will be challenging since the photometric activity of the giant star must be well characterised, but the detection of such transits is within the detection capabilities of PLATO.

2.1.6 Planets around post-RGB stars

To date not a single bona fide planet has been identified orbiting an isolated white dwarf (e.g., Hogan et al. 2009). Therefore, we remain ignorant about the final evolutionary configuration of > 95% of planetary systems. Theoretical models (e.g., Nordhaus & Spiegel 2013) predict a gap in the final distribution of orbital periods, due to the opposite effects of stellar mass loss (planets pushed outwards) and tidal interactions (planets pushed inwards) during the red giant branch (RGB) and asymptotic giant branch (AGB) phases. If a planet enters the envelope of the expanding giant star, its survival depends a number of poorly constrained parameters, particularly its mass. Currently, the lowest mass brown dwarf companion known to have survived such “common envelope” evolution to the WD stage has 25-30 M_J (Casewell et al. 2012), but theoretical models suggest much lower mass gas giants may survive.

Over its five year primary mission, Gaia is expected to astrometrically detect several hundreds of WD planets ($M > 1\ M_J$) in long period orbits, but the likelihood of planets surviving in close orbits around WDs will likely remain an open question for some years. Recently, more than 15 planets around post-RGB were detected, orbiting extreme horizontal branch subdwarf B (sdB) stars, or cataclysmic variables. Most of them were on long-period orbits and discovered from eclipse or pulsation timing (e.g., Silvotti et al. 2007), while two sdB planetary systems with very short orbital periods of few hours were detected by Kepler through illumination effects (Charpinet et al. 2011; Silvotti et al. 2013). The Kepler discoveries suggest that ~10% of sdB stars could have close planets (or planetary remnants) and 1/40 of sdB stars could show a transit. Although we expect that some new results may come in the next years from ground-based Doppler surveys, PLATO can easily collect large-number statistics on these objects, allowing detecting sdB planets not only from illumination effects but also from the first transits, giving first estimates of their radii. Even more importantly, PLATO has the capabilities to detect the first WD planet transits, which requires large statistics (Faedi et al. 2011).

PLATO can easily detect gas giants eclipsing WDs, placing limits on the masses of planets that can survive "common envelope" evolution. In addition, since WDs are similar in radius to Earth, PLATO can detect transiting bodies down to sub-lunar sizes. Such objects may exist in close orbits to WDs, possibly through perturbations with other planets in a complex and unstable post-main sequence system. Indeed, at periods of ~10-30 hours, these rocky bodies would exist in the WD's "habitable zones" (Agol 2011), and their atmospheres would be detectable with JWST (Loeb & Maoz 2013).

Discovery and characterisation of post-RGB planets is essential to study planetary system evolution and planet-star interaction during the most critical phases of stellar evolution: RGB and AGB expansion, thermal pulses, planetary nebula ejection. We note that sdB/WD asteroseismology allows a very good characterisation of these stars and their planets.

2.1.7 Circumbinary planets

Planets that orbit around both components of a stellar binary were suggested as favourable targets for transit surveys (Borucki 1984) due to the expected alignment between the planetary and the stellar orbital planes, which strongly increases detection probabilities on eclipsing binaries with near edge-on orbits. Some early surveys (e.g., Deeg et al. 1998) subsequently centred on them, but it was not until the Kepler mission that the first transiting circumbinary planets (CBPs) were found (Doyle et al. 2011). The discovery of 7 CBPs in 6 systems has been announced to date. Their characteristics are rather distinct to those found by timing methods, with orbital periods on the order of several months and planet-masses that are relatively low, the heaviest one being Kepler-16b with 0.33 M_J. All CBP orbits have an inner limit to their stability (e.g., Dvorak et al., 1989; Chambers et al., 2002) and most of the transiting CBPs orbit rather close to that limit (Welsh et al. 2012). It is also notable that all planet-hosting binaries have orbital periods on the order of 10 days or longer. An additional photometric method to detect CBPs, based on the detection of the binaries' eclipses in the planet's reflected light has been presented by Deeg & Doyle (2011). In Kepler data, this method could detect CBPs that are not far from the inner stability limit around short-periodic binaries in a large range of orbital inclinations, but no discoveries have been reported yet.

Formation and evolution models predict in general the formation of circumbinary protoplanets in relatively distant disks and subsequent migration, combined with the further accretion of matter, to the planet's observed positions. In particular, the accumulation of CBPs near the inner stability limit has been foreseen by Pierens & Nelson (2007), who predicted that an inward drift of a protoplanet can be stopped near the edge of the cavity formed by the binary. In more general terms however, any generic theory on planet system formation and evolution needs to be compatible with planets found around binary stars, making this population of planets therefore an interesting test-bed for many theoretical advances.

For PLATO, this presents the following objectives:

- What are the properties of the circumbinary planetary systems? What are their masses, orbital periods and the types and ages of host stars? Can their special features be explained by existing planet formation theories, and/or do they need modifications?

- Do other classes of CBPs besides currently known ones exist? In particular, no CBPs on short-period binaries have been found to date, although these binaries are by far the most common ones and there are no special obstacles to the detection of their planets.

The number of CBP detections that was found to date in Kepler data is likely limited by the number of light curves sampled and not so much by its photometric precision, e.g. all known CBP transits can be identified "by eye" in the light curves. This indicates that the discovery of these systems in Kepler data may be rather complete, although some efforts to detect shallow transit CBPs are still on-going.

With the sample size and observing duration of PLATO, we can expect that the sample of transiting circumbinary planets (CBPs) of the types that are currently known will multiply several-fold. We can also expect a clear answer on the existence of short-periodic CBPs.

2.1.8 Evolution of planetary systems

The ability to derive the age of planetary systems is one of the key assets of PLATO. The age of stars is traditionally very poorly constrained, to within at best only a few Gyrs for stars on the main sequence. Furthermore, young planets, that are the most important in order to decipher the conditions under which planetary systems are formed, orbit around active stars and the determination of their parameters has remained elusive (see e.g., Gillon et al. 2010; Czelsa et al. 2009; Guillot & Havel 2011).

With relative ages of main sequence stars known to within 10 %, PLATO will remove the age ambiguity in planet evolution. A large sample of planetary systems with known age will allow us to search for type cases of planet and planetary system evolution, identify correlations with the host star parameters, as well as with the planet interior composition and structure. The characteristics of planetary systems discovered by PLATO will be invaluable to future large missions that will spectroscopically characterise the atmospheres of nearby Earth-like planets for signatures of life.

Planets and planetary systems evolve with age in several aspects, which we briefly summarize here:

- Gas giant planets progressively cool and contract, a process that lasts up to several Gyrs (see Section 2.1.4). An accurate knowledge of age is therefore crucial for the interpretation of measured radii and a determination of interior structure (ESA/SRE(2011)13).
- Terrestrial planets evolve with time, as exemplified by the planets in our Solar System (see also Section 2.1.3). The atmospheres of the terrestrial planets in our Solar System are secondary atmospheres produced by outgassing from the interior and impacts, both processes being more intense in the young Solar System. In the case of e.g. Mars a possible denser young atmosphere has meanwhile been lost to space. Hence, the atmospheric composition and pressure of the terrestrial planets can change with time. In the case of Earth its atmosphere has been further modified by the development of oxygen-producing life (tertiary atmosphere) since about 2.5 Gyrs. The distinct evolution of the terrestrial planets in our Solar Systems is far from being fully understood. Exoplanets can complement our investigations of terrestrial planet evolution by contributing parameters not accessible in the Solar System: A large number of planets over a wide bulk parameter range and at different ages. This will allow us to search for type cases and possible correlations of planetary evolution processes with stellar and planetary system parameters, which will provide a breakthrough in our understanding of the evolution of atmospheric composition and habitability. PLATO will provide the initial key steps towards this ultimate goal: it will detect a large sample of terrestrial planets at intermediate orbital distances; it will measure their bulk densities and masses needed to estimate outgassing efficiencies and atmospheric scale heights and it will determine accurate ages of planets. Since PLATO target stars are bright, they will be targets for direct spectral detections of atmospheric absorptions in future proposed L-class missions.
- Host stars evolve with time and expose young planets to much higher UV and high-energy radiation levels than found on Earth today (see Section 2.1.10). This affects processes like atmospheric losses, but also radiation levels affecting life on the surface of terrestrial planets. Therefore, a good characterisation and dating of the host stars is crucial to obtain an understanding of the evolution of planetary

atmospheres and habitable conditions. The significance of atmospheric loss processes is also crucial to understand whether small planets are able to retain their extended primary, hydrogen-dominated, atmospheres over a significant part of the lifetime of a planetary system (see Section 2.1.9). An observational constraint on the presence of primary atmospheres for planets with different ages will allow us to test the predicted formation of such planets from planet synthesis models (e.g. Mordasini et al. 2009, 2012b; Section 2.1.2). Crucial here are planets at intermediate orbital distances, which are less affected by loss processes due to interaction with strong stellar radiation.

- The architecture of planetary systems is shaped through physical (e.g., from planet formation) and dynamical processes covering a wide range of timescales, up to billions of years. The comparison of planet system populations of different ages will allow us to investigate whether typical scenarios at different ages exist (e.g., hot Jupiters: disk or Kozai migration). Furthermore, TTV observations over long time periods, e.g. by combining PLATO with already available Kepler observations, would allow constraining the Q-factor describing internal tidal energy dissipation of planets, a factor crucial to understand the tidal evolution of close-in planets.

The accurate determination of planetary system ages for thousands of systems is among the key features of PLATO. This crucial goal will not be achieved by any other on-going or planned future transit mission. Key science questions PLATO can answer are:

- What are the ages of planetary systems?
- How do planet parameters (e.g., mean densities, radii of gas giants, planet star distance distributions, and (if combined with spectroscopic follow-up) atmospheres) correlate with age?
- How many super-Earths retain their primary atmosphere? Is there a correlation of small planet primary atmospheres with system age? What are the main parameters governing the presence of primary atmospheres (e.g., formation mechanism, stellar type, orbital distance, age, metallicity)?
- What is the planetary evolution timescale compared to the lifetime of the system?
- How does the structure/architecture of planetary systems vary and evolve with age?

2.1.9 Planetary atmospheres

In the past decade, numerous studies have been published on the use of wavelength-dependent primary transits and secondary eclipses to characterise the atmospheres of exoplanets, including, e.g., GJ 1214b (e.g., Charbonneau et al. 2009; Bean et al. 2010; Berta et al. 2012; de Mooij et al. 2012) and 55 Cancri e (e.g., Crossfield et al. 2012; Demory et al. 2012; Ehrenreich et al. 2012). Highlights include the claimed detections of molecular features in the infrared (e.g., Knutson et al. 2011) to the inferred presence of clouds/hazes in the visible (e.g., Pont et al. 2013) in the atmospheres of hot Jupiters, and even the detection of the exosphere (Vidal-Madjar et al. 2003; Lecavelier des Etangs et al. 2012). Visible data determine the albedo, the identity of the major spectroscopically inert molecule and the relative abundance of clouds/hazes of the atmosphere. Clouds have long been an obstacle in our understanding of the atmospheres of Earth, Solar System objects and brown dwarfs, and are rapidly emerging as a major theme in the study of hot Jupiters, super Earths and directly imaged exoplanets. For small exoplanets, visible data help to determine if a thick, gaseous atmosphere is present and thus identify the exoplanet as a prime candidate for follow-up, atmospheric spectroscopy with JWST, E-ELT and future L-class missions.

The albedo measures the fraction of starlight reflected by an atmosphere and therefore its energy budget. It is of central importance in determining the thermal structure of the atmosphere. Measuring the secondary eclipse (occultation depth) in the visible directly yields the geometric albedo, which is the albedo of the atmosphere at full orbital phase (e.g., Demory et al. 2011b). Detecting reflected light over the planet orbit, the spherical albedo can be derived. For the hottest objects (~2000 to 3000 K) thermal emission from the exoplanet may contaminate the broadband visible data, thus confusing the measurement of reflected light versus thermal emission. In these situations, the two broadbands of the fast cameras of PLATO will be useful in decontaminating the occultation depth measurements for the brightest stars.

The spectroscopically active molecules of an atmosphere typically contribute spectral features in the infrared, but these molecules are often minor constituents of an atmosphere (by mass). Of central importance in interpreting an exoplanetary atmosphere is the knowledge of the pressure scale height, which is set by the mean molecular weight. This is determined by the dominant (by mass) inert molecule, and the gravity of the planet. On Earth, the dominant, inert molecule is nitrogen; in gas giants like Jupiter, it is believed to be molecular hydrogen. Analyses of the spectra of hot Jupiters often assume the atmosphere to be hydrogen dominated (Madhusudhan & Seager 2009). For rocky or terrestrial exoplanets with secondary atmospheres, the mean molecular weight cannot be assumed. A robust way to directly compute the mean molecular weight is to measure the primary transits at two visible wavelengths (Benneke & Seager 2012), which can be accomplished using the two broadbands of the fast cameras of PLATO. If only one broadband measurement is made, then one may be able to distinguish between hypothesized atmospheres (e.g., hydrogen-dominated versus water-dominated models; de Mooij et al. 2012). Alternative methods include the detailed analysis of the line shape of a certain molecular species or the relative strength of its features at different wavelengths (Benneke & Seager 2012), but such an approach requires the line opacity list in question to be robust, which is not always the case. Visible data thus provides an important check on the analysis of infrared data of exoplanetary atmospheres. Identifying the dominant, inert molecule in an atmosphere has significant implications for inferring its thermal structure and spectrum, as the inert component often exerts an indirect influence on the spectroscopically active molecules via processes such as pressure broadening and collision-induced absorption.

Phase curves show the flux as a function of orbital phase, which may be deconvolved to obtain the flux versus longitude on the exoplanet, known as a "brightness map" (Cowan & Agol 2008). Infrared phase curves contain information about the efficiency of heat redistribution from the dayside to the nightside of an exoplanet (Showman & Guillot 2002; Cooper & Showman 2005; Showman et al. 2009; Cowan & Agol 2011; Heng et al. 2011), as previously demonstrated for hot Jupiters (e.g., Knutson et al. 2007, 2009). To a lesser extent, infrared phase curves constrain the atmospheric albedo and drag mechanisms (shocks, magnetic drag). By contrast, visible phase curves encode the reflectivity of the atmosphere versus longitude, which in turn constrains the relative abundance of clouds or hazes if they are present. The cloud/haze abundance depends on the size and mass density of the particles, as well as the local velocity, density, pressure and temperature of the flow, implying that a robust prediction of the cloud properties requires one to understand atmospheric chemistry and dynamics in tandem. Examples of exoplanets where clouds are likely to be present include Kepler-7b, which has a high albedo (~ 0.3) and a phase curve containing a surprising amount of structure (Demory et al. 2011a). The feasibility of obtaining visible phase curves has already been demonstrated for the CoRoT (Alonso et al. 2009a,b; Snellen et al. 2009, 2010) and Kepler (Borucki et al. 2009; Batalha et al. 2011) missions.

A more ambitious goal is the use of the information from the phase light curve of the planet to constrain the temporal evolution of the temperature distribution of its upper atmosphere and set the first constraints on the dynamics of its atmosphere (e.g., Knutson et al. 2009). An interesting goal would be to establish the frequency of planets showing superrotation on their atmospheres, a phenomenon which involves displacement of the hottest atmospheric spot of a tidally locked planet by an equatorial super-rotating jet stream (see Faigler et al. 2013 and references therein). PLATO will provide bright targets for such investigations. High-accuracy photometry also allows for the measurement of the tidal distortion created by a transiting planet on its star (Welsh et al. 2010), which can provide a wealth of information about the star-planet interaction. Among the PLATO detections will also be nearby giant planets on wide orbits for which transit spectroscopy and direct imaging spectroscopy will be possible. The comparison of these two approaches will then allow us to study the vertical structure of the planet atmosphere.

As the scientific community prepares for the launch of the JWST and also ground-based telescopes such as E-ELT, a central question to ask is: what are the best targets for follow-up, atmospheric spectroscopy of small exoplanets? Earth-like exoplanets with sizes of about 2 Earth radii are believed to be either composed predominantly of rock or scaled-down versions of Neptune with thick gaseous envelopes. If the bulk composition of an exoplanet cannot be made from a material lighter than water, then one can calculate the thickness of the atmosphere, relative to the measured radius, by utilising the mass-radius relation of pure water (Kipping et al. 2013). It was shown that such simple approach can be used to imply a mostly rocky composition (e.g., Earth, Kepler-36b; Kipping et al. 2013). By quantifying this metric for the entire PLATO catalogue of small exoplanets, one can construct a valuable database of optimal follow-up targets.

Knowledge of the fraction of small exoplanets with and without thick atmospheres, as a function of their other properties, provides a direct constraint on planet formation theories (see Section 2.1.2).

In summary, the key science questions that PLATO can answer about the atmospheres of exoplanets are:

- What is the diversity of albedos present in exoplanetary atmospheres? How does the albedo correlate with the other properties of the exoplanet (incident flux, metallicity, etc)? Are these albedos associated with the presence of clouds or hazes?
- What are the dominant, inert molecules present in exoplanetary atmospheres? What are the mean molecular weights?
- When are clouds present in exoplanetary atmospheres? What is the diversity of the cloud properties (particle size, reflectivity, etc)?
- For small exoplanets (of ~2 R_E in size), what are the best targets for follow-up, atmospheric spectroscopy? Here, small planets at intermediate orbital separations are of particular interest.

2.1.10 Characterising stellar-exoplanet environments

Transit observations of exoplanets around bright host stars together with advanced numerical modelling techniques and known astrophysical parameters, such as the host-star age and radiation environment, offer a unique tool for understanding the exoplanet upper atmosphere-magnetosphere interaction with the star.

Observations around bright enough stars with the Hubble (HST) and Spitzer Space Telescopes, combined with theoretical studies of transiting exoplanets, have indicated that obtained UV spectra related to the upper atmospheres can be used to study a number of issues, e.g.: space weather events on exoplanets (Lammer et al. 2011a; Lecavelier des Etangs et al. 2012), properties such as the thermospheric structure (e.g., Koskinen et al. 2012), the exosphere-magnetosphere-stellar plasma environment (Holmström et al. 2008; Ekenbäck et al. 2010; Llama et al. 2011), outflow of planetary gas including hydrogen atoms (Vidal-Madjar et al. 2003; Ben-Jaffel 2007; 2010; Ehrenreich et al. 2012), and heavy species such as carbon, oxygen and metals (Vidal-Madjar et al. 2004; Linsky et al. 2010; Fosatti et al. 2010).

Moreover, the detection of transiting Earth-size or super-Earth-type exoplanets with PLATO orbiting bright M-stars can be used as a proxy for early Solar System planets like young Venus, Earth and Mars, which faced a much harsher UV radiation environment than today, closer to that of active M dwarf stars (Lammer et al. 2011b; Lammer et al. 2012). PLATO detections of such terrestrial planets will give the possibility to study EUV heated and extended upper atmospheres around Earth-type exoplanets by UV follow up observations. The expected results of such observations are essential for testing e.g. early terrestrial atmosphere evolution hypotheses.

Due to the present lack of bright target stars, only four exoplanets, namely HD 209458b, WASP-12b, HD 189733b, and 55 Cancri b, have host stars that are bright enough to allow UV follow-up transit observations with HST that can be used to enhance our understanding in these fundamental science cases. The detection and observation of hundreds of exoplanets around bright and nearby host stars with PLATO will allow for a detailed follow-up analysis of high precision attenuation spectra obtained for transiting close-in planets by near future space observatories such as the World Space Observatory-UV (WSO-UV) (Shustov et al. 2009; 2011; Gómez de Castro et al. 2011), or other future UV observing facilities taking advantage of this PLATO legacy. Such observations will improve our knowledge of the exoplanet-upper atmosphere-magnetosphere environments fundamentally.

2.1.11 Detection of rings, moons, Trojans and comets

High-precision photometry, the large number of planets detected by PLATO, together with the well-characterised host stars will significantly increase our chances to detect planetary rings, moons, Trojan planets and exo-comets.

Modulations in the transit light curve also allows for the detection of planetary rings (Barnes & Fortney 2004, Ohta et al. 2009) and large moons (Sartoretti & Schneider 1999). One of the main drivers for the search of moons is that they might share the orbits of Jupiter-sized planets in the habitable zone (Heller & Barnes 2012), and therefore be interesting targets for atmospheric characterisation. There is a well-developed project searching for moons around transiting extrasolar planets in the Kepler mission (Kipping et al. 2012, Simon et al. 2012), but so far the search has proven to be elusive.

Moons produce two types of observable effects, photometric transits superimposed on the planetary transits and perturbations in the timing and length of the transits of the host planet. Unfortunately, for typical regular satellites in the Solar System, such as Ganymede around Jupiter, the amplitude of the timing perturbations is extremely small, in the order of several seconds, which is well below current detection limits, and the photometric transit of a moon, when superimposed onto planetary transits, can very well be confused with the patterns produced by spot crossing (Silva-Valio & Lanza 2011; Sanchís-Ojeda et al. 2012) or instrumental systematics. On the other hand, moons are not thought to be stable for orbital periods of the host planet below 0.1 au. This means that we can only aim at finding moons at planets with large orbital periods, which reduces the number of transit events for a given length of the observations. The scarcity of the observations and the fact that the orbital phase of the moon is sampled at the orbital period of the planet, or below the Nyquist frequency of the moon's orbit, makes the characterisation of these systems extremely challenging. Kepler photometric precision is around 30 ppm in 6.5 h at magnitude 12 (Gilliland et al. 2011). PLATO expects to achieve 27 ppm in 1h at magnitude 10.8, therefore outperforming Kepler by at least a factor of 2, in the cases where stellar noise sources do not dominate. A factor of 2 in noise means a factor of 4 in the detectable radius, because the transit depth is proportional to the square of the radius ratio between the transiting object and the star, which can make a difference regarding which systems can be detected with PLATO in comparison with Kepler. Still, the challenges for the characterisation of the planet-moon system will remain important.

Nevertheless, even if the moon orbital period cannot be inferred from TTVs, its radius can be measured for large moons, by the depth of its transit superposed to the planet transit. And for transiting moons, their atmosphere can be detected by further transit spectroscopy (Kipping et al. 2009).

A more favourable scenario is the possibility of detecting binary planetary systems, or systems close to binary such as Pluto-Charon or the Earth-Moon system. In these cases, the combined signal of the planet and the moon is clearly distinguishable in the photometry and the TTVs can be much larger, up to some minutes in the case of the Moon orbiting the Earth. Such binary systems have not been found yet and determining their frequency remains a science case for PLATO.

Trojan-planets moving close to the Lagrange points L4 and L5 in 1:1 mean-motion resonance with planets are thought to be in very stable configurations, even if they reach the size of super-Earth planets. In our Solar System there are multiple examples of bodies in such orbits, albeit with sizes comparable with asteroids, so planetary objects in Trojan orbits would be a new class of system. PLATO would have the precision to detect Trojan-planets as small as Earth. However, so far such systems have not been detected by any other survey (see Cabrera 2008 and references therein).

While controversial it has been suggested that comets can be expected to redistribute organic material in a planetary system (as well as water). Exo-cometary tails lead to transit light curves that could be as steep as those produced by earth-sized planets (Lecavelier des Etangs 1999) and hence detectable by PLATO.

2.2 Science Goals II: Probing stellar structure and evolution by asteroseismology

Asteroseismology is the study of the global oscillations of stars. The frequencies of these oscillations, which can be either trapped acoustic waves (also called p-modes) or internal gravity waves (also called g-modes) or a mixture of the two, depend on the radially varying density and internal speed of sound of the star. Thus, measurements of oscillation frequencies can be used to infer the internal structure of stars. The data acquired by the CoRoT and Kepler missions have clearly demonstrated that it is possible to accurately measure the radii, masses and ages of pulsating stars. While this is now carried out for tens to hundreds of stars, PLATO

will do it for many tens of thousands of stars and thus provide very stringent constraints on the theory of stellar structure and evolution.

PLATO is the first exoplanet mission to make systematic use of asteroseismology to characterise the masses, radii, and ages of planet host stars with much higher precision than is possible using classical methods. Asteroseismology is therefore of key importance to derive accurate planet parameters. Furthermore it is the most accurate method to date exoplanetary systems.

PLATO will measure the oscillation frequencies of over 80,000 dwarf and subgiant stars with magnitudes less than 11, and 1,000,000 stellar light curves in total, over the course of the full mission. It will thus be a powerful new tool for the characterisation and study of the evolution of star-planet systems.

2.2.1 Stellar parameters as key to exoplanet parameter accuracy

The main focus of the asteroseismology programme of PLATO will be to support exoplanet science by providing:

- stellar masses with an accuracy better than 10%,
- stellar radii to 1-2%,
- and stellar ages to 10% of the main sequence lifetime.

Gaia will provide the distances to the stars via direct, geometrical measurements, and hence the true absolute luminosity of the star can be derived with high accuracy. Combining the luminosity with the effective surface temperature of the star obtained from (ground-based) high-resolution spectroscopy, we will obtain the radius of the star with 1-2% accuracy. Also, luminosities from Gaia can be used in cases where T_{eff} has not been measured. In case Gaia data should not become available in the future, the stellar radius can also be directly determined by using asteroseismic scaling relations together with the effective temperature.

In the past, performing asteroseismology was far from straightforward, i.e., even for stars very similar to our Sun. However, real breakthroughs in asteroseismology have recently been achieved through the space missions MOST, CoRoT and Kepler. Asteroseismology will provide the mean density of the star, e.g., via the scaling relationships or inversion techniques. These scaling relations based on solar values have already been tested and validated on Kepler targets by comparing the asteroseismic radii and distances with interferometric observations and Hipparcos parallaxes (Huber et al. 2012; Silva Aguirre et al. 2012). By combining the very precise mean density values of PLATO's asteroseismic analysis and the stellar radii from Gaia we will obtain accurate stellar masses.

The asteroseismic age-determination is more complex and requires invoking models of stellar evolution. Age estimates will be made by comparing grids of stellar models computed for different initial parameters (mass, metallicities, helium abundances, convection parameters) to the combined non-asteroseismic and asteroseismic observational constraints. The models will themselves be improved using the asteroseismology of PLATO observations (Section 2.2). Several publications in recent years have shown that ages can indeed be determined from asteroseismology with high precision, e.g. Metcalfe et al. (2009, 2010) and recently for 22 Kepler targets by Mathur et al. (2012) and the bright stars 16 Cyg A and B by Metcalfe et al. (2012). These examples show that even higher precisions than 10% can be achieved.

Other examples come from the CoRoT satellite which has observed several solar-type stars in its asteroseismic programme. One of the cool stars observed is the G0V type star (m_V = *6.3*) HD52265, a planet hosting star, which was observed with CoRoT for 117 days (Ballot et al. 2011; Gizon et al. 2013). About 31 oscillation modes were present with sufficient S/N in the power spectrum of the light curve (Figure 2.10). A grid of stellar models was computed (Escobar et al. 2012) and further analysis of convection and rotation performed (Lebreton & Goupil 2012; Gizon et al. 2013). A seismic radius of 1.34 ± 0.02 R_{Sun} and a seismic mass of 1.27 ± 0.03 M_{Sun} were derived. The age was determined as 2.37 ± 0.29 Gyr. More solar-type stars have been observed by CoRoT in this fashion and several of them are known to have (large) planets.

The Kepler mission allows for asteroseismology down to about at least m_V = 12. Kepler has carried out asteroseismic observations on a large number of stars, including many with transiting planets. Recent examples of such planetary systems containing icy/rocky planets are Kepler-36b (Carter et al. 2012), Kepler-68 (Gilliland et al. 2013) and the smallest planet detected so far, Kepler-37b (Barclay et al. 2013). Based on the asteroseismic analysis of 66 Kepler planet host stars, Huber et al. (2013) claim typical uncertainties of 3% and 7% in radius and mass, respectively, from the analysis of global asteroseismic parameters. PLATO will provide at least similar performances in thousands of stars with planets.

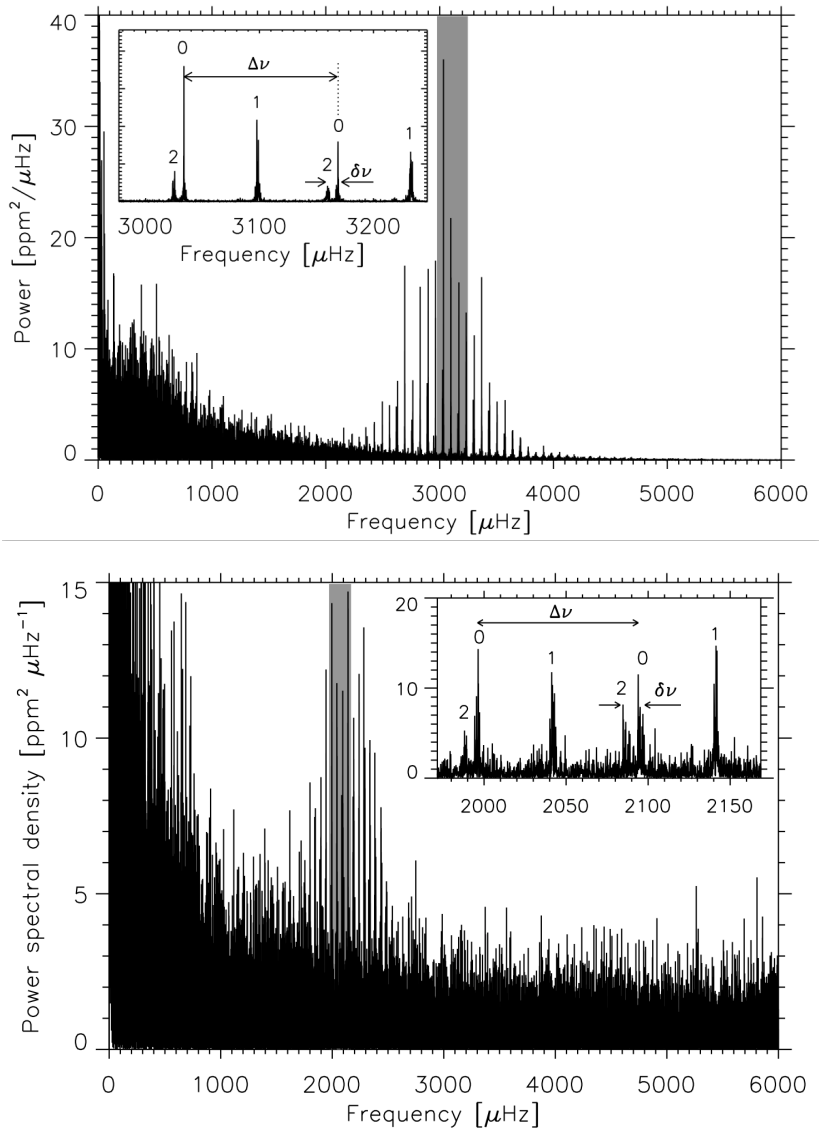

Figure 2.10: Top: Solar power spectrum from 2 years of SOHO/VIRGO photometric data. Bottom: Power spectrum of HD 52265 from 117 days of observation with CoRoT (Gizon et al. 2013). The inset figures zoom on the sections of the power spectra highlighted in gray.

CoRoT and Kepler results clearly demonstrate the feasibility of achieving highly accurate star and planet parameters. It should be noted that measurements of effective temperature to within 1% will be achievable through dedicated high-resolution, high signal-to-noise spectroscopic observations obtained as part of the ground-based follow-up program. The determination of the chemical abundances and effective temperature will be based on state-of-the-art techniques and model atmospheres taking 3D and non-LTE effects into account (Bergemann et al. 2012; Magic et al. 2013). Taken together with the luminosities expected from ESA's Gaia mission the effective temperature will lead to stellar radii with a relative precision within 2% for un-reddened stars, as is the case for most of the PLATO targets, as illustrated above.

Finally, the frequency analysis can also provide information about stellar interior rotation (e.g., Beck et al. 2012; Deheuvels et al. 2012; Gizon et al. 2013). Furthermore, the relative amplitudes of the split components depend on the inclination of the rotation axis relative to the line of sight and hence may reveal a possible misalignment between the stellar equator and the orbital planes of transiting exoplanets (Gizon & Solanki 2003; Gizon et al. 2013; Chaplin et al. 2013).

2.2.2 Stellar models and evolution

With sufficiently good data the asteroseismic determination of mass and radius is essentially independent of stellar models. For other quantities, particularly the age, the inferences involve fitting models to the observables and their accuracy depends on our ability to model stellar evolution. Thus the asteroseismic investigation of stellar structure and evolution is an essential part of the characterisation of planet hosts and to put the discovered planetary systems into an evolutionary context. Asteroseismic investigation of a large number of stars of various masses and ages is a necessary tool to constrain models of stellar interiors, identify missing physics, and thereby improve our understanding of stellar evolution.

A long standing problem in stellar modelling is the description of the transport by convection. Prescriptions or such transport in 1D stellar model computation, require the knowledge of quantities which cannot be derived easily from first principles. One therefore needs information from numerical simulations and most importantly from observations of stars in various evolutionary stages and chemical composition. One example is the filling factor of downdraft plumes carrying energy from the top of a convection zone to the bottom. This type of observational constraints can only be obtained with highly precise seismic measurements (frequencies, amplitudes, mode lifetimes) and only for bright enough stars. The necessary seismic precision demands these stars be observed over long runs.

Another main source of uncertainty affecting age determination is the presence and efficiency of transport mechanisms in radiative zones (Zahn 1992, Maeder 2009). While these mechanisms can have a significant impact on the main-sequence lifetime, they are still poorly understood and crudely modelled.

Rotational mixing is one of such processes that is not yet well understood. Angular momentum and chemical elements can be transported in the radiative zones of rotating stars through meridional circulation and hydrodynamical instabilities. This results in a change of the global and asteroseismic properties of stars when rotational effects are taken into account, and in particular to an increase of the main-sequence lifetime due to the transport of fresh hydrogen fuel in the stellar core (e.g., Eggenberger et al. 2010). These changes depend on the poorly-known efficiency of rotational mixing, which can be constrained by obtaining information about the internal rotation profiles in stellar radiative zones. Radial differential rotation can be inferred by asteroseismology for stars that have mixed modes (e.g., Suárez et al. 2006). These modes have a g-mode character in the core and a p-mode character in the envelope. They are therefore sensitive to the core, while having amplitudes large enough to be detected at the surface. Mixed modes are present in subgiant and red-giant stars (e.g., Beck et al. 2011), and depth variation of internal rotation has already been measured using Kepler data (e.g., Beck et al. 2012; Deheuvels et al. 2012). However, only the longest observing runs (2 years with Kepler) provided sufficient precision to derive the information on the core rotation of these evolved stars, and on the evolution of the core rotation with time. This brings valuable constraints on the transport processes during and, perhaps more importantly, prior to the post main sequence stage. The sample of available Kepler subgiant stars is too small to allow for an unbiased statistical study. To proceed further, we will need a larger sample of bright post main sequence stars.

Thorough investigation of stellar evolution requires a large number of bright stars sampling all relevant stellar parameters (mass, age, rotation, chemical composition, environment). The PLATO mission will, for the first time, provide such necessary data in order to:

- Improve understanding of internal stellar structure, including the identification of missing physics.
- Better understand the pulsation content and its interaction with the physics of the star, in particular with respect to rotation.
- Improve our understanding of stellar evolution.

2.3 Science Goals III: Complementary and Legacy Science

In addition to its focus on relatively bright stars, one major and crucial advantage of PLATO over the CoRoT and Kepler space missions is its ability to observe in many directions of the sky. This will enable us to sample a much wider variety of time-variable phenomena in various populations of the Galaxy than hitherto. Moreover, PLATO's asteroseismic characterisation of stellar ensembles, binaries, clusters and populations will be a significant addition to the Gaia data for about 50% of the sky. This capability will obviously give rise to a very rich legacy for stellar and galactic physics, promising major breakthroughs in a variety of subjects, some of which are discussed in this section.

2.3.1 Stellar structure and evolution

Low-mass red Giants: Red giants are cool and luminous stars, which, by virtue of covering a wide domain in mass, age, chemical composition, and evolutionary state, are an important source of information for testing chemo-dynamical models. An important legacy from the CoRoT and Kepler missions has been the discovery of solar-like oscillations in thousands of G-K red giants (De Ridder et al. 2009; Bedding et al. 2010; Hekker et al. 2011). The occurrence of non-radial modes was only unambiguously proven from CoRoT observations (De Ridder et al. 2009). This opened up the field of asteroseismology of low-mass evolved stars. Thanks to the discovery of gravity-dominated mixed modes in more than 300 days of continuous Kepler data of red giants (Beck et al. 2011, Bedding et al. 2011), the promise of asteroseismology being able to discriminate between different nuclear burning phases was finally delivered. Indeed, with PLATO we will be able to probe the properties of the core structure of red giants and reveal if they are already in the helium core burning stage or are still climbing up the red giant branch while burning hydrogen in a shell (Bedding et al. 2011, Mosser et al. 2012). PLATO will be able to separate these two kinds of stars, because they have different positions in the frequency spacing-diagrams. PLATO will also improve the luminosity-period relationships of these kind of bright objects, which helps to use them as galactic or even extragalactic distance-indicators with higher precision than nowadays.

PLATO will improve our understanding of the internal structure of red-giant stars by providing accurate oscillation frequencies for an unprecedented number of targets in different directions of the galaxy.

Hot B subdwarf (sdB) stars: These are core He-burning stars with an extremely thin H-rich envelope (Heber 2009). They exhibit pulsation instabilities driving both acoustic modes of a few minutes and gravity modes with 1−4 h periods. It is only recently, with CoRoT and Kepler, that data of sufficiently high quality could be obtained for the gravity mode sdB pulsators (Charpinet et al. 2010; Østensen et al. 2010). Asteroseismic modelling determine their global parameters (e.g., mass and radius) with a precision of typically 1% (Van Grootel et al. 2013). The recent discoveries of planets around single sdB stars (Charpinet et al. 2011; see Section 2.1.6) support the idea that planets could influence the evolution of their host star, by triggering the mass loss necessary for sdB star formation.

PLATO will be the only space-based facility able to further do deep seismic probing of sdB stars (data that cannot be obtained from the ground). It will also discover new planets around these objects, permitting to disentangle the question of the origin of such stars and explore star-planet interactions in the advanced stages of stellar evolution.

Massive stars: Despite their scarcity compared to low-mass stars, stars massive enough to end their lives in core-collapse supernovae dominate the chemical enrichment of galaxies and the Universe as a whole. Most of the heavy elements (by mass fraction) are created by stars with birth masses above about 9 M_{Sun}. Gravity-mode oscillations in such evolved massive supergiants (e.g., Saio et al. 2006; Lefever et al. 2007) hold similar potential to probe the stellar core as the gravity-dominated mixed modes found in red giants (Moravveji et al. 2012a).

PLATO can provide a homogeneous sample of blue supergiants studied by asteroseismology with a broad range of pulsation periods.

White Dwarfs (WDs): White dwarfs are the endpoint of the evolution of the vast majority (~ 95%) of stars in the Universe. They no longer undergo fusion reactions but gradually evolve along the cooling sequence, where several classes of g-modes pulsations allow asteroseismic probing of the final stages of stellar evolution (Fontaine & Brassard 2008). WDs can be used to constrain the ages of the various populations of

stars in the Galaxy, during their later evolved stages (cosmochronology, Fontaine et al. 2001; Liebert et al. 2013). The cooling tracks are very sensitive to the exact core composition and envelope layering, two parameters that are inaccessible from direct observations and poorly constrained from theory, but that can be determined from asteroseismology (Giammichele et al. 2013). WD cosmochronology interacts well with the Gaia mission adding accurate age estimates to the 3D mapping of the Galaxy. Internal dynamics can also be probed by asteroseismology, (e.g., rotation and angular momentum evolution, Charpinet et al. 2009). Finally, "exotic" physics due to the extreme compact nature of white dwarfs can be calibrated (neutrino production rates, conductive opacities, interior liquid/solid equations of state, crystallization).

PLATO will be the very first mission to bring WD seismology into the space era, allowing for significant asteroseismic probing of the final stages of stellar evolution.

2.3.2 Asteroseismology of globular and young open clusters

Testing stellar evolution theory through asteroseismology will be most successful if applied to the extremes of evolutionary stages within a cluster. This should include both young open clusters with (pre-) main-sequence and pre-supernova supergiant pulsators on the one hand, and old globular clusters of various metallicities that contain main-sequence, horizontal branch, and white dwarf stars, on the other hand.

Current asteroseismic studies involved, for example, the study of solar-like oscillations of the red giant members (Stello et al. 2011; Hekker et al. 2012) and led to the first seismic cluster constraints on age, metallicity, and mass-loss rates on the red giant branch (Basu et al. 2011; Miglio et al. 2012a; Corsaro et al. 2012). Unfortunately, only clusters in a relatively narrow range of ages, from 0.4 Gyr for the youngest to ~ 8 Gyrs for the oldest, were studied.

Due to the pointing restrictions of Kepler and CoRoT, no young clusters (i.e., with ages younger than a few tens of million years) can be observed by Kepler, and only one young cluster, NGC 2264, could be observed in two short runs by CoRoT. Recent asteroseismic results from the NGC 2264 observations include, e.g., the discovery of the first two pre-main sequence ϒ Doradus pulsators (Zwintz et al. 2013) and a homogeneous study of the relation between pulsations and stellar evolution from the early stages to the main sequence phase (Zwintz et al. 2013).

PLATO will lead to major breakthroughs when observing clusters at different ages, thanks to its large-sky accessibility and its step-and-stare phase. No other astronomical experiment with the capability to investigate stellar evolution at the level of full cluster asteroseismology is presently on the horizon.

2.3.3 Probing the structure and evolution of the Milky Way

The chemical enrichment of the Universe is one of the main thrusts of modern astrophysics and the Milky Way (MW) can be seen as the Rosetta stone of this evolution. The origin and evolution of the MW is encoded in the motion and chemical composition of stars of different ages. In particular, the MW halo contains the oldest and most metal-poor stars observable, which were born at times, or equivalent redshifts, still out of reach for the deepest surveys of primordial galaxies. These stars retain the memory of the unique nucleosynthesis in the First Stars, as revealed by their striking abundance patterns observed at very low metallicities (Chiappini et al. 2006). A serious obstacle to discriminate between different scenarios of formation and evolution of the Galaxy components (halo, thin and thick disk and bulge) is the difficulty of measuring distances and more importantly ages for individual field stars. Crucial ingredients to study evolutionary processes in the disk are, e.g., the age-metallicity and age-velocity dispersion relations for different directions and at different galactic radii and heights from the plane.

Even if not completely free from stellar modelling, the mass of a red giant star, given its evolution rate, is a good proxy of its age. In addition, oscillation spectra also allow one to distinguish between H-shell burning and central He-burning phases (Bedding et al. 2011, Mosser et al. 2011). So, once the chemical composition is known, asteroseismology can provide stellar ages within a 15% uncertainty, while classical methods such as isochrones may be uncertain by a factor two. Using seismic data from CoRoT and Kepler, Miglio et al. (2012b, 2013) showed that pulsating red giants can efficiently be used to map and date the Galactic disc in the regions probed by the observations (Figure 2.11). Note that given the high intrinsic luminosity of red

giants compared to dwarfs, these data allow us to see quite far in the Galaxy, up to about 10 kpc, whereas Hipparcos precise parallaxes are available only up to 100 pc. The capability of seismic data to derive individual stellar ages indicates a clear vertical gradient in the ages of disc red giants. These results show the enormous potential of red giant seismology with PLATO, which will not be limited to pencil-beam surveys as is the case for CoRoT and Kepler.

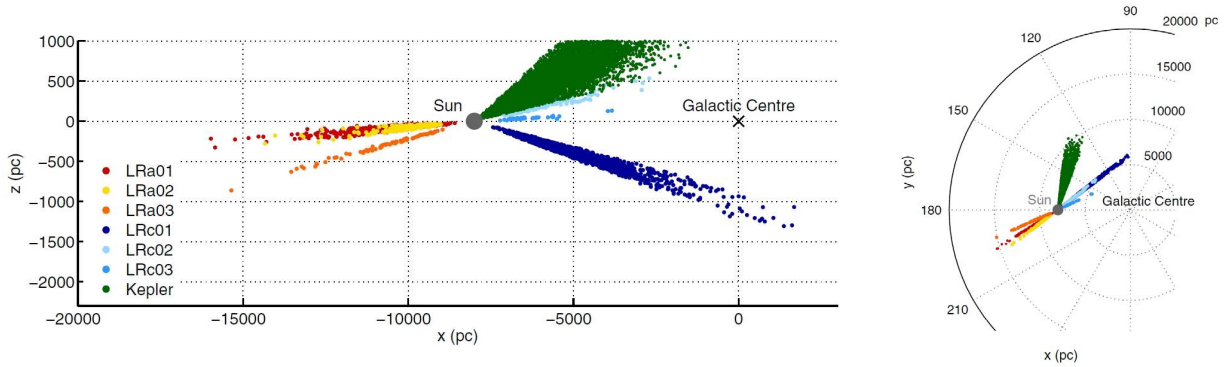

Figure 2.11: Distribution on the galactic plane of the red giants with asteroseismic characterisation from the light curves obtained in the CoRoT exofield for six long runs: LRa01 (red), LRa02 (yellow), LRa03 (orange), LRc01 (blue), LRc02 (green), LRc03 (cyan). From Miglio et al. (2012b).

The European Gaia satellite will create a 3-D map of stars throughout our Galaxy, hence providing an observational test bench to theoretical predictions on the origin, structure and evolutionary history of our Galaxy. Additional crucial information both, on velocities and chemical abundances, will come even earlier from several on-going/planned spectroscopic surveys such as SEGUE-2, APOGEE and the Gaia-ESO surveys.

The combination of chemical compositions from spectroscopic surveys with distances from Gaia and ages from seismic data, as provided by PLATO for large samples of stars, will allow us to comprehensively study chemical gradients and their time evolution in different directions. It will provide information on the metallicity distribution of thick and thin disk stars at different positions in the galaxy, and their time evolution. In addition, the evolution of the stellar velocity dispersions in the disk can be studied. All of these crucial constraints will allow us to quantify the importance of stellar radial migration in the formation of the Milky Way, otherwise difficult to quantify from first principles. This will represent invaluable information not only for the formation of the Milky Way, but also for the formation of spiral galaxies in general.

2.3.4 Stellar activity and flaring

Starspots dim the star when they transit across the surface, allowing us to determine the surface rotation rate and even the surface differential rotation. While the fixed pointing of CoRoT and Kepler limited their stellar diversity, PLATO will give a full picture of the evolution of angular momentum loss among different populations of stars. PLATO will be able to provide both: precise ages from asteroseismology and rotation periods from the analysis of light curves.

The study of stellar activity by PLATO will allow us to:

- calibrate the stellar age-rotation relationship (gyrochronology: e.g., Barnes 2007);
- study magnetic activity cycles and constrain stellar dynamo models;
- perform stellar coronal seismology.

2.3.5 Accretion physics near compact objects

Accretion phenomena in compact binaries, such as cataclysmic variables or X-ray binaries (XRBs), display variability on a range of timescales, involving both the orbital and spin periods of the components. In such systems, the secondary transfers material to the primary, which is either a white dwarf, a neutron star or a black hole. XRBs show variability due to accretion ranging from milliseconds to hours, while the time scales for cataclysmic variables are in the range from minutes to days.

PLATO's wide field and cadence of 25 and 2.5 seconds for normal and fast telescopes, respectively, is well suited to shed new light on the physical processes involved in disc accretion of compact objects, by studying a sample of carefully selected cataclysmic variables and XRBs with m_V below, say, 16.

2.3.6 Classical pulsators

PLATO will obtain high-precision photometric light curves for classical pulsators. Besides making significant progress in essentially all areas of pulsating stars. The availability of accurate asteroseismological measurements and radial mode pulsational period estimates, combined with a detailed evolutionary framework could be of pivotal importance in order to shed light on the explanation of different pulsation mechanisms and problems with them.

The precision of the PLATO data and the expected number of β Cephei stars may also be key to understand their pulsational properties by the analysis of the splitting asymmetries, as well as the internal rotation profile. For those stars the convective core is expected to rotate between 3 and 5 times faster than the surface (Dziembowski & Pamyatnykh 2008; Suárez et al. 2009). The study of Cepheids and RR Lyrae stars will benefit greatly from the large number of PLATO targets. A rough estimate gives 550 (730) Cepheids (of both classical and Type II) down to 13th (15th) magnitude compared to about a half dozen observed with CoRoT, and only one well documented case in the Kepler field (Szabó et al. 2011). The improvement is similarly large for RR Lyrae stars: the current design and observing strategy of PLATO promises the observation of at least 800 (3600) of such stars down to the 13th (15th) magnitude limit, as opposed to ~30 and ~50 found in CoRoT and Kepler fields respectively. These calculations used the GCVS catalogue (Samus et al. 2012) and neglected the results of recent all-sky surveys, and therefore these numbers should be regarded as lower limits.

In summary, PLATO will reveal significantly more features of classical pulsators that will lead to a better understanding of the underlying physical processes and their influences on stellar evolution.

2.3.7 Classical eclipsing binaries, beaming binaries and low-mass stellar and sub-stellar companions

PLATO will provide the opportunity to significantly increase the samples of binaries and sub-stellar companions studied in the following areas:

- Classical eclipsing binaries as observational tests of stellar evolution models.
- Detect low-mass stellar companions via the so-called beaming effect.
- Measure the gravity darkening effect, related to the internal heat-distribution of stars via radial and meridional circulations (Rafert & Twigg 1980).
- Observe contact binaries to study the formation process, internal structure, acitvity and especially the final evolutionary stage of binary systems (Eggleton 2012; Csizmadia et al. 2004; Tran et al. 2013).

2.3.8 Additional complimentary science themes

Apart from the above short, non-exhaustive list of themes in stellar and galactic physics that PLATO is able to deal with, various additional subjects are within reach. Examples from stellar physics are common-envelope and Roche-Lobe overflow evolution of close binaries, tidal asteroseismology, mass-loss and structure of stars rotating at critical velocity. On top of this, PLATO can address a number of science topics in different areas of planetary, stellar and galactic physics. Topics discussed for further investigations using PLATO are, e.g., transiting phenomena such as super-novae, GRBs, or even microlensing searches for black

holes (Griest et al. 2013), as well as Kuiper-belt and Oort clouds objects in our Solar System. PLATO will also make precision measurements on a small well-selected sample of compact objects – both galactic and extragalactic, where the high cadence and precision will benefit the interpretation of poorly understood phenomena.

2.3.9 PLATO's long-term legacy

The PLATO catalogue of thousands of characterised planets and of about 1,000,000 stellar light curves will provide the fundament for a huge long-lasting legacy programme for the science community. Planets, around bright stars, detected and characterised by PLATO will be a rich input catalogue for spectroscopic studies to investigate their atmospheres and link them with the planetary bulk properties. Observing further transits of large planets around suitably bright objects from the ground over long periods, well beyond the mission lifetime, will allow searching for planets or exomoons by TTVs and Transit Duration Variations (TDVs) over a very long time baseline. During the PLATO mission lifetime, RV follow-up to determine planet masses will focus on the scientifically most interesting targets. However, science interests develop with time and there is always room for surprising discoveries. Planet candidates detected by PLATO, but not confirmed by RV within the mission lifetime, will provide a wealth of targets for future mass determinations by the science community, resulting in thousands of further characterised planets.

The PLATO catalogue of about 85,000 stars with known ages and of about 1,000,000 highly accurate photometric stellar light curves complements the results of the Gaia mission and will provide a huge legacy for stellar and galactic science, which will be explored by the community in the years to come after the PLATO mission.

2.4 PLATO follow-up observations

The prime science product of PLATO consists of a sample of fully characterised planets of various masses, sizes, temperatures, and ages, with a special emphasis on terrestrial planets in the habitable zone of their parent stars. To reach this ambitious goal, a ground-based support is absolutely required, mostly for the follow-up of planetary system candidates.

The role of the follow-up is multiple. We first need to discard false positive configurations leading to photometric signatures similar to the ones induced by planetary transits. Then, complementary observations provide information on the planet properties not available from the light curves, the most important among them being the planet masses derived from radial velocities. The most efficient transit surveys on the ground still have 5 to 10 times more false positives than real planets in their candidate list. From the Kepler experience, we are learning that this ratio seems to get more favourable in space with high quality photometric data (Morton and Johnson 2011, Santerne et al. 2013), but the number of false positives will nevertheless be non-negligible. The final performance of the PLATO space-based transit mission is thus ultimately determined by the associated follow-up capabilities. It is therefore particularly important to include these considerations in the planning of the mission. An important part of the preparatory work includes estimates of the expected planet yield and false-positive rate in order to plan and organize in an optimum way the ground-based telescope observations.

2.4.1 False-positive estimation

The first step of planet detection is to separate false alarms from real planet signals. False alarms can be caused by e.g., stellar spots or by diluted signals from eclipsing binaries within the large pixel scale of PLATO. Many causes of false alarms can be identified already from close inspection of the stellar light curve. Taking advantage of the expertise gained with the successful ground-based transit search surveys, and with the CoRoT and Kepler space missions, a battery of diagnostics has been developed to detect some of the most common false positive configurations directly from the photometric observations. The light curves undergo several checks, e.g., for out-of-transit photometric variations (ellipsoidal variation, beaming effect) as found for binary stars, a check for adequate transit and occultation depth and duration consistent with a planet-sized object, and most importantly from a pre-spectroscopic validation procedure providing a reliable probability that the signal is of planetary nature.

Such a planet *validation* approach consists in comparing the relative capabilities of these blend scenarios and of the transiting planet scenario to explain the available data. For space-based surveys, which explore the small-size planetary domain, the so-called "Blender" (Torres et al. 2011) and "PASTIS" (Almenara et al. 2012) software perform this procedure. They combine a detailed analysis of the transit light curve with a statistical study of the stellar background (or foreground) population, which may mimic the planetary signal. One of the key pieces of information in this procedure is the measurement of the transit signal at different wavelengths, especially in the infrared, which constrains the colour difference between the target and the potential false-positive system. This procedure has been successfully applied to several Kepler and CoRoT cases (Fressin et al. 2012a,b; Moutou et al. 2013), but its performance is severely limited if the transit is observed in only one wavelength. The exquisite photometric precision of PLATO and the simultaneous observations with the two fast cameras, which will observe in different photometric bands, will allow for a first-order rejection of potential blend scenarios with the planet-validation analysis.

Many false alarms can already be rejected in this way before putting planet candidates on the observational follow-up list. These analysis methods help to separate planetary candidates from binary stars or intrinsic stellar brightness variations, such as the one caused by spots, give confidence in the planetary nature of the detected object, and provide an upper limit to the planetary mass. The expected rate of remaining false positives should then be determined in order to estimate the need of ground-based follow-up required on top of planet characterisation. For the CoRoT space mission, the false-positive rate, estimated from the follow-up effort made during the past years, is up to 70% (Moutou et al. 2009; Cabrera et al. 2009). For the Kepler space mission, the false-positive rate is estimated around 11% for small-size planets (Morton and Johnson 2011, Santerne et al. 2013). The main difference with CoRoT comes from the capability of Kepler to determine the relative position of the image centroid during and outside of the transit epoch (Bryson et al. 2011) as will also be done by PLATO. We may then reasonably assume that the rate of false- positives among PLATO candidates will be less than 15%.

In addition, it is important to obtain high spatial resolution imaging of the planetary transit hosts to exclude contaminating objects in the PLATO PSF, and to verify that the transit is indeed observed from the target star. This is especially crucial for shallow transits that are candidates for the most interesting terrestrial planets that are also the more demanding in RV follow-up time.

2.4.2 Optimisation of the radial velocity follow-up

The planet minimum mass estimated from Doppler measurements is directly proportional to the amplitude of the reflex motion of the primary star. The characterisation of the lowest possible mass planets detected with PLATO will then be intimately linked to the ultimate long-term precision achieved on the radial velocity (RV) measurements of the star.

2.4.2.1 Limitations to precise radial velocity follow-up measurements

Looking for the highest RV precision, several sources of uncertainty have to be considered. They can be classified into several broad categories: photon count, technical, and astrophysical. Each of these sources is essentially independent from the others and thus the actual precision eventually obtained on the measurements will be a quadratic combination of the different contributions.

Instrumental requirements: The exciting results obtained with the HARPS spectrograph (ESO, Chile), and its twin at the TNG (La Palma, Spain) in operation since May 2012, have motivated new studies to push down the limits of Doppler spectroscopy. These instruments demonstrate sub-m/s long-term RV precision (typically 80 cm/s for published planetary systems). From the instrumental perspective, reaching a precision level of a few cm/s should be possible with especially-designed spectrographs, provided that special care is applied to some aspects (Pepe & Lovis 2008): spectrograph stability, high spectral resolution to resolve the spectral lines, adequate sampling, precise wavelength reference, efficient image scrambling, and precise guiding and centring. The ESO ESPRESSO/VLT project materializes the efforts in this direction. New spectrographs designed according to the requirements set for high-precision RV's and pushing in the IR domain are also in development. For example, the two Spirou/CFHT and Carmenes/Calar-Alto projects are proceeding now with a secured budget and should become operational on sky within a few years.

Photon noise: The uncertainty on the RV's associated with photon noise roughly scales with the measurement signal-to-noise ratio (S/N) of the spectra, i.e. with the square root of the flux, or also with the

telescope diameter. With HARPS, a photon noise level of 1 m/s is achieved in 1 min for a m_V = 7 K dwarf. This precision corresponds to an exposure time of close to 4 hours for a m_V = 13 star. Assuming a similar spectral window (0.38 − 0.68 μm), considering an expected efficiency about 4 times better for ESPRESSO (from phase A study), and taking into account the difference in collecting areas, we estimate that with ESPRESSO on the VLT we will reach 10 cm/s in 15 min for a m_V = 8 star, or 20 cm/s in 1 hour for a m_V = 11 star. These estimates demonstrate the need for bright stars and large collecting areas when considering the radial velocity follow- up of very low-mass planet candidates.

Contamination effects: the contamination of the target spectrum by an external source is also a potential limitation for the precision of the RV measurements. The most disturbing cases are the light from a close-by object and the Moonlight. The light of faint objects close to the science target may fall on the spectrograph fibre and contaminate the science target spectrum. This is in particular the case for transit false-positive detections due to triple-star blends. High-resolution, high-contrast follow-up observations with instruments equipped with AO capabilities will be required to point out visible companions of any magnitude close to the science target. In the same way, we have to avoid as much as possible that direct or indirect sunlight reaches the detector with a contrast magnitude compared to the science target smaller than ~ 8−10 for the highest RV precision.

Stellar jitter: Besides instrumental, environmental, and photon-noise limitations, other phenomena intrinsic to stellar atmospheres, often called “stellar noise” or “stellar jitter”, have to be taken into account. They cover different timescale intervals depending on their origin.

i) *p-mode oscillations:* Solar-like oscillations induced in stars with convective envelopes have typical periods of a few minutes in solar-type stars and amplitudes per mode of a few tens of cm/s in radial velocity (Kjeldsen et al. 2005). The observed integrated signal is the superposition of a large number of these modes, possibly adding up to several m/s. Amplitudes of the RV variation become larger for early-type and evolved stars.

ii) *Granulation and super-granulation:* Granulation is the photospheric signature of the large-scale convective motions in the outer layers of stars with convective envelopes. The granulation pattern is made of a large number of cells with upward and downward motions tracing hot matter coming from deeper layers and matter having cooled down at the surface. On the Sun, the typical velocities of these convective motions are 1-2 km/s in the vertical direction. However, the large number of granules on the visible stellar surface efficiently averages out these velocity fields, leaving some remaining jitter at the m/s level for the Sun, probably less for K dwarfs (e.g., Palle et al. 1995; Dravins 1990). The timescale for granule evolution is about 10 minutes for the Sun. On timescales of several hours, evolution of larger convective structures in the photosphere may induce additional stellar noise, similar in amplitude to granulation itself (meso- and super-granulation).

iii) *Magnetic activity:* Magnetic phenomena at the surface of dwarf stars induce radial-velocity variations through the temporal and spatial evolution of spots, plages, and convective inhomogeneities (Saar & Donahue 1997; Saar et al. 1998). Induced variations in the spectral line asymmetry are modulated by the rotational period of the star and can mimic a planetary signal (e.g., Queloz et al. 2001; Bonfils et al. 2007) or potentially inhibit the detection of planetary signals of low amplitude. Granulation is also damped within the spots, changing for spotted stars the balance of granulation effect over the surface. Stellar jitter depends on effective temperature, stellar activity, and projected rotational velocity (e.g., Wright et al. 2004). Typical values are below 1 m/s for slowly rotating, quiet G-K dwarfs (Mayor et al. 2009). To quantify the activity level of their targets, Doppler planet searches traditionally use the log(R’HK) indicator representing the fraction of a star’s bolometric flux emitted by the chromosphere in the Ca II H & K lines (Noyes et al. 1984). The bottom level of the stellar-induced velocity jitter for the quietest stars is not known yet.

iv) *Magnetic cycles:* Longer-term changes in the spot coverage of the stellar surface (over several years), often referred to as the star magnetic cycle (11-year cycle for the Sun), are also inducing a slow low-amplitude variation of the observed RV’s. This effect can fortunately be tracked and corrected with activity-indicator monitoring (as e.g., the log(R’HK); Lovis et al. 2011).

2.4.2.2 Stellar intrinsic variation and optimal observing strategy

Although stellar noise is a major limitation on very high precision Doppler measurements, adequate observing strategies help diminish its effect. The strategy adopted to minimise the stellar oscillation noise consists of integrating over a few typical oscillation periods. Estimates based on HARPS observations and asteroseismology models show that, for quiet stars, an exposure time of 15 minutes is sufficient to average out the "perturbing" signal well below 1 m/s, and the noise even gets down below 10 cm/s in about 20-30 minutes. On intermediate and long timescales, Doppler measurements are affected by stellar granulation and stellar activity. A strategy aiming at statistically averaging the perturbing effects is possible with enough observations covering a span larger than the typical timescale of the effects (hours to stellar rotation periods).

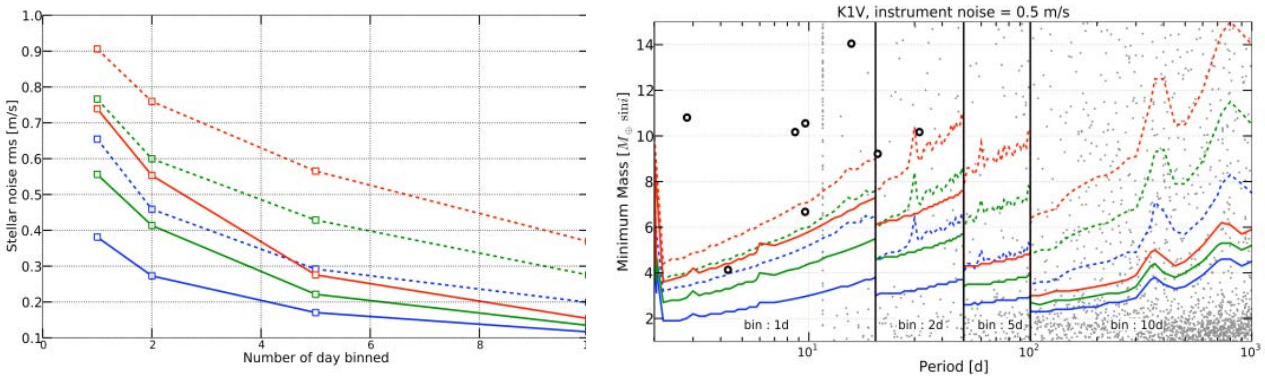

Figure 2.12: Left: Estimate of stellar noise effect on RV rms as a function of the binning of the measurements, for Alpha Cen B (K1V). The 2 types of lines correspond to different observing strategies: dashed for the typical strategy used for the HARPS high-precision programs (1 measure per night of 15 minutes, on 10 consecutive nights each month); solid lines for a more efficient strategy with 3 measures per night of 10 minutes each, 2 hours apart, every 3 nights. The different colours correspond to different stellar activity levels (blue for log(R'HK)=−5.0, green for log(R'HK)=−4.9, and red for log(R'HK)=−4.8). Right: Corresponding limits of planet mass detection as a function of orbital period derived from Monte-Carlo simulations. The open circles represent small-mass planets found with HARPS around G and K dwarfs, and the lighter dots correspond to the expected planets from the Bern population synthesis models (Mordasini et al. 2009). Lines and colours have the same meaning as for the left panel. The diagram is separated in 4 period regimes, each one using a different binning, well adapted to the corresponding period range.

Simulations of synthetic observations including stellar effects on RV measurements have been performed in order to quantify the amount of measurements required to reach a given level of precision, taking into account oscillations, granulations and activity-related effects (Dumusque et al. 2011a, 2011b). The observed combined effect of the different stellar noises is presented in Figure 2.12 for Alpha Cen B (K1V), for different activity levels and observing strategies. The obtained improvement of the measured RV rms is very encouraging and demonstrates the pertinence of the approach. Proceeding in this way, an equivalent precision of 35 cm/s has already been obtained on the 3-Neptune host HD 69830 (Lovis et al. 2006). Very interesting detection limits are obtained in the case of a realistic observing strategy (optimised precision versus cost in observation time) consisting in a set of three 10-minutes observations, individually separated by 2 hours, every 3 nights. A binning over several days can then be applied when looking for longer period planets (Figure 2.12, right). The interesting point to note here is that, for a given planet mass, the detection limit is weakly depending on the period. Indeed, the lower amplitude of the signal is then compensated by the larger temporal bins considered for the average. The estimated yield of the PLATO survey is using results of these simulations to realistically take into account limitations set by stellar noise for the radial velocity follow-up. Over the past few years, 10 quiet stars have been monitored with HARPS following the proposed optimum strategy. Half of them are already found to host planetary systems (Pepe et al. 2011), including two planets with detected RV amplitudes in the 50 to 90 cm/s range. A third system, HD 192310 (K3V), hosts a Neptune beyond the habitable zone of the star (P = 526 d), demonstrating the efficiency of the approach for the characterisation of PLATO low-mass candidates. These early results are still including HARPS instrumental limitations (with centring and guiding effects) and a contribution from photon noise. Improvements are then expected with more stable instruments as ESPRESSO/VLT and longer exposure

times to better average the stellar oscillations. Another promising approach to characterise stellar noise will be to simultaneously monitor activity indicators at the same time as the velocity observations and use correlation between them to correct the velocity from the stellar intrinsic contribution. Studies are being conducted in this direction using photometric, activity indicators, and line-shape measurements (Lovis et al. 2011).

2.4.3 Organisation of the follow-up

The main aspect of the ground-based follow-up of PLATO transit candidates will reside in the basic planet characterisation through radial velocity measurements. As seen in previous paragraphs, the same level of precision cannot be reached for all stars due to various sources of stellar intrinsic limitations: spectral type, luminosity class, activity level, star brightness. In particular, photon-noise limitations and activity-related jitter require a large amount of telescope time in order to detect the lower-mass planets.

False positives related to stellar diluted blends will usually not display large radial velocity variations. Due to the PLATO large pixel size on the sky, the situation will appear often. It is thus important to point out these cases before spending expensive time on large telescopes. As mentioned previously, many cases will be discarded from the light curve analysis. For the remaining cases, it will be important to check that the low-depth transit is not due to a deeper eclipse of a fainter star very close to the primary target. This can be achieved at higher spatial resolution, checking for transits on the neighbouring stars. The radial velocity follow-up coupled with the high-angular confirmation that the transit is indeed taking place on the primary target should be sufficient to safely characterise the planet candidates.

Due to the number of expected PLATO candidates, a systematic observation of all detected transits with large telescopes will be unfeasible and an optimised follow-up scheme has to be organised. Facilities of given precision should be mainly used for the characterisation of planets accessible to that precision. In practice for the characterisation follow-up, a multi-step approach going from moderate- to high-precision instruments is already successfully used in most of the on-going surveys. It will also nicely apply to PLATO candidates. It is sketched in Figure 2.13.

1. The candidate list has to be cleaned as much as possible from false positives by diagnoses applied directly on the high-precision light curves, as described above.
2. Small telescopes will be used for a first screening of the remaining transit candidates, rapidly discarding unrecognised binaries from the list. As PLATO prime targets consist of bright stars, low- to intermediate-precision instruments (similar to FEROS on the ESO 2.2-m telescope, or CORALIE on the 1.2m Swiss telescope at La Silla) will be perfectly suited for this part of the follow-up.
3. Given that the host star's brightness and activity level will define the expected ultimately achievable radial velocity precision, this will dictate which telescope + spectrograph facility has to be used for the planet characterisation.
4. HARPS on the ESO 3.6-m telescope at La Silla, HARPS-N on the Italian TNG at La Palma, SOPHIE on the 1.93-m telescope at OHP, or similar instruments in development (Spirou/CFHT, Carmenes/Calar-Alto) will be the working horses for planets with masses down to the super-Earth regime not too far from their central stars, as well as for the most active part of the sample (anyway limited by stellar noise to a level comparable to the instrument precision).
5. Finally, the most interesting and demanding lower-mass, longer-period planets will require the best possible radial velocity precision that should be available with ESPRESSO on the VLT (on the sky in 2017) and possibly with future super-stable spectrograph on the ELTs.

Even with a rigorous pre-selection of planetary candidates, a significant amount of telescope time will be required for PLATO follow-up. Efforts will therefore concentrate on the most interesting prime targets, leaving cases like e.g., 'hot-Jupiter candidates' as a legacy for the community to study over a longer future time period, depending on science interest. In priority it is planned to concentrate on low-mass planets at large orbital separations, but it is also assumed that several hundred/thousands of low-mass planets with short periods will be followed-up with high precision. It is furthermore assumed that 20 observations per planet are adequate to characterize the candidates. With these assumptions for a follow-up over the 6-year mission lifetime, the required observing time for the RV follow-up is approximately 50 nights/year for

several 1-2m and three 4m-class telescopes, and up to 40 nights/year on one 8m-class telescope (ESA/SRE(2011)13). Such follow-up effort would provide on the order of 1500 accurately characterised Earths to super-Earths on short to medium period orbits and long period gas giants, and about 100 terrestrial planets out to 1 au. The real number of confirmed planets with highly accurate RV mass measurements will depend on the actual telescope time invested. We only provide a conservative estimate here. Clearly, further developments of data analysis procedures as well as the availability of smaller telescopes will be important to identify potential false alarm scenarios early in the analysis and thereby limit the number of candidates which go to high-precision RV follow-up. Also, we strongly emphasize that follow-up for interesting targets will continue as a legacy. Thus, if more telescope time is required to cover all interesting targets, this can, and likely will be, performed on a longer timescale after the end of the mission.

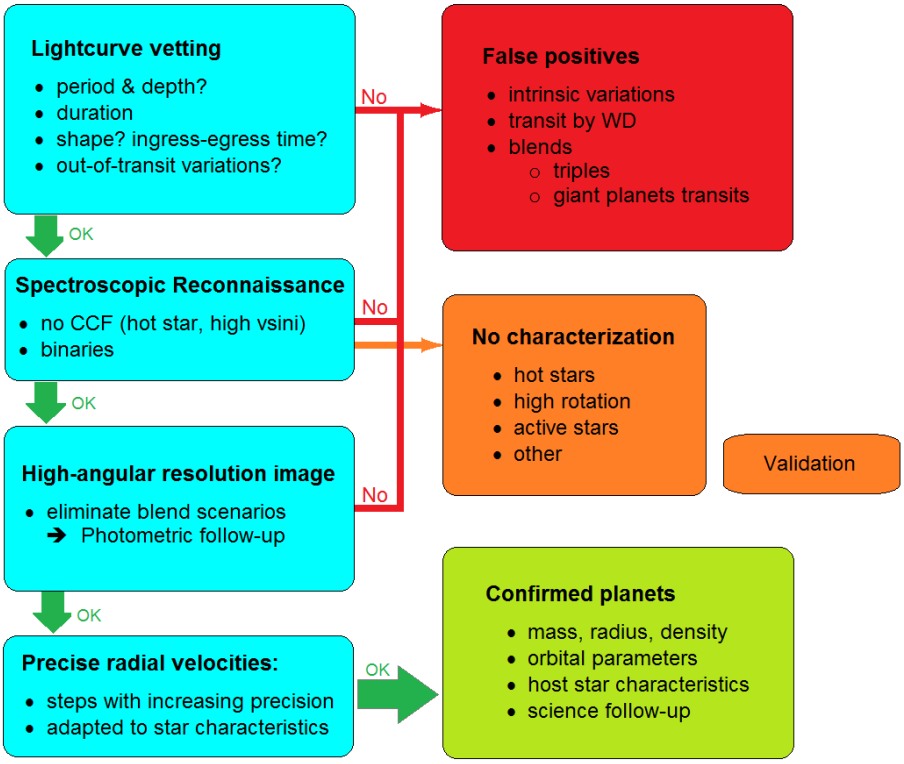

Figure 2.13: PLATO follow-up organisation describing the different steps making use, in an optimum way, of different observing facilities. WD is a White Dwarf, CCF is the Cross Correlation Function used in radial velocity (RV) observations, SB2 stands for double-line Spectroscopic Binary.

A very important but affordable (de Zeeuw, private communication) amount of telescope time will be required for the PLATO follow-up. It is the duty of the PLATO Consortium through its mission lead and follow-up scientist and/or of ESA to discuss with the institutes or organisations running the observing facilities about a scheme to secure the observing time required for the PLATO candidates. This has to be a global effort of the community, in the line of the open data property policy of ESA. It is worth noticing here, that a similar effort is already being discussed for the follow-up of the candidates provided by the TESS/NASA mission that will focusing on short-period planets orbiting bright low-mass stars. Such measurements can already be seen as an advanced PLATO follow-up effort.

3 Scientific requirements

The main scientific objective of PLATO is to detect and thoroughly characterise a very large number of exoplanetary systems, including both the exoplanets and their host stars. To achieve this goal PLATO will require monitoring the visible flux from a large number of bright stars, with very high accuracy, during a long time and with a high cadence. These light curves will show the signatures of planets transiting in front of their parent stars. The same light curves will allow us to measure the micro-variations in flux of these stars, which will be used to perform a seismic analysis of them. The exoplanet transits and the stellar seismic analysis will yield the fundamental physical parameters of the exoplanets and their stars with ultra-high precision. Combining the long uninterrupted high precision photometric monitoring from space with ground-based follow-up observations, such as high-resolution radial velocity spectroscopy, a full characterisation of the planetary systems will be obtained. The primary targets of PLATO are therefore stars that are sufficiently bright to allow both high photometric accuracy from space and precise follow-up measurements from ground to determine their mass. Additional ground-based high resolution spectroscopy will be used to confirm or measure the stellar fundamental parameters ($T_{\rm eff}$, $\log(g)$, chemical composition, rotation velocity, etc).

The knowledge of the planet orbital period, the planet/star radius ratio and the planet/star mass function, coupled to the measurement of the star's radius, mass and evolutionary state, will therefore allow us to derive the planets fundamental physical parameters (mass, radius, orbit, age). Additional ground- and space-based follow-up observations will also be obtained for the brightest targets providing information on the planet atmospheric composition and dynamics.

This chapter describes in detail the scientific high level requirements needed to achieve the objectives of the PLATO mission, including the stellar sample definition, the observation strategy and the required photometric accuracy. These are the basic requirements from which the lower level engineering requirements that define the design of the mission have been derived, leading to the payload concept described later in this report.

The depth of a planetary transit is given by the ratio of the areas of the planet and its transited star, which is of the order of $\Delta F_{\rm star}/F_{\rm star} \approx 10^{-4}$ in the case of Sun-Earth analogues, while transit durations are typically of the order of 12 hours. In order to detect such transits at more than 4σ, a dimensioning requirement, we need to obtain a photometric noise level lower than about 2.5×10^{-5} in 12 hours, i.e. about 8×10^{-5} in one hour. This is the minimum requirement for the detection of an Earth-like planet in front of a solar-like star.

However, the measurement of several points across the transits will be necessary, implying lower levels of noise. We therefore require a photometric noise level below 3.4×10^{-5} in one hour, for the highest priority star sample of the mission.

Results from CoRoT and Kepler have shown that detecting, measuring and identifying oscillation modes in solar type stars requires a noise level in amplitude Fourier space below about 2.0 ppm per $(\mu\text{Hz})^{1/2}$ (Michel et al. 2008; Deheuvels et al. 2010; García et al. 2009; Ballot et al. 2011), which is equivalent to 3.2 ppm in 5 days, or 1.3 ppm in 1 month, and which translates approximately into a noise level of 3.4×10^{-5} in 1 hour, i.e., similar to that for the detection and characterisation of Earth-like transits.

The duration of the observations needs to be longer than 2 (goal 3) years, so that at least 2 (goal 3) consecutive transits for Sun-Earth analogues can be detected. For the seismic analysis of the target stars, the total monitoring time must be sufficient to yield a relative precision of 10^{-4} for the measurement of individual mode frequencies, which is needed to perform the inversion of the oscillation spectra. For solar-type stars, this comes down to an absolute precision of 0.2 to 0.1 μHz, which translates into a minimum monitoring time of 5 months for a reasonable S/N of 10 in the power spectrum.

In the following sections we describe the specific requirements that define the PLATO mission.

3.1 PLATO light curves and additional products

R0a: PLATO must provide long, high duty cycle, high precision photometric time series in visible light of a large number of bright stars. The basic PLATO data products consist of the white-light curves with derived characteristics of the stellar samples specified by the requirements below (see R2 and R5).

R0b: In addition, it is required that part of the payload (e.g., a small subset of the telescopes or individual detectors if a multi-telescope concept is chosen) provides photometric time series in at least two separate broad bands (see R8). These will be used in particular to constrain the identification of the detected oscillation modes in bright classical pulsators.

R0c: PLATO must also provide relative astrometric measurements of the targets of the bright samples (defined in R2 below). These astrometric measurements will allow us to search for giant planets through the detection of the associated star wobble, and will also be used to identify false positives, due for instance to background eclipsing binaries. Astrometric measurements may also be used to evaluate a posteriori instrument jitter properties.

3.2 Surveyed fields

R1: Two long duration fields must be monitored in addition to step-and-stare phases, during which additional fields will be surveyed. During the step-and-stare phases, the instrument may also have to come back to the two fields observed during the two long monitoring phases. During the step-and-stare phase, the instrument must be capable of accessing other fields at any position in the sky, at a proper time for these observations to be feasible.

3.3 Stellar samples and corresponding photometric noise levels

Because the transit depth is inversely proportional to the square of the star's radius, transiting planets will be preferentially searched around the small radii cool dwarf stars, which indeed will be similar to our Sun. However, the stellar sample will be extended also to sub-giants, which have radii only slightly larger than dwarfs. The restriction to cool stars is also motivated by the need for subsequent radial velocity follow-up observations. Their spectra supply the large number of lines necessary to get very accurate radial velocity measurements, and are thus eminently suited for the programme. Consequently, the core star sample for the PLATO mission will consist of cool dwarf and sub giant stars that are bright enough for the photometric precision required for the detection of small planets, for seismic analysis and radial velocity follow-up to be reached.

R2: Five complementary stellar samples have been defined as targets of the PLATO mission, and are described below by order of priority.

P1: Given the probability to detect transits of planet in the habitable zone of solar-type stars, estimated to be about 0.1% (geometric probability × fraction of stars with such planets), we estimate that at least 20,000 cool dwarfs and sub-giants need to be surveyed for a sufficient amount of time to detect long period orbits (~1 year), i.e., typically for 2 to 3 years. This number of surveyed stars implies an expected number of characterised telluric planets in the habitable zone of G type stars of the order of 20, which we consider as the main objective for PLATO. Additionally, we would expect to detect many transits of larger planets and/or closer around these stars. Therefore, more than 20,000 dwarfs and sub-giants later than spectral type F5, with a noise level below 3.4×10^{-5} in 1 hour, must be observed with the required duty cycle for more than 2 (goal 3) years. This sample, with $8 \leq m_V \leq 11$, is the backbone of the PLATO mission, and is considered as the highest priority objective.

P2: The search for planetary transits around very bright and nearby stars presents a specific interest, as these sources will become privileged targets for further ground- and space-based observations. We therefore request the monitoring of a relatively large number of very bright stars with the goal of detecting a few telluric planets in their habitable zone. Hence, more than 1,000 dwarfs and sub-giants later than spectral type F5 and brighter than $m_V = 8$ must be monitored with a noise level below 3.4×10^{-5} in 1 hour, with the required duty cycle for more than 2 (goal 3) years.

P3: The detection of an even larger number of short period planets around such very bright stars will also be used as input for further instruments aimed at characterising their planetary atmospheres. Hence, more than 3,000 dwarfs and sub-giants later than spectral type F5 and brighter than $m_V = 8$ must be monitored with a noise level below 3.4×10^{-5} in 1 hour, with the required duty cycle for more than 2 months. The P3 sample is an extension of the P2 sample, i.e., P2 sample is included in P3 sample.

P4: Due to the specific interest of investigating planets around cool dwarfs, an additional sample of more than 5,000 cool dwarfs brighter than $m_V = 16$ must be monitored with a noise level better than 8.0×10^{-4} in 1 hour, with the required duty cycle for more than 2 (goal 3) years. In addition, an equivalent number of such cool dwarfs must be monitored during the step-and-stare phase of the mission, with the same noise and duty cycle characteristics.

P5: Finally, to increase the statistics we need to observe a very large number of stars with the required precision to detect telluric planets around solar-type stars, i.e., 8×10^{-5} in 1 hour, even if accurate seismic analysis will not be available. For these detections, we will rely on other, less precise and less reliable techniques to assess the mass and age of the host stars. These other methods, e.g., based on a correlation of stellar rotation with age, will likely be improved by a proper calibration using the seismological measurements of the P1 sample. The minimum number of such stars required to get a statistically significant result is around 245,000, out of which we expect several hundred transits from telluric planets. As for the first sample we would also expect many more larger transiting planets. Hence, more than 245,000 dwarfs and sub-giants later than spectral type F5, with a noise level below 8×10^{-5} in 1 hour, with m_V typically between 8 and 13, must be observed with the required duty cycle for more than 2 (goal 3) years.

The above noise levels are specified as corresponding to photon noise only. With the addition of requirement R6b below, ensuring that the measurements remain photon-noise limited, similar noise levels are expected when taking into account all sources of noise.

3.4 Duration of monitoring

R3a & b: The total duration of the monitoring of the long-duration fields must be longer than 2 (goal 3) years.

R3c: The step-and-stare phases at the end of the mission must have a duration of at least 1 (goal 2) year in total. During this phase, previously monitored fields, as well as additional fields, will be surveyed for at least 2 months and up to 5 months each. In addition, further visits to the previously surveyed fields will be organised in an optimised way to study long period exoplanets (several years), whose transits could occur at any time during the step-and-stare phase.

3.5 Time sampling

The duration Δt_{tr} of a transit of a planet with semi-major axis a and orbital period P in front of a star with radius R_{star} is given by $\Delta t_{tr} = P\ R_{star}\ /(a/\pi)$. For true Earth analogues Δt_{tr} = 13 hours. More generally, the duration of a transit around a single star may last from about 2 hours (a “hot giant'” planet around a low-mass star) to over one day, for planets on Jupiter-like orbits (5 au distance). Planets in the habitable zone, however, will cause transits lasting between 5 hours (around M stars) and 15 hours (for F stars), for equatorial transits.

Because individual transits have durations longer than 2 hours, a time sampling of about 10 to 15 minutes is in principle sufficient to detect all types of transits, as well as to measure transit durations and periods. However, a higher time resolution is needed for an accurate time ingress and egress of the planet transits for which the S/N in the light curve is sufficient. The accurate timing will allow us to detect third bodies, which cause offsets in transit times of a few seconds to minutes, and will allow us to solve ambiguities among possible transit configurations through the determination of ingress and egress times of the planet. In practice, a time sampling of about 50 sec will be necessary to analyse in such detail the detected transits.

The needed time sampling for the asteroseismology objectives can be derived directly from the frequency interval we need to explore, which is from 0.02 to 10 mHz. In order to reach 10 mHz, the time sampling must correspond to at least twice this frequency, i.e. of the order of 50 s.

R4a: The sampling time for intensity measurements of stellar samples P1, P2 and P3 must be shorter than 50 s.

R4b & c: The sampling time for intensity measurements of stellar sample P4 & P5 must be shorter than 10 min, and shorter than 50 s after a first transit detection, for a precise timing of further transits.

R4d: The sampling time for relative astrometric measurements of stellar samples P1, P2, P3, must be shorter than 10 min, and shorter than 50 s after a first transit detection. Astrometric measurements with a time sampling of 50 s are also required for samples P4 and P5 after a first transit detection.

3.6 Photon noise versus non-photonic noise

R6a: The photon flux of the target stars must be sufficiently high to ensure that photon noise allows achieving the photometric noise requirements.

R6b: All other sources of noise must remain at least 3 times below that of the photon noise, at least for stars of sample P1, in the frequency range 0.02−10 mHz. Downward of 0.02 mHz, the non-photonic noise level is allowed to rise gradually, to reach a maximum of 50 ppm per $(\mu Hz)^{1/2}$ in Fourier amplitude space at a frequency of 3 μHz, for stars with $m_V = 11$.

3.7 Overall duty cycle

The probability that N successive transits of the same planet are observed is given by $p_N = d_f^N$, where d_f is the fractional duty cycle of the instrument. In order to achieve an 80% probability that all transits of a three transit sequence are observed, a duty cycle of 93% is needed, ignoring gaps that are much shorter than individual transits. The requirement for planet-finding is therefore that gaps which are longer than a few tens of minutes do not occur over more than 7% of the time, with a loss by gaps as small as 5% being desirable.

A similar requirement is also imposed for seismology. Gaps in the data produce side lobes in the power spectrum, which make mode identification ambiguous. Periodic gaps in the data must be minimised, as they will produce the most severe side lobes in the power spectra. It can be shown that periodic outages representing 5% of the total time produce aliases with a power of about 1.5% of that of the real signal. Such side lobes are just acceptable, as they will remain within the noise for most of the stars observed. It is therefore required that periodic data gaps are below 5%.

Non-periodic interruptions have a less catastrophic influence on the power spectrum, and can therefore be tolerated at a higher level, provided the time lost is compensated by a longer elapsed time for the observation. Random gaps in the data representing a total of 10% of the monitoring time yield side lobes with a power lower than 1% of that of the real signal, which will be adequate for this mission. The requirement on random data gaps is therefore that they do not exceed 10% of the elapsed time.

R7a: Gaps longer than 10 minutes must represent less than 7% (goal 5%) of the total observing time per target, for the longest possible observation period (3 years).

R7b: Periodic gaps of any duration must represent less than 5% (goal 3%) of the total observing time, and less than 2% at any given frequency in Fourier space, over periods of 5 months.

R7c: The total amount of gaps, periodic or non-periodic, of any duration, must represent less than 10% (goal 5%) of the total observing time over periods of 5 months.

3.8 Colour information

In addition to the measurement of oscillation frequencies, asteroseismology requires the identification (ℓ,m) of the detected modes. Knowing the ℓ identification for the dominant modes of each of the bright target stars of PLATO implies a significant reduction of the free parameter space of stellar models, and is a requirement to guarantee successful seismic inference of their interior structure parameters and ages. For oscillations in the asymptotic frequency regime, the derivation of frequency spacing's is enough to identify the modes. For most main-sequence stars excited by the κ mechanism, when the modes do not follow particular frequency patterns, the identification of ℓ can be achieved by exploiting the difference in amplitude and phase of the mode at different wavelengths. Therefore, some degree of colour information must be present in the PLATO data.

R8: Part of the payload must provide photometric time series in at least two separate broad bands (see R0b). At least two of the telescopes, or a dedicated subset of individual detectors, must provide photometric monitoring in at least two separate broad bands (one band per telescope). The photometric bands must be maximally separated, in such a way that the photon flux integrated in the common wavelength range

represents less than 10% of the total photon flux. Less than 50% of the photons are allowed to be lost due to this broadband photometry.

3.9 The need to go to space

The science goals of PLATO require the detection and characterisation of a very large number of planetary transits, as well as the seismic analysis of their host stars. As explained above, this requires very high precision, very long duration and high duty cycle photometric monitoring, which cannot be done from the ground. The Earth's atmosphere causes indeed strong disturbances that limit the achievable performance to milli-magnitude accuracies, mostly through scintillation noise. The small amplitude of the photometric dips caused by terrestrial planets is therefore beyond the range of ground-based observations.

Alternative techniques can be used from the ground to detect new exoplanets, and this field has seen tremendous progress in recent years. The most efficient of these relies on radial velocity measurements, performed by high resolution spectroscopy. The most severe drawback of the radial velocity technique is that the resulting mass determination suffers from the sin *i* ambiguity, except in the rare cases where the inclination angle *i* can be estimated. Photometric transit techniques are the only ones that can overcome this difficulty. In addition, long, uninterrupted observations, that only space-based instruments can provide, are necessary to optimise the probability of transit detection, as well as to avoid side lobes in stellar oscillation power spectra. Achieving a high duty cycle ($\geq$ 95%) is very difficult from ground, even if a network of multiple telescopes, or a powerful observatory in Antarctica, would be available. Space is therefore necessary to achieve the goals of PLATO, on one hand because of its stability and the absence of photometric disturbances, and on the other hand because it offers the possibility to perform the long, uninterrupted observations that are needed to detect and bulk characterise exoplanets and to perform seismic analysis of their host stars.

3.10 PLATO target and field selection

Telemetry limitations impose the pre-selection of PLATO targets for the detection of planets. The optimal field selection is closely related to the target selection. The success of the mission is related to our ability to select fields that maximise the number of F5 or later spectral type dwarfs and sub-giants for which we can have photometry with the required S/N, i.e., fields in which P1 to P5 targets are maximised. We need to prepare a PLATO input catalogue (PIC) which includes P1-P5 targets, and provide their main parameters.

A limited number of additional targets may be added to the PIC, to monitor special objects (e.g., in star formation regions or star clusters within the long monitoring fields) for the main and complementary science.

Finally, the PIC will help us to assess the nature of the detected transiting bodies: a good knowledge of the host star will help us to exclude false alarms and will trigger the most appropriate follow up strategy. It will also allow us to get a first estimate of the size of the planet.

The PIC will serve to: 1) finally select the optimal PLATO fields; 2) select all appropriate >F5 dwarf and sub-giants within them (samples P1 – P5); 3) characterise as much as possible the selected targets, i.e., estimate their temperature, gravity, variability, metallicity, binarity, chromospheric activity; 4) provide a list of neighbours that contaminate the target star flux; 5) give a first estimate of the transit object radius; 6) optimise the follow-up strategy.

Pre-launch characterisation of PLATO targets will provide us with the basis for a statistical analysis of planetary system properties on a large scale.

The building of the PIC will require the assembly of information from very different input catalogues on a wide range of targets (from mid-F to M-dwarfs and subgiants).

The main source for the PIC will be Gaia early, intermediate, and final release catalogues. A complementary survey of available photometric, spectroscopic catalogues and other data bases for the assessment of stellar activity will be carried out. This survey can also be used as back up for the PIC target selection and characterisations in the case of delays in the publication of Gaia catalogues. We have demonstrated that available and forthcoming catalogues are sufficient to select the main PLATO targets (P1, P2, P3, and P4),

and to provide us with their basic parameters, assuring the success of PLATO mission, independently from Gaia performances.

3.10.1 Statistical analysis of available stellar catalogues

A first approach to the target/field selection is the statistical analysis of the existing catalogues. For each star down to the PLATO limiting magnitude (that is V~13.5 for the P5 sample, and even fainter for the P4 sample), we will collect all parameters needed for a complete stellar characterisation (parallaxes, absolute magnitudes, $T_{\rm eff}$, log (g), metallicity, activity diagnostics, variability, binarity, etc.).

No single catalogues including all of such information are available, at the moment.

For this analysis, we can take advantage of a) existing catalogues of parallaxes, spectroscopic parameters or narrow-band photometry with a bright limiting magnitude (i.e., $m_V < 7.2$ for the Hipparcos catalogues, $m_V < 8$ for the MK/HD/Geneva-Copenhagen surveys) or limited to specific areas of the sky (i.e., RAVE for southern targets with $|b| > 20$); b) catalogues derived from stellar classification techniques based upon broad-band infrared/visible colours and proper motions (see also "complementary target selection"). The latter are limited by completeness, the magnitude range, and the accuracy of the source catalogues. The most useful source catalogues are: i) Tycho-2 for proper motions and *BV* photometry; ii) 2MASS for *JHK* infrared photometry; iii) UCAC3 for proper motions. No deep, all-sky source of precise $m_V \sim 0.01$ is available so far, except for the space-based Tycho-2 which is complete down to $m_V \sim 11$. In any case, we note here that the brightest PLATO stellar samples (P1, P2, P3) are the most scientifically relevant ones, and that the selection of the PLATO fields will be driven by the intent of maximising the number and the photometric quality of these bright targets. This holds in particular for the P1 sample, due to its relevance for the mission.

As for the P2-P3 sample (very bright stars with $m_V \leq 8$) the existing catalogues provide us with a nearly complete astrophysical characterisation, based especially upon Hipparcos parallaxes and spectra/*uvby* Strömgren photometry from the Geneva-Copenhagen survey. These stars are very close to the Sun (< 80 pc, which is the distance of a F5V star at $m_V = 8$). They are nearly reddening-free and isotropically distributed over the sky. Indeed, the all-sky counts of suitable P2-P3 targets from the above-mentioned sources demonstrate that their angular density is nearly uniform, and that we can meet the scientific requirement of ~1,000 targets observed during the long-duration phase (that is, over two PLATO fields) in any directions.

Catalogues from broad-band classification techniques (e.g., Ammons et al. 2006) give us density maps for the P1 (bright stars with $m_V \leq 11$) sample by selecting suitable targets in the ($T_{\rm eff}$, log g) plane (Figure 3.1). We verified that the resulting star density is in agreement (within 20−30%) with the Trilegal (Girardi et al. 2005) and Besançon Galactic models (Robin et al. 2003), both in the number and spatial distribution of targets.

Empirical estimate from Ammons (2006) catalogue and synthetic fields from Trilegal and Besançon Galactic models, sampled at different Galactic latitudes b, shows that the density of P1 targets lies in the range 5−8 stars per deg^2, i.e., it changes only by a factor smaller than two, moving from the Galactic disc to the Galactic pole. This weak dependence is mainly due to the F star components of the sample, while the GK dwarfs are nearly isotropically distributed.

As for the P4 sample (M dwarfs down to $m_V \sim 15-16$), by using the nearby luminosity function by Kroupa (2001) obtained by Hipparcos data for objects brighter than $m_V = 11$, and from ground-based data for fainter objects, in the range $9 \leq m_V \leq 13$ and for spectral type M1−M7, the number of M dwarf stars expected in a 1000 deg^2 is 2,795 for $m_V < 15$ and 11,125 for $m_V < 16$, well within the scientific requirements.

3.10.2 False alarms

Astrophysical false alarms, mainly due to eclipsing binaries, were shown to outnumber true transiting planets in ground-based and space-based photometric surveys for planets. In the case of PLATO, this problem is minimised, thanks to the brightness of the targets. Complementary techniques are also foreseen in the PLATO project to identify astrophysical false alarms from the detailed analysis of light curves, the analysis of centroids to identify blended eclipsing binaries, the comparison of transits at different colours from the FAST telescopes, as well as the photometric and spectroscopic ground-based follow-up observations. Experience gained by Kepler and CoRoT missions will be extremely valuable for the removal of false positives (e.g., Torres et al. 2011).

3.10.3 Reddening analysis

PLATO targets are located close to the Sun. At the limiting magnitude of sample P1 (m_V = 11) we have that the brightest (F5) stars can be observed out to ~300 pc (~ 200 pc for the G0 stars). For a magnitude limit at m_V = 13 the limiting distances increase by a factor 2.5. It is very well known that the Sun is located in a local bubble, with a radius of about 150 − 200 pc (Lallement et al. 2003; Vergely et al. 2010) where the reddening is negligible. At increasing distances the reddening increases depending on the specific directions. An estimate of the reddening from the all sky survey of the Holmberg Geneva-Copenhagen Catalogue (2009) shows that it remains very low [$E(B\text{-}V)$ < 0.02 mag] out to 300−400 pc from the Sun. This distance includes basically all targets limited to m_V = 11 and the influence of the distance from the Galactic plane is marginal.

This guarantees that, even independently from Gaia, sample P1, P2, P3 can be selected from available catalogues with high completeness and a very low contamination level. The reddening between 400 and 800 pc (corresponding to the deeper P5 samples) can be determined from other distance limited maps of the reddening, typically obtained measuring individual bright stars, such as those published by Neckle and Klare (1980). These maps show that, in general, the reddening rapidly increases just before 1 kpc, in agreement with the average values obtained by infrared measurements of Marshall et al. (2006). A consequence of this analysis is that the rapid increase of the reddening beyond about 1 kpc can be used for a colour separation of much more distant, contaminating sources, such as bright giants, enabling us to select P1, P4, and P5 samples from available catalogues (UCAC3 and 2MASS).

3.10.4 Field selection and field content

The two long-duration PLATO fields will represent the core of the mission. Their centres must stay within two regions imposed by the observational constraints. These “allowed regions” are spherical caps defined by an ecliptic latitude |β| > 63°, and are located respectively in the southern and northern hemispheres, mostly at high declinations (|δ| > 40°).

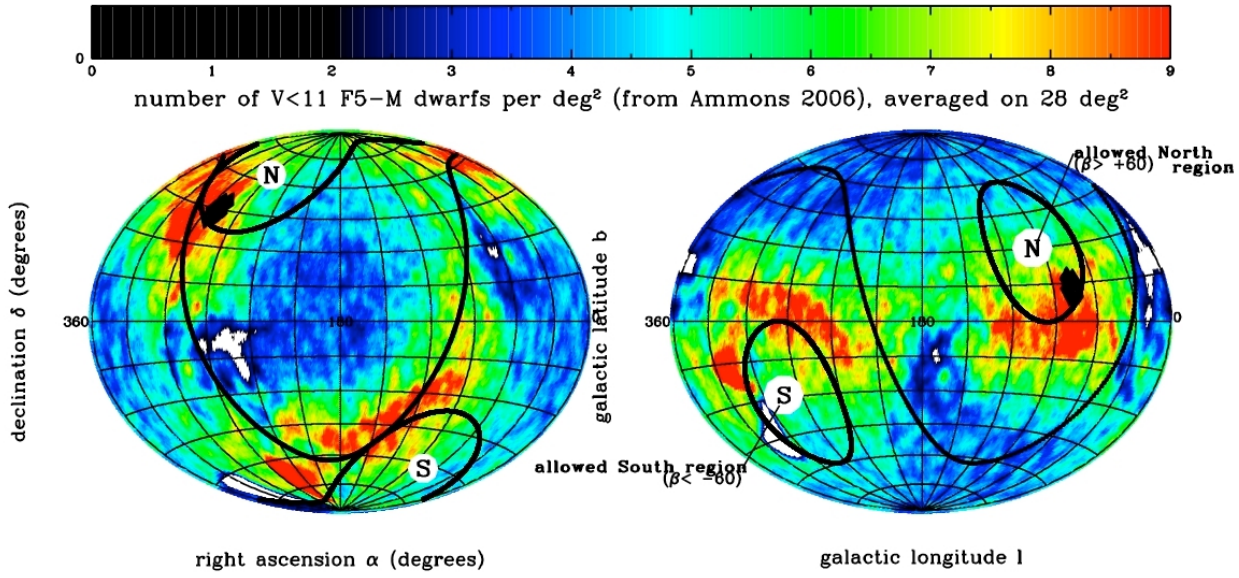

Figure 3.1: All-sky angular density of P1 targets as selected by Ammons et al. (2006), in equatorial (left panel) and galactic coordinates (right).

The choice of the long-duration fields should be driven by 1) the fulfilment of the requirements concerning the number of observable targets for all five P1-P5 samples, and the maximisation of the P1-P2 samples; 2) the minimisation rate of expected astrophysical false positives due to crowding, above all from blended eclipsing binaries. Both Galactic models and catalogues tell us that for every field choice, within the allowed

southern and northern regions, the requirements for the P2 (> 1,000 targets summed on both fields) and the P1 (> 20,000) samples are always met, with a large margin (see Figure 3.2).

The requirement for the P5 sample (> 245,000) is conservatively met for fields centred at $|b| < 40°$. M-dwarfs with $m_V < 16$ are a factor of 10 more numerous than the P4 requirements, and therefore are overabundant with respect to the science requirements. On the other hand, both the number of expected false positives and the number of nearby dust clouds rise steeply for $|b| < 30°$. The best trade-off strategy is then to select fields centred at about $|b| \sim 30°$. As for the Galactic longitude, we note that the regions at low declination $|\delta| < 60°$ are on average less affected by interstellar extinction as visible on the dust maps. Also, low-declination regions have the advantage of a more efficient observations during the ground-based follow-up phase. A proposed conservative choice (to minimise contaminants, still satisfying the scientific requirements in terms of target numbers) for the field centres is ($l = 253°$, $b = -30°$) for a Southern sky field and ($l = 65°$, $b = 30°$) for a Northern sky field (see Figure 3.2). These fields are centred approximately on Pictor (South) and Lyra/Hercules (North) constellations. The northern field includes the Kepler field on a corner. An additional, thorough study of the contaminant problem will allow us to verify whether the field centre can be moved to lower Galactic latitudes ($|b| \sim 25°$), thus increasing the number of targets.

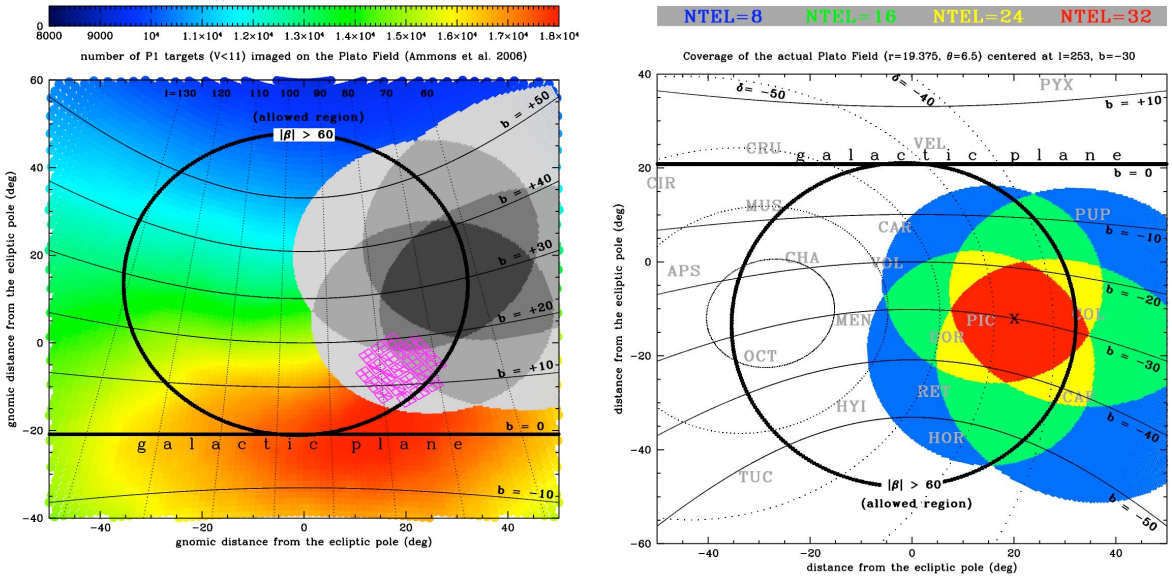

Figure 3.2: Left Panel: Density of P1 targets for the northern region, averaged over the area of the PLATO field, following Ammons et al. (2006). The preliminary long-duration PLATO field is shown in grey. The Kepler field is indicated in pink colours. Right Panel: The preliminary long-duration PLATO field chosen for the southern allowed region, with the number of telescopes covering the single sub-regions indicated by different colours.

3.10.5 Target selection and characterisation from Gaia catalogue

Gaia all-sky survey, due to launch in late 2013, will monitor astrometrically, photometrically, and, in part, spectroscopically, during its 5-yr nominal mission lifetime, all point sources with $6 < m_V < 20$, which will generate a huge database encompassing ~10^9 objects. Using the continuous scanning principle first adopted for Hipparcos, Gaia will determine the five basic astrometric parameters (two positional coordinates α and δ, two proper motion components μ_α and μ_δ, and the parallax π) for all objects, with end-of-mission precision between 7 μas (at $m_V = 6$) and 200 μas (at $m_V = 20$).

The precise determination of fundamental stellar parameters with Gaia will be instrumental in helping us to identify bright, nearby cool F-, G-, K-, M-dwarfs and sub-giants across the huge sky region (almost 50% of the sky) covered by the PLATO fields.

During the implementation phase, the first objective will be to coordinate the analysis of all available information (astrometric, photometric, and spectroscopic), initially from detailed simulations of Gaia observations, and then from Gaia early, intermediate and possibly final release catalogues. This will provide a highly complete reservoir of well-classified nearby dwarf/sub-giant stars from which to choose, in order to populate the PIC, ahead of launch. To this end, a collaboration agreement has been established between the

PLATO Consortium and the Data Processing & Analysis Consortium (DPAC) of the Gaia mission (www.rssd.esa.int/gaia/dpac), responsible for the preparation of the data analysis algorithms to reduce the astrometric, photometric, and spectroscopic data.

The analysis of the first simulations, provided by DPAC's Coordination Unit 2 (CU2), indicates that a "clean" sample of main-sequence dwarfs later than F5, with only ~1% "contamination" from cool giants, could be easily selected with simple cut-offs in distance and reddening-corrected absolute magnitude in the Gaia main photometric pass-band MG. This was the result of the exquisite precision estimates of Gaia parallaxes (<< 1% uncertainty for all potential PLATO PIC targets), based on detailed error models, taking into account the selection of specific gate schemes in order to avoid saturation on bright ($m_V < 13$) stars. The contaminants can be reduced to a negligible fraction (~ 0.1%) using the information on effective temperature $T_{\rm eff}$ and surface gravity $\log(g)$ from Gaia spectro-photometry, which will be accurate to $\sim 200-300$ K and $0.2-0.3$ dex, respectively, for bright stars ($m_V < 14$).

Upon release of the Gaia early and intermediate release catalogues, in-depth investigations of the quality of Gaia astro-spectrophotometric measurements will be carried out for both "primary" stars included in the core data analysis (processed by CU3) as well as for stars showing hints of variability (processed by other CUs).

The reassessment of Gaia performance in astrometry, photometry, and spectroscopy on bright stars will continue into PLATO until the publication of the final Gaia catalogue (ca. 2021).

Though the Gaia catalogue will provide us the best data source for the PIC target selection and characterisation, we also analysed our capability to build the PLATO PIC in case of reduced performances by Gaia.

The advent of accurate all-sky catalogues such as Hipparcos, Tycho-2, and 2MASS made the extraction of stellar main parameters from wide-band photometry and proper motions possible (Ammons et al. 2006; Belikov & Roeser 2008; Ofek 2008; Bilir et al. 2006; Pickles & Depagne 2010). These authors defined the main techniques we can use to extract P1 sample targets (P2 and P3 samples will be available mainly from Hipparcos and MK/HD/Geneva-Copenhagen surveys).

Most of these works employ similar input catalogues, usually Tycho-2 and 2MASS magnitudes, as they provide uniform, precise all-sky photometry over passbands that contain useful information on [M/H] and $\log(g)$. Proper motions, when used, are extracted also from Tycho-2. We carried out an external validation of these techniques by selecting stars with "photometric" $T_{\rm eff}$ and $\log(g)$ suitable for the inclusion in the P1 sample, and then checking how many of them are confirmed as P1 targets by the spectroscopic parameters from RAVE dr3 (Siebert et al. 2011). We find on average < 20% of contaminating giants in such a selected sample, which is still acceptable (but shall be reduced during the implementation phase) as PLATO telemetry will allow us to monitor more P1 targets than the 20,000 stated by the scientific requirements. Further contaminants can be identified by on-board photometry and discarded afterwards.

Unfortunately, most photometric classifications are limited to about $m_V < 11$ (and therefore to the PLATO stellar samples P1-P3) by the completeness limit of Tycho-2. Though 2MASS provides very good photometry ($\sigma < 0.05$ mag) down to $m_V \sim 15$ and Tycho-2 proper motions are also well complemented by UCAC3 for stars brighter than $m_V \sim 15$, no reliable source of visual magnitudes is available for $m_V > 11$ on the whole sky, making stellar classification more difficult (i.e., affected by a larger contamination level), with the only exception of M-dwarfs (P4). However, once full-coverage catalogues (e.g., from APASS and SkyMapper) will be released, it will be possible to extend photometric spectral and luminosity classification of stars to fill P5 target requirements. Meanwhile, we note that "reduced proper motion" (RPM) techniques from UCAC3 proper motions coupled with 2MASS *JHK* colours are already able to perform an acceptable selection of M-dwarfs (which, by far, outnumber the minimal P4 science requirement) and a minimal giant/dwarf separation for the P5 sample. Preliminary estimates done on RAVE dr3 entries with UCAC3/2MASS data show that it is possible to perform a P4 target selection with > 60% efficiency, and < 30% contamination, and a P5 target selection with < 30% contamination and > 80% completeness. This implies that we will be able to prepare the PIC even in case of failure or reduced performances by Gaia.

3.10.6 PIC target characterisation

After field selection and the identification of the targets to be observed with PLATO, we will focus our attention on the determination of the target properties. A thorough astrophysical characterisation of the PIC

target stars will help, for example, minimising false positives, and the optimisation of expensive, time-consuming follow-up work. The target characterisation will normally involve the determination of a complete set of stellar parameters (e.g., distance, proper motion, magnitudes, $T_{\rm eff}$, surface gravity $\log(g)$, metallicity [M/H], extinction, stellar activity, age indicators) for each PIC entry. This, combined with information on binarity/multiplicity and/or the presence of planetary-mass companions (likely available at the level of Gaia intermediate data releases), will also allow for detailed prioritisation of the PIC targets.

The principal source of target parameters will be the Gaia catalogues. Cross-matching of other catalogues will help to complete target characterisation, and will be performed at the ASI Data Centre (ASDC). The level of magnetic activity will be collected from available catalogues in the literature and archives (e.g., X-rays, UV emission lines, Ca II H&K indices, H-alpha EWs) in order to define subsamples of stars with different activity levels. Recalling that high magnetic activity is an indicator of youth, choosing stars having different activity levels will allow us to investigate the properties of planetary systems in an evolutionary contest.

Archival spectra of PLATO targets will also be used for characterisation. Dedicated surveys for further characterisation are also being considered. Small aperture telescopes equipped with suitable narrow-band filters might provide reliable temperature and gravity for PLATO targets in a limited amount of time. Observations of the PLATO field using dedicated telescopes might provide information on stellar content around PLATO targets at 1 arcsec spatial resolution, very useful to evaluate blend scenarios, as well as temperature and activity characterisation of PLATO targets (including the P5 sample) by means of narrow-band observations. An extension of the RAVE survey devoted to PLATO targets is also being considered.

3.10.7 Gaia parameters extraction and target characterisation

In any case, we expect that the bright PLATO stellar sample ($m_V \leq 11$) will have distance, proper motion, magnitudes, $T_{\rm eff}$, surface gravity $\log(g)$, metallicity [M/H], extinction, stellar activity and age indicators provided with high precision by Gaia. During the implementation phase, dedicated algorithms will be created, implemented and tested for cross-examination of the Gaia astrometric, spectroscopic and photometric information for the definition and prioritisation of the set of parameters utilised for the selection of PIC targets, based on extensive simulations of the PLATO fields, and the completeness assessment described above. The algorithms will be adapted for ingestion, and extraction of the relevant parameters from Gaia early as well as intermediate release data.

4 Payload

The PLATO instrument covers the cameras, their focal planes, all related electronics and the on-board data processing system (DPS). The PLATO instrument (provided by the PLATO Mission Consortium) plus the optical bench on which the 34 cameras are mounted (provided by the satellite contractor), constitute the PLATO payload.

The PLATO payload was studied in an assessment phase, followed by a definition phase completed in 2011. The results were summarised in a definition study report (ESA/SRE(2011)13), which is the basis for the payload description provided here. Furthermore, PLATO underwent part of a B1 study phase during the M1/M2 mission competition.

4.1 Basic instrument overview

The instrument concept is based on a multi-telescope approach, involving a set of 32 "normal" cameras working at a cadence of 25 s and monitoring stars fainter than $m_V = 8$, plus two "fast" cameras working at a cadence of 2.5 s, and observing stars in the m_V range from 4 to 8.

A camera includes a Telescope Optical Unit (TOU), a Focal Plane Assembly (FPA) which supports four CCD detectors, the Front End Electronics (FEE) box and related thermal equipment. The TOUs are based on a fully dioptric telescope including 6 lenses. Each camera has a 1100 deg^2 field-of-view and a pupil diameter of 120 mm.

The 32 "normal" cameras are arranged in 4 groups of 8 cameras (Figure 4.1). All 8 cameras of each group have exactly the same field-of-view. However, the lines of sight of the four groups are offset by an angle of 9.2° from the PLM +Z axis. This particular configuration allows us to survey a total field of about 2250 deg^2 per pointing, with various parts of the field monitored by 32, 24, 16 or 8 cameras. This strategy optimises both the number of targets observed at a given noise level and their brightness. The satellite will be rotated around the mean line of sight by 90° every 3 months, resulting in a continuous survey of exactly the same region of the sky.

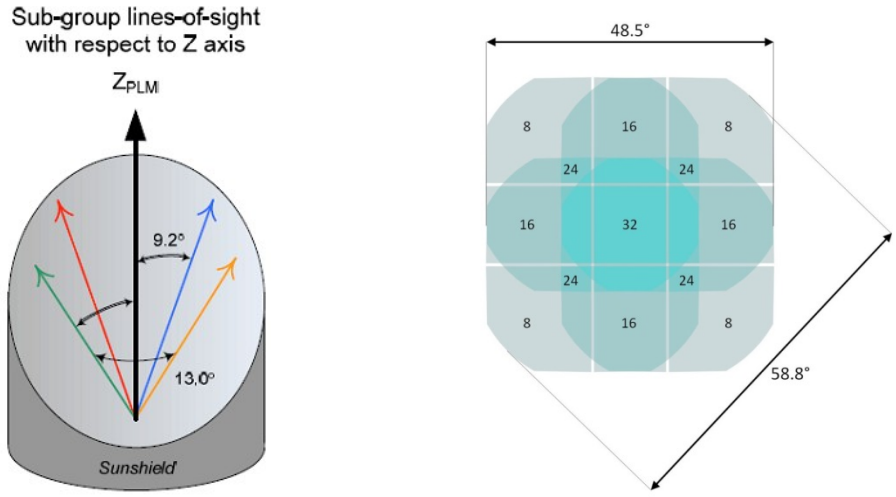

Figure 4.1: The overlapping line-of-sight concept (left) and the resulting field-of-view configuration (right).

Each camera is equipped with its own, cooled FPA, comprised of 4 CCDs with 4510 × 4510 pixels each, working in full frame mode for the "normal" cameras, and in frame transfer mode for the "fast" cameras.

Each assigned target star will be allocated a CCD window around it from which all the pixel values will be read out and transmitted to ground, forming a small image called an "imagette". The size of this window is

typically 6×6 pixels (9×9 pixels for the fast cameras), large enough to contain the whole image of the target star. These imagettes will be used on ground to derive the PSF at different positions of the detector, a step which is needed to define the photometric extraction masks, and to verify the quality of the photometric and centroiding data being obtained by the on-board automatic processing.

There is one Data Processing Unit (DPU) per two cameras performing the basic photometric tasks and delivering a set of light curves, centroid curves and imagettes to a central Instrument Control Unit (ICU), which stacks and compresses the data, then transmits them to the SVM for downlink. Data from all individual cameras are transmitted to the ground, where final instrumental corrections, such as jitter correction, are performed. The DPUs of the fast cameras will also deliver a pointing error signal to the AOCS, at a cadence of 2.5 s.

Each DPU of the "normal" cameras (N-DPU) is associated with two FEEs. They are grouped together by 4 in the same box called Main Electronics Unit (MEU). There are 4 MEUs (16 N-DPUs) for the 32 normal cameras, each one including its own power supply electronics. The fast DPUs (F-DPU) are functionally associated to the fast FEE. There are 2 Fast DPUs, one per fast FEE, grouped in one box called Fast Electronics Unit (FEU), also including its power supply.

Additional components of the electronics unit include the Ancillary Electronics Units (AEUs), used to power the associated FEE and the synchronisation board used to have a fully synchronised acquisition by all the cameras, and two Instrument Control Units (ICU) used in cold redundancy. The two ICUs are grouped in a single box with their own power supply. In addition, the instrument includes on-board software, operating on the DPUs and ICUs, which can be modified during the flight. See Figure 4.2 for an overview on the on-board data treatment architecture. More details of the system architecture are provided in the Definition Study Report (ESA/SRE(2011)13, Section 4.4) and have to be omitted here due to space limitations. Table 4.1 provides an overview of the instrument.

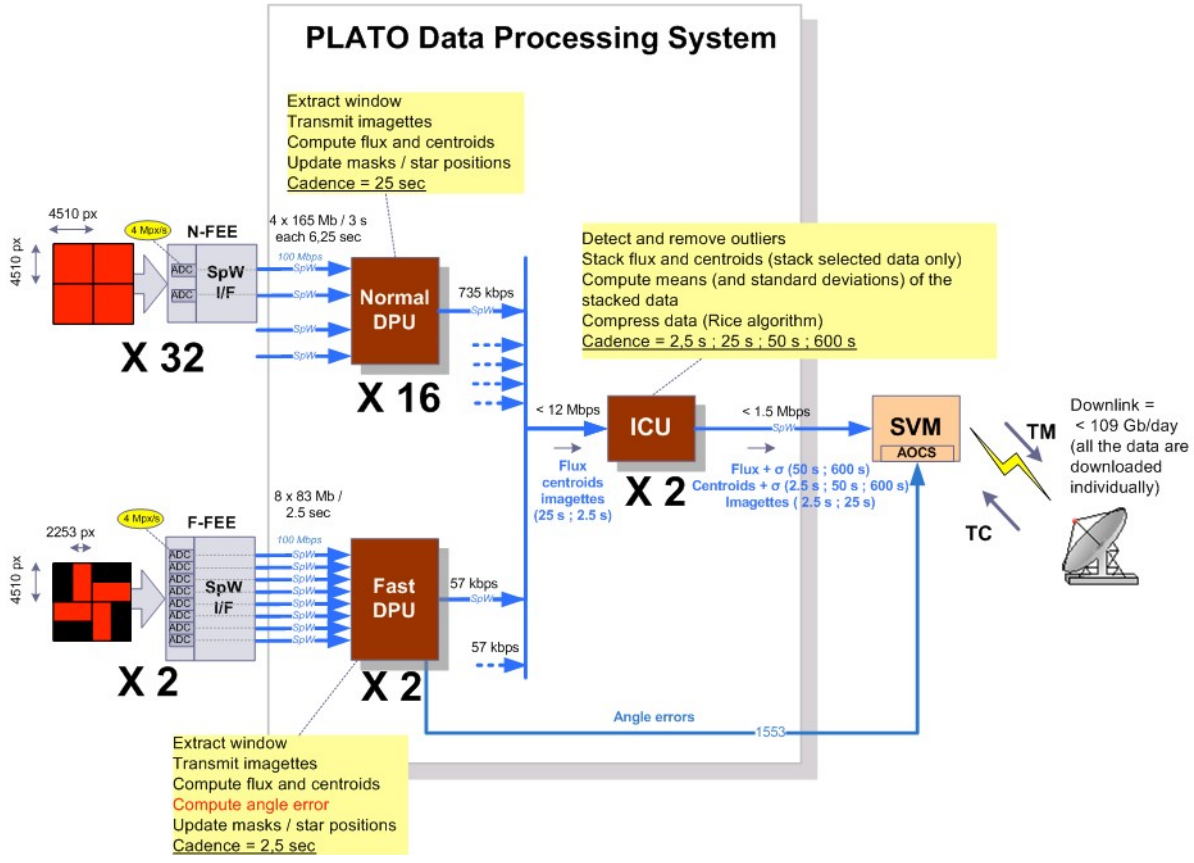

Figure 4.2: The PLATO on-board data treatment architecture.

Table 4.1: Summary of the instrument

Characteristics	Value	Comments
Optics	Full refractive design with 6 lenses and 1 entrance window	Axi-symmetric design
Optics spectral range	500 – 1050 nm	
Pupil diameter	120.0 mm	For one telescope
Normal camera field of view	~ 1100 deg² ~ circular, diameter 38.7°	For each telescope
Normal camera detector	Full frame CCD 4510 x 4510 18 µm square pixels	
Fast camera field of view	~ 550 deg²	For each telescope. Only 50% of the focal plane light sensitive.
Fast camera detector	Frame transfer CCD 4510 x 2255 light sensitive, 18 µm square pixels	
Plate scale	15.0 arcsec / px	For both normal and fast telescope
PSF surface	Always included within 9 px	
Payload field-of-view	Overlapping FoV of 2232 deg²	32 cameras looking on 301 deg² 24 cameras looking on 247 deg² 16 cameras looking on 735 deg² 8 cameras looking on 949 deg²
Equivalent pupil size	678.8 mm for 32 cam 587.9 mm for 24 cam 480.0 mm for 16 cam 339.4 mm for 8 cam	
Focal plane layout	4 CCDs in a square	
CCD temperature	< –65°C	By passive cooling
Read-out frequency	4 Mpx/s	For both normal or fast telescope
Read-out noise	55 e- rms/px	Global for detector and electronics, at nominal read-out frequency
Read-out noise fast cameras	90 e- rms/px	Global for detector and electronics, at nominal read-out frequency
Normal camera CCD cycle period	25.0 s fixed	
Fast camera CCD cycle period	2.5 s fixed	To be confirmed with AOCS needs
Normal camera exposure time	~ 22.0 s fixed	+ a shorter exposure time for on-ground, at room temperature, tests
Fast camera exposure time	~ 2.3 s fixed	
Pointing error rate	2.5 s fixed	
Number of telescopes	32 Normal + 2 Fast	
Power needed by payload	~ 820 W	Including 20% uncertainties
Mass of the payload	~ 600 kg	Including 20% uncertainties
Electronics	1 FEE / camera 1 DPU / 2 cameras 2 ICUs in cold redundancy	FEE and CCD activities are fully synchronised
Science Operation Centre	Under ESA responsibility	
Orbit type	Sun-Earth system L2	
Life time in orbit	> 8 years	
Eclipse	none	
Observation phases	1st and 2nd: 2 or 3 years	1 pointing / phase
Step-and-stare phase	> 1 year	With several pointings
Attitude	90° rotation around the LoS every 3 months	

4.2 Telescope Optical Unit (TOU)

There is no general difference in the TOU design for normal and fast telescopes, but the latter will include filters in form of special coatings on an optical surface of the optical train. The optical configuration consists of 6 lenses, plus one window, placed at the entrance of the telescope, providing protection against radiation and thermal shocks. The first surface of the first lens contains even aspherical terms (K, a4, a6), while the second surface is flat in order to facilitate the interferometric surface measure during the aspheric manufacturing. All the other lenses are standard spherical surfaces. The first surface of the third lens is the optical system stop and guarantees a real entrance pupil diameter of 120 mm. This configuration provides a corrected field-of-view up to 13.7° (90% of encircled energy within less than 2×2 pixels), while the full field of view is up to 14.3°, accepting slightly degraded image quality, as well as a ~7% vignetting, in this small region at the edge of the field. A layout of the design is shown in Figure 4.3 and the general performance and parameters of the baseline optical configuration are summarised in Table 4.2.

Table 4.2: Camera parameters

Spectral range	500 – 1000 nm
Entrance Pupil Diameter	120 mm
Working f/#	2.06 @ 700 nm
Field of View	~ 1100 deg^2
Image quality	90% Enclosed energy < 2×2 $pixel^2$ over 1108.3 deg^2
Maximum Field Distortion	5.043%
Plate scale	15 arcsec/pixel
Pixel size	Square, 18 microns
CCD format	4510 × 4510 (×4) $pixel^2$
FPA size	164.36 mm (2 mm CCDs gap)
Working Temperature	–80°C (at telescope TRP)
Working Pressure	0 atm

The TOU main structure consists of a machined tube with all the interface planes, threads and holes necessary to mount the other components. The heat dissipated by the CCD needs to be transported through the TOU structure, which therefore must be made of material with high thermal conductivity. In addition, the large temperature difference between integration and operation requires a design able to accommodate the dimensional changes of the assembled components without leading to unacceptable mechanical stresses.

TOU integration and verification procedures have been defined and tested by breadboarding and prototyping activities. A breadboard with 4 out of 6 lenses identical to the nominal ones (other than using the non-radiation hardened glass) has already been manufactured, integrated, aligned in the warm, and the optical performances measured, and re-measured in a cryo-vacuum chamber under conditions very similar to the nominal ones (see Figure 4.4). Details can be found in PLATO-INAF-TOU-RP-0013 (issue 02). At the same time, two blank in CaF_2 with similar size of L3 have been mounted on the same current mechanical design of the holder foreseen in the TOU and subject to vibrational and thermal tests, following the specifications given in the launcher manual with an uneventful result.

The thermal design of the TOUs is such that the mean temperature at TRP is –90° ± 1.5°C with the heaters switched off. The TRP location is at a distance of 244 mm from the CCD (near L3).

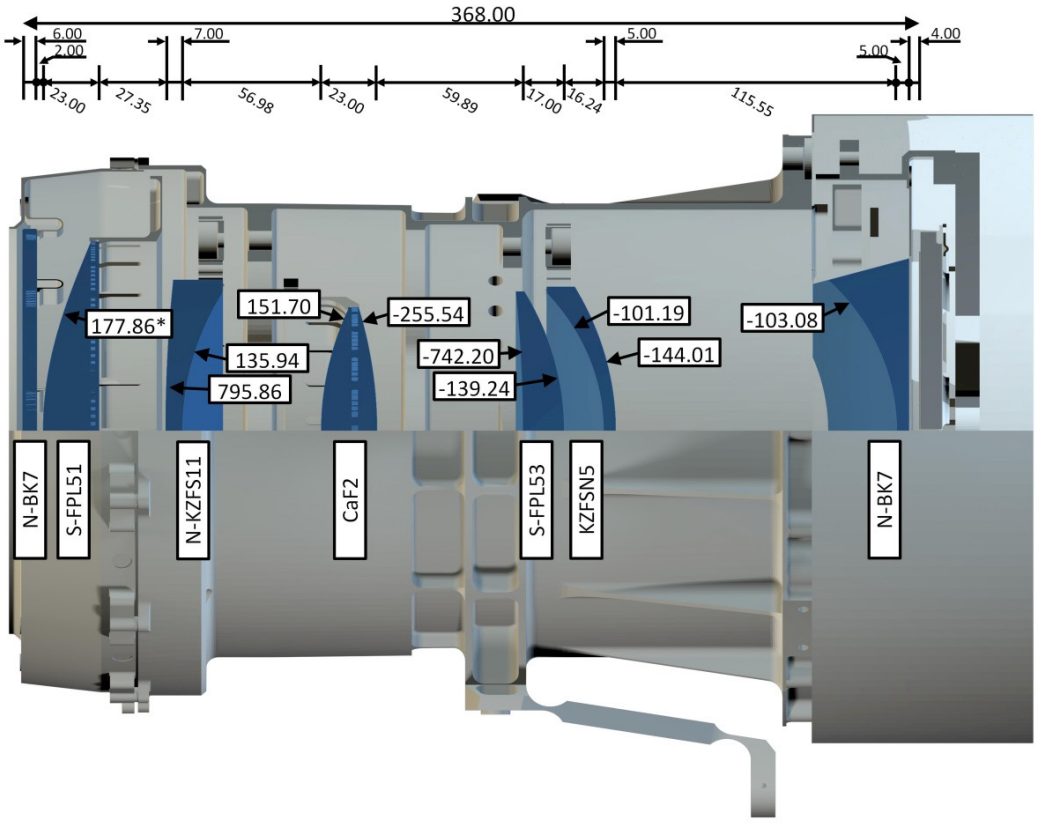

Figure 4.3: The baseline optical layout is shown together with a cross section of the mechanical envelope. One of the point attachments to the optical bench is visible in the lower part while the baffle is missing in this drawing. The structure of the focal plane assembly with the detectors is also seen (at the right side).

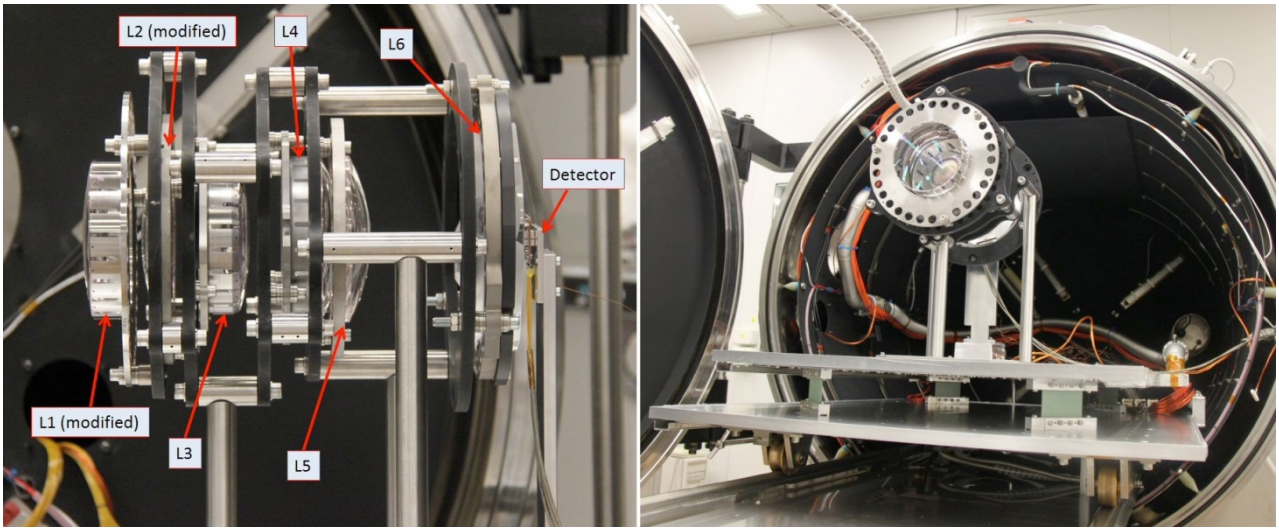

Figure 4.4: Left: The TOU Breadboard shown on its side with the lenses indicated. Four out of six are nominal ones (including the one for the pupil stop in Calcium Fluoride). Right: The TOU Breadboard while entering the cryo-vacuum chamber for the alignment tests.

4.3 Focal Plane Assembly (FPA)

The PLATO detector is a CCD with two separately connected sections to allow full frame (FF) or frame transfer (FT) modes. It is a back-illuminated, back-thinned device, non-inverted type, whose characteristics

are summarised in Table 4.1. An antireflection coating is required on its sensitive surface for quantum efficiency increase. Only one readout register with two outputs is required for both the FF and FT devices. The detector will work at a temperature lower than –65°C.

The Focal Plane Assembly structure supports the 4 CCDs via quasi-static mount on a support plate, ensuring a good planarity. The support plate is attached to the telescope structure by a stiff interface ring of the same material as the TOU. It has the possibility to be adjusted in position (along ZCAM and around the camera transverse axes) by using 3 shims located between FPA and telescope. It is electrically isolated from the telescope, and the thermal power dissipated at FPA level is evacuated by the mechanical interface with the telescope, the CCD packages being thermally connected to the FPA-telescope interface via flexible thermal straps.

Figure 4.5 shows the CCD array configuration for both normal and fast cameras, while Figure 4.6 depicts the Focal Plane Assembly.

The flexi-cables have a free length of ~ 80 mm (TBC) from the bottom of the FPA to the top of the FEE. The distance between FPA and FEE is limited to a nominal value of 65 mm to get slightly bended flexi-cables allowing small misalignments, displacements or rotations between them during AIT, and launch.

Extensive analysis has been performed to guarantee the PLATO FPA performances, in terms of vibration robustness, flatness, CCD temperature, while remaining within mass and power budget. Finally, integration and verification procedures for the FPA have been defined and tested using a mock-up manufactured in Al with the current design (see Figure 4.7) already integrated.

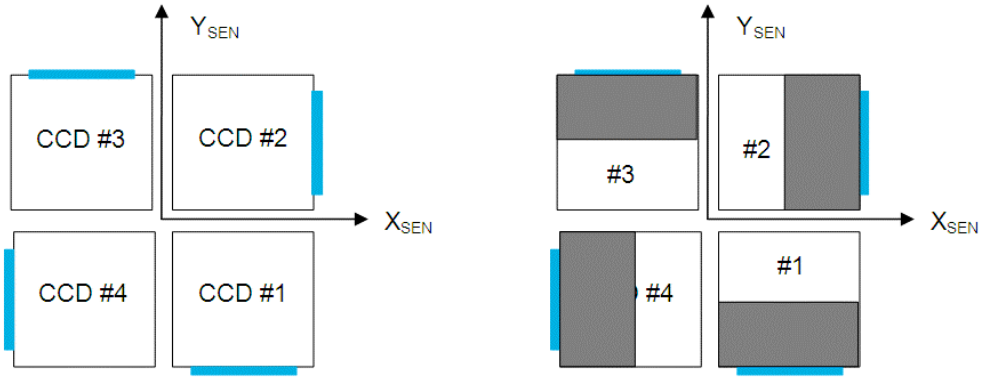

Figure 4.5: The CCD array configuration for normal cameras (left) and fast cameras (right). Blue rectangles represent the flexi-cables. The shaded area in the fast cameras CCD corresponds to the frame transfer storage area, and is not light sensitive.

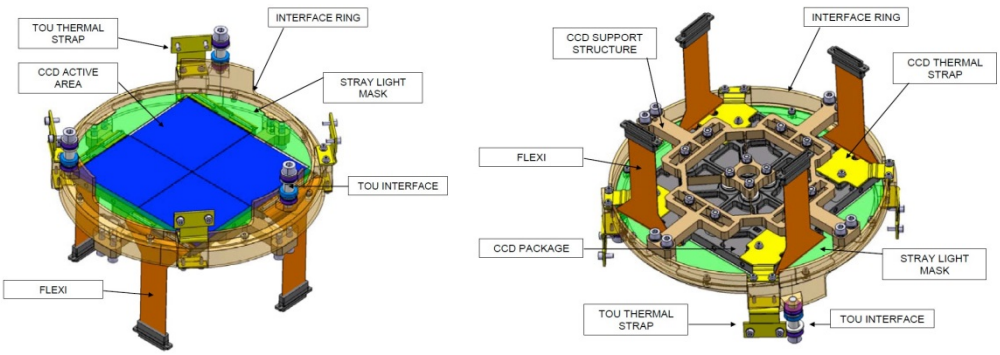

Figure 4.6: The Focal Plane Assembly seen from top (left) and from bottom (right).

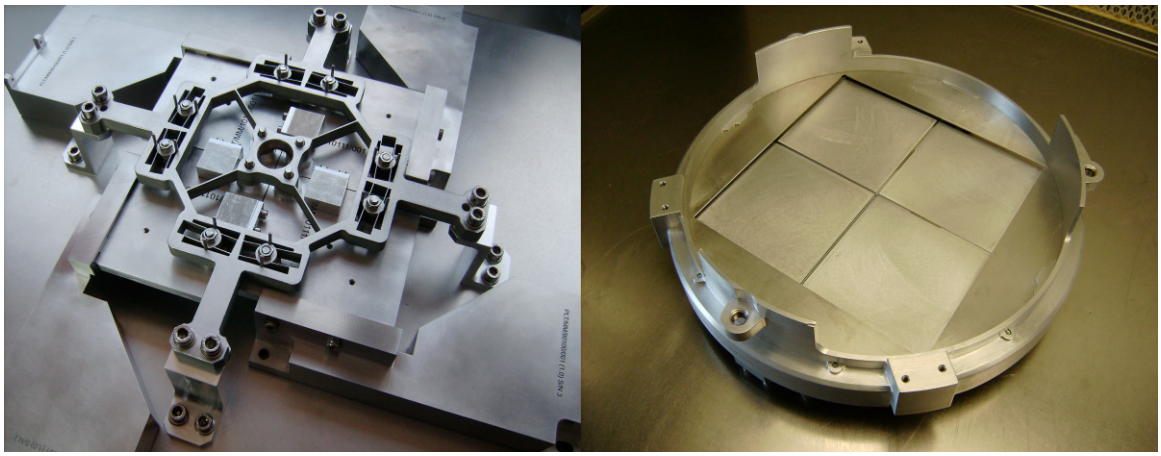

Figure 4.7: The Focal Plane Assembly mock-up. Left, CCD support structure; right, top view with 4 dummy CCDs.

4.4 Front End Electronics (FEE)

The N-FEE operates the 4 CCDs of a normal camera, digitizes the image data and transfers them to the DPU. Each CCD has an integration time of ~22 s and a readout time of ~3 s. The readouts are staggered at equal intervals of the 25 s period. The readout and data transfer to the DPU are arranged such that the readout of one CCD is finished before the next begins, in order to minimise crosstalk and interference effects.

An FPGA is the core of the N-FEE, and receives command packets from the DPU and timing and synchronisation data from the AEU. It generates all the clocks necessary for driving the 4 CCDs and drives the DACs responsible for providing the bias voltages.

The interface between N-FEE and N-DPU is made by two SpaceWire links. The protocol used is RMAP in all cases, but the command interface is actually simulated RMAP with e.g. control registers, HK data, memory mapped for simple access.

The F-FEE operates the CCDs of the two fast cameras. It has many aspects in common with the N-FEE: commanding, CCD bias supplies, clock waveforms, and housekeeping. Other aspects are significantly different due to the use of frame-transfer devices and shorter integration times: FPGA and programming, number of SpaceWire interfaces and data rate.

For the fast cameras, the 4 CCDs are read out simultaneously every 2.5 s. Due to less critical noise requirements, the F-FEE uses an integrated analogue front-end (AFE) electronics, instead of the non-integrated 16-bit AFE used by N-FEE. As for the N-FEE, synchronisation of the two cameras is ensured by receiving from the associated F-AEU a high frequency signal (50 MHz) and a signal giving the information of the 2.5 sec period beginning, also synchronised with the 25.0 sec period of the normal cameras.

The AEU powers the associated FEEs and includes the synchronization board. The N- and F-AEU boxes are located in the SVM. There are 4 N-AEU boxes, one for each group of cameras. Each box contains 8 independent DC/DC converters, dedicated to one N-FEE. There is one F-AEU box for the two F-FEEs, containing two fully independent DC/DC converters, one for each F-FEE.

4.5 On-board data treatment subsystem

4.5.1 Main Electronics Unit (MEU) and Data Processing Units (DPU)

Each Main Electronics Unit (MEU) gathers in the same box (see Figure 4.8 for the MEU architecture):

- 4 N-DPU boards: each N-DPU board is responsible for handling two normal cameras.
- 2 SpaceWire routers: one main and one redundant.

- A Power Supply Unit that converts the primary voltage received from the SVM into the secondary voltages needed for powering the N-DPU boards and the routers.
- A Motherboard for internal connections.

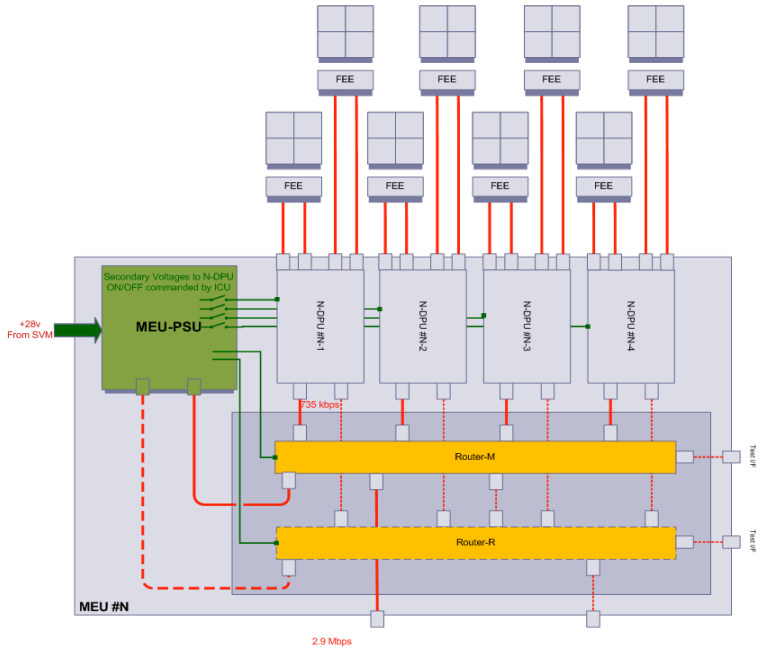

Figure 4.8: MEU box architecture.

Each N-DPU board is connected to 2 N-FEE thanks to 4 SpaceWire links configured to run at 100 Mbps (one SpaceWire link per CCD FEE readout output). Each N-DPU board is connected to the nominal router and to the redundant router. Nominally, both MEU routers are working in cold redundancy. However, to handle certain failure cases, both MEU routers can be switched on simultaneously and can work in hot redundancy.

The instantaneous data rate between 2×N-FEE and N-DPU is: 2×2×4 Mpx/s × 1.25 = 4×80 = 320 Mbps. With two SpaceWire links between 1 N-FEE and 1 N-DPU, the instantaneous data rate over one link is 80 Mbps, compatible with a SpaceWire link configured to run at a bit rate of 100 Mbps. On the other end, the data rate towards the ICU includes a 50% margin on star count (accounting for the uncertainty on the star field content), the SpaceWire overhead and the packetisation overhead. The data rate between one N-DPU and the MEU router is 735 kbps, corresponding to the transmission of about 21 packets per second. The full data rate between one MEU and the active ICU is 4×735 kbps = 2.9 Mbps, corresponding to the transmission of about 83 packets per second. The count of extracted windows for 4 CCDs is:

Sample P1	2×6720, with margin 50% = 2 ×10080
Sample P4	2×102200, with margin 50% = 2 × 153300
Background windows	2×400
Imagettes	up to 2×2000
Offset windows	2×2×4 offset windows (2255 pixels)
Smearing rows	2×4×10 over-scan rows

The application software running on each DPU performs the complete data reduction and photometrical extraction process. It is triggered as soon as a set of windows extracted from a full-frame image is available.

The needed processing power has been estimated by prototyping the main algorithms in C language on a LEON2@100 MHz processor simulator. The measured CPU occupation rate is 37% (CPU load margin = 170%). The conclusion is that the normal N-DPU board can be implemented with one LEON AT697F processor working at 100 MHz. The CPU load margin can be used to improve the algorithms, to implement new algorithms, to process more targets, to update with a higher frequency the photometric masks or to reduce the processor frequency. The total memory required per N-DPU board will be 256 Mbytes, assuming +50% margin in the number of stars to be monitored per CCD.

Data of the two fast telescopes are processed by the F-DPU. The processing of each exposure is identical to that of the N-DPU, except that (i) the cadence is 2.5 s instead of 25 s; (ii) pointing error measurements will be performed with an accuracy better than 0.032 arcsec/√Hz and transmitted to the AOCS (Fine Guidance System: FGS).

The distribution of the extracted windows is the following (counts for the 4 CCDs):

Stars	400
Background windows	100 (7×7 pixels)
Imagettes	40
Offset windows	2×4 offset windows
Smearing rows	4×10 over-scan rows

The photometric algorithms will be based on the optimal mask method which gives the best results for the fast camera configuration (TBC). The FGS algorithms are based on an extended Kalman filter (EKF) used for recursive nonlinear optimisation. Pixels will be digitised at a rate of 4 Mpixel/s, thus the maximum rate per half CCD is 64 Mbps. With 8 links (one per half CCD output), including the SpaceWire overhead, it gives 80 Mbps as a peak rate. In order to cope with this bit rate with margin, the link is configured at 100 Mbps for 8 links. The expected mean rate will be 1.25 (SpaceWire overhead) image size / 1.5 (readout time) so it is 1.25×81/ 1.5 = 68 Mbps, leaving 30% margin.

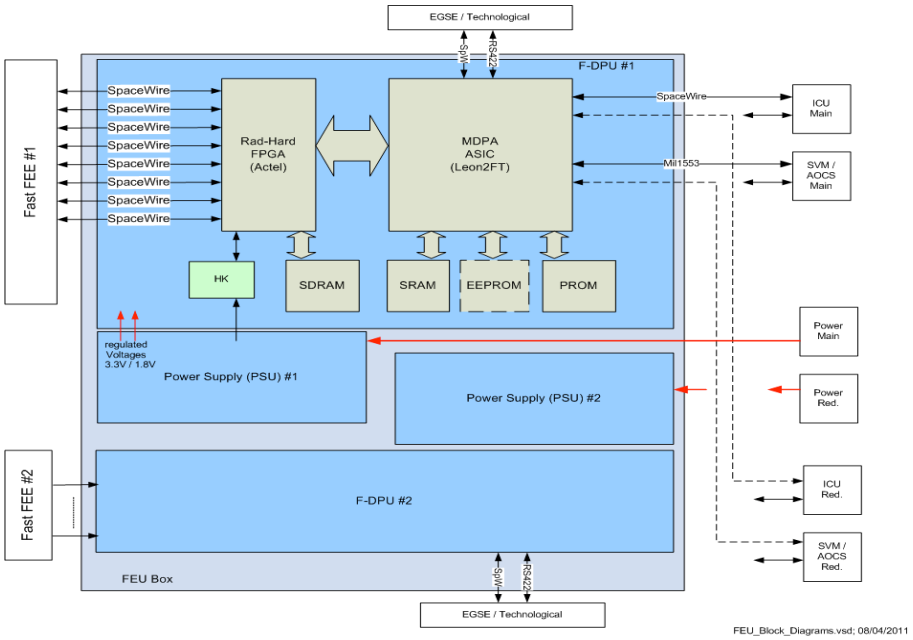

Figure 4.9: FEU Architecture Block Diagram

The CPU load needed by the data acquisition, correction and reduction process is about 40% with a MDPA LEON2 FT processor running at 80 MHz. In total 512 Mbytes of SDRAM will be needed per F-DPU.

The FEU is an integrated electronics box, which consists of two data processing (F-DPU) boards (each within one module frame) and 2 power converters (PSU) integrated into a single frame. Figure 4.9 shows the FEU architecture.

4.5.2 Instrument Control Unit (ICU)

Both ICUs (main and redundant) are gathered in a single box and work in cold redundancy. Each ICU shall implement the following common functions (non-exhaustive list):

- Handle communications with spacecraft.
- Receive and process telecommands.
- Format and transmit cyclic and sporadic HK telemetry packets.
- Format and transmit the scientific payload telemetry packets.
- Manage the SpaceWire network: the ICU is a remote network manager (router configuration, router monitoring, router status reporting…).
- Receive the on-board time (Central Time Reference) from the S/C, handle the time stamping of the data transmitted in HK TM and forward the CTR to the DPUs.
- Receive a SpaceWire time code from the S/C and forward it to the DPUs.
- Produce state and diagnosis information (cyclic status, progress event).
- Schedule the DPU tasks (by the way of commands sent to the DPUs).
- Manage the data flow (especially in configuration mode).
- Manage the mode transitions.
- Manage the software parameters.
- Manage the maintenance of the ICU software.
- Manage the maintenance of the N-DPU software.
- Manage the star catalogue.
- Compress the data using a lossless compression algorithm. A compression factor of at least 2.0 is required.
- Acquire and transmit to the S/C its own voltage and current consumptions.

Every 2.5 s, the active ICU processes the data (flux, centroids and imagettes) sent by the F-DPUs. The imagettes are compressed before being transmitted to the SVM. The fluxes and centroids are stacked: N measurements are stacked for each F-DPU. Every 25 s, the active ICU processes the data (flux, centroids and imagettes) sent by the N-DPUs.

The imagettes are compressed before being transmitted to the SVM. An outlier detection is performed on the fluxes and centroids by comparing the data corresponding to the same star as sent from N cameras (N=8, 16, 24 or 32). The selected measurements are stacked.

The active ICU performs a detection of the outliers on fluxes and centroids of stacked data. The mean of the valid stacked measurements (flux and centroids) are computed and buffered waiting for compression and transmission to the SVM.

In configuration mode, the main functions of ICU are to transmit the star catalogues and all other configuration parameters to the DPUs, to compress full-frame images sent by the DPUs, to pack and transfer to SVM all the data from DPUs necessary for subsequent validation of on-ground operations.

The expected data volume (adding 40% contingency) is roughly 212 Gb/day (imagettes, photometric data, centroid data, raw images, etc). Presently, the available TM rate is 106 Gb/day; therefore, ICU will compress the data by a factor of 2 at least, without loss of information.

The ICU shall manage an input average data-rate from N-DPU and F-DPU of about 12 Mbps and an average output data-rate to the SVM of about 1.5 Mbps (16×735 kbps from the N-DPUs + 2×57 kbps from the F-DPUs). These average data-rates can be easily managed by the standard SpaceWire link, running up to 100 Mbps.

The ICU shall be in charge of the in-flight maintenance of the N-DPU application software (scientific SW) and its own SW. The N-DPU and ICU application software shall be reconfigurable during the flight.

The ICU electronics architecture is shown in Figure 4.10. It includes a Motherboard, 2 processor modules (AT697F - LEON2, SPARC V8), 2 I/O & Memory modules, and 2 Power supply modules.

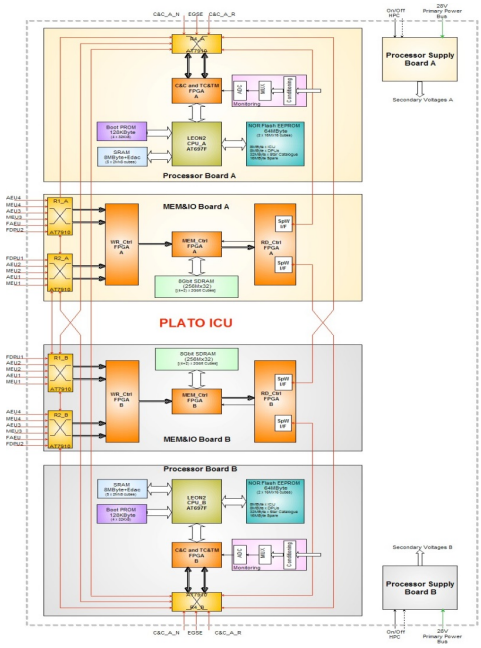

Figure 4.10: ICU overall architecture block diagram (main and redundant).

4.6 Payload Budgets

4.6.1 Telemetry data budget

Overall TM budget	
Daily volume for all normal cameras (science data)	97.6 Gb
Daily volume for all fast cameras (science data)	2.2 Gb
Daily for all cameras (with compression, without header)	99.8 Gb
CCSDS packet header overhead	0.6%
Data auxiliary header overhead	2.5%
Total daily volume (with compression, with headers)	**103 Gb**
Available data rate	**109 Gb**
Margin	6 Gb (6%)
Instantaneous rate ICU to SVM	*1.19 Mbps*

4.6.2 Payload mass budget

(in kg)	Per unit w/o uncert.	N Unit	Total w/o uncert.	Total with 20% uncert.
Fast camera				
TOU w/o baffle	8.856		17.712	
Baffle assembly	0.740		1.480	
Baffle cone	0.262		0.524	
FPA	1.320		2.640	
I/F TOU-FPA	0.104		0.208	
Therm. equipment	0.400		0.800	
Total w/o FEE	(11.682)		(23.364)	
F-FEE	1.400		2.800	
Total fast camera	**13.082**	**2**	**26.164**	**31.397**
Norm. Camera 1&4				
TOU w/o baffle	8.856		141.696	
Baffle assembly	0.740		11.840	
Baffle cone	0.320		5.120	
FPA	1.550		24.800	
I/F TOU-FPA	0.104		1.664	
Therm. equipment	0.400		6.400	
Total w/o FEE	(11.970)		(191.520)	
N-FEE	1.300		20.800	
Total norm. camera	**13.270**	**16**	**212.320**	**254.784**
Norm. Camera 2&3				
TOU w/o baffle	8.856		141.696	
Baffle assembly	0.740		11.840	
Baffle cone	0.234		3.744	
FPA	1.550		24.800	
I/F TOU-FPA	0.104		1.664	
Therm. equipment	0.400		6.400	
Total w/o FEE	(11.884)		(190.144)	
N-FEE	1.300		20.800	
Total norm. camera	**13.184**	**16**	**210.944**	**253.133**
Electronics				
N-AEU	4.650	4	(18.6)	(2.3)
F-AEU	2.300	1	(2.3)	(2.8)
MEU	4.500	4	(18.0)	(21.6)
FEU	4.500	1	(4.5)	(5.4)
ICU	6.500	1	(6.5)	(7.8)
Total electronics			**49.9**	**59.9**
Total payload			**499.3**	**599.2**

This mass budget is compliant with the allocated mass of 600.0 kg, including 20% uncertainties. Note that it is based on a design with good maturity, especially for the cameras, which represent a large fraction of instrument mass.

4.6.3 Payload power budget

(in W)	Per unit	Number of box	Power w/o uncertainties	Power with 20% of uncertainties	Remarks
Camera					
Telescope thermal	2.0	34	68.0	81.6	2W shall be considered as the mean value per camera. It depends on location on the OB
Normal FPA	0.55	32	17.6	21.1	
Normal FEE	6.4	32	204.8	245.8	
Fast FPA	0.8	2	1.6	1.9	
Fast FEE	13.0	2	26.0	31.2	
Electronics boxes					
Normal AEU	28.0	4	112.0	134.4	
Fast AEU	19.0	1	19.0	22.8	
MEU (4 DPU)	43.8	4	175.2	210.2	
FEU (2 DPU)	20.0	1	20.0	24.0	
ICU	19.8	1	19.8	23.8	
Heating			**68.0**	**81.6**	
Others			**596.0**	**715.2**	
Total			**664.0**	**796.8**	

This budget is fully compliant to the allocated power consumption of 820 W including 20% uncertainties.

4.7 Flexibility of the PLATO payload design

Four major scientific performance indicators can be identified for the PLATO mission:

- The total number of stars that will be monitored for long intervals of time (2 to 3 years), down to a given photometric noise level. This performance indicator depends in a complex way on a combination of the field-of-view of each individual camera, the configuration of the cameras in the proposed overlapping-line-of-sight concept, the pupil size of each camera, and finally the total duration of the mission, i.e., the number of long monitoring phases that the mission can afford.
- The total number of stars that will be monitored for shorter intervals of time (2 to 5 months), down to a given photometric noise level. In addition to the characteristics listed in the previous item, this indicator also depends on the exact strategy of the step-and-stare phase.
- The total number of stars that will be monitored for long intervals of time (2 to 3 years), down to a given magnitude. This performance indicator depends on the global field of view of the instrument and on the total duration of the mission.
- The total number of stars that will be monitored for shorter intervals of time (2 to 5 months), down to a given magnitude. In addition to the characteristics listed in the previous item, this indicator also depends on the exact strategy of the step-and-stare phase.

It is clear from the list of indicators above, that in order to maximise the science impact of PLATO, we need to maximise at the same time:

- the total duration of the mission,

- the field-of-view of each camera,
- the global field-of-view of the instrument,
- the pupil size of each camera,
- the number of cameras,
- the flexibility of the step-and-stare phase observation strategy.

The current instrument and mission baseline as described in the previous sections is one possible point in this complex multi-dimensional parameter space. The PLATO assessment and definition study have shown that this point indeed corresponds to a globally optimised situation.

However, should some of the characteristics of the present baseline be descoped in future phases of the project, the impact of such potential descoping would have to be studied in detail. Descoping one of the above characteristics might be compensated by an upgrade in other characteristics. Trade-offs for departures from the current baseline may be imposed in the future by technical, financial or programmatic considerations. In such circumstances, the PLATO Science Team, with the help of the PMC, will have to review and rank the scientific performance indicators listed above, in order to provide guidance to the PLATO mission management teams as to the best compromise for an updated baseline.

PLATO, with its concept involving a set of identical instruments, and its observation strategy divided into long and short monitoring phases, is an extremely flexible mission, and certainly offers several satisfactory configurations.

4.8 Payload performance

Here we describe the expected scientific performances of the current mission baseline. These estimates are based on the best knowledge of the instrument, of the characteristics of the fields and of the behaviour of the targets to be observed. Most of these performances are derived from models (e.g., star density in the observed fields) and from the instrument end-to-end simulator developed during the study and updated with the latest parameters of the instrument baseline.

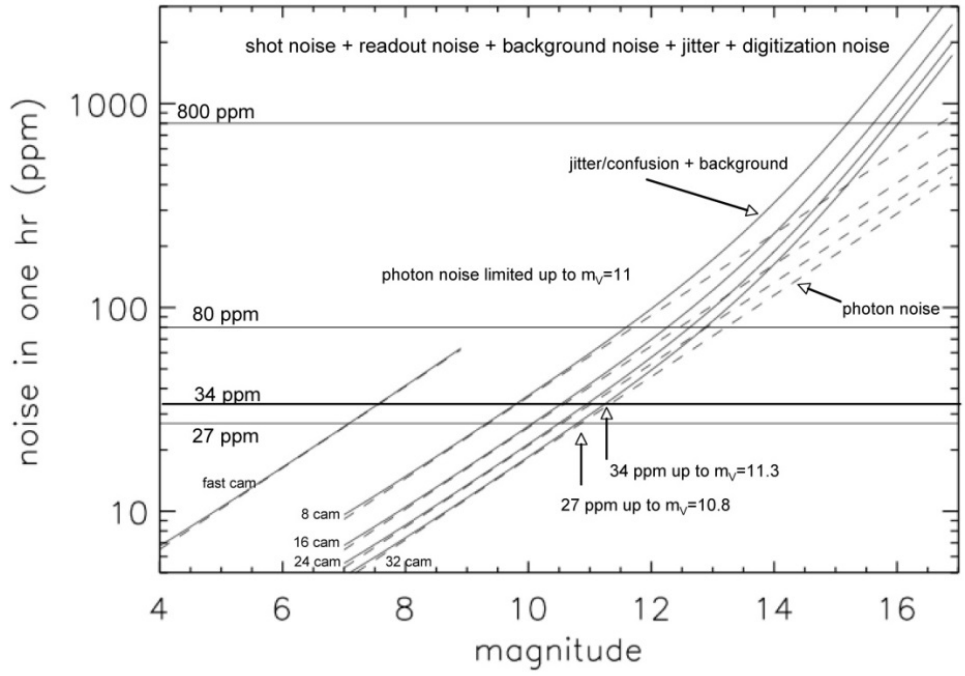

Figure 4.11: Overall noise performances of the PLATO instrument, including jitter correction

The PLATO end-to-end simulator was used to generate simulated light curves for various sets of stars representing realistic portions of the fields to observe. All known sources of noise were introduced in these simulations, including photon noise, readout noise, jitter noise, background noise, etc. The simulations also assume the standard on-board and on-ground data treatment system, including on-board weighted mask photometry, and on-ground a posteriori jitter correction.

Table 4.3: A summary of PLATO scientific performance evaluation

PLATO star sample	# of stars			
	after two long monitoring phases 4,300 deg^2	science requirement	incl. step-and-stare phase 20,000 deg^2	science requirement
P1: dwarfs/sub-giants later than F5, noise ≤ 34 ppm in 1 hour	21,300	20,000	85,000	n/a
P2, P3: dwarfs/sub-giants later than F5, $m_V \leq 8$, noise ≤ 34 ppm in 1 hour	1,250	1,000	3,100 (≥ 5 months)	3,000
P4: M dwarfs, noise ≤ 800 ppm in 1 hour	> 5,000 (TBC)	5,000	> 5,000 (TBC)	5,000
P5: dwarfs/sub-giants later than F5, noise ≤ 80 ppm in 1 hour	267,000	245,000	1,000,000	n/a
# dwarfs/sub-giants later than F5, $m_V \leq 11$	36,000	maximise	145,000	n/a

The results of these simulations were used to validate simplified models of the instrument and data treatment system, with which extensive computations were performed in order to evaluate the global performance of the mission, as shown in Figure 4.11.

For each portion of the global field-of-view of the instrument, covered by either 8, 16, 24 or 32 normal cameras, the mean magnitude down to which various levels of noise are reached were computed using this model, then the star density model was used to derive the corresponding numbers of stars observable during the mission. Similar performance calculations were also performed for the two fast cameras.

The basic outcome of these performance evaluations is summarised in Table 4.3. For this evaluation, we have assumed two long runs of 2 years each, and a 2 year step-and-stare including the following successive runs: 3×5 months, 1×4 months, 1×3 months, 1×2 months.

As can be seen, in this evaluation of the performance of the instrument baseline all scientific requirements are well met, and some are even significantly exceeded.

5 Mission design

5.1 Mission implementation

PLATO will perform the scientific observations in an "operational orbit" around the Earth-Sun Lagrange Point 2 (L2). Such operational orbit is defined in as a free-insertion, large amplitude, **eclipse-free** libration orbit around L2. This orbit is unstable and shall be maintained by regular station-keeping manoeuvres every 30 days. The angular size of the libration orbit seen from the Earth is approximately 33° in the ecliptic plane and 25° out of this plane. The launch window for reaching such an orbit opens every day for at least 45 minutes over a period of at least 2 weeks out of every 4 weeks. PLATO will be launched from Kourou by a Soyuz 2-1b rocket with Fregat upper stage into a direct transfer trajectory to the operational orbit. The transfer will last approximately 30 days. Trajectory correction manoeuvres shall be performed by the spacecraft 2, 5 and 20 days after the separation from the Fregat (occurring about 1500 s after lift-off) in order to remove the launcher dispersions and correct the perigee velocity.

The PLATO mission profile consists of the following phases:

- Pre-launch Phase, from launch campaign preparation to launch vehicle lift-off.
- Launch and Early Orbit Phase (LEOP), from lift-off to the completion of the first trajectory correction manoeuvre performed by the spacecraft on day 2 after the separation from the Fregat upper stage.
- Transfer Phase, from the end of the LEOP to the attainment of the operational orbit around L2.
- Commissioning Phase, starting during the Transfer Phase and running in parallel to it (and after if necessary) till the completion of the check-out of the spacecraft and of the check-out and calibration of the Payload with completion maximum 2 months after the arrival in the operational orbit.
- Nominal Science Operations Phase, starting at the end of the Commissioning, consisting of a *Long-Duration Observation Phase* and a *Step-and-Stare Observation Phase* lasting 6 years in total.
- Extended Science Operations Phase, starting at the completion of the Nominal Science Operations Phase and lasting up to 2 years.

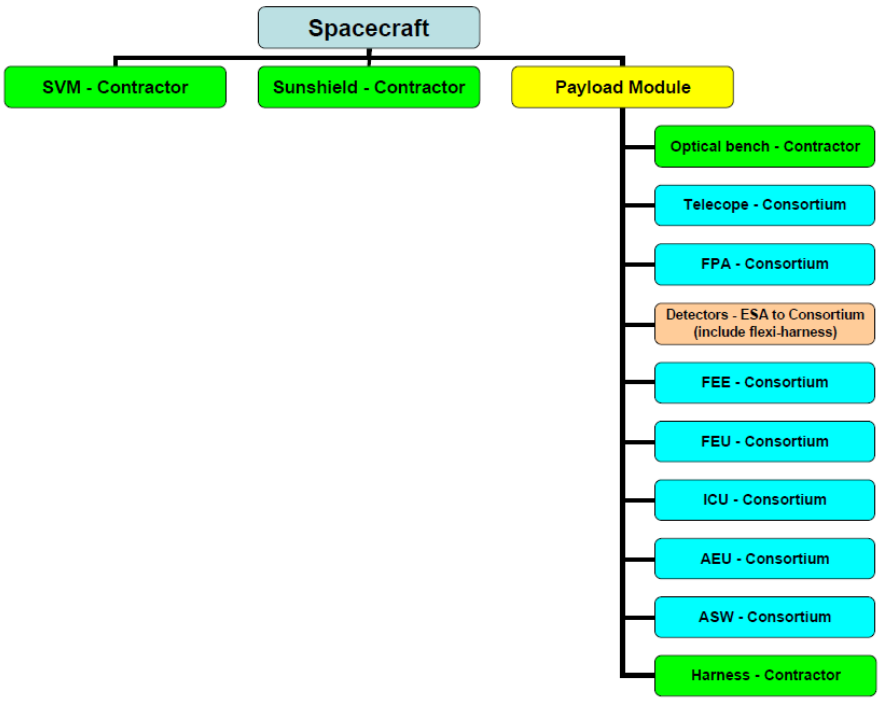

Figure 5.1: The PLATO Product Tree

5.2 Overall spacecraft configuration

The PLATO spacecraft is configured with three main modules that can be individually integrated and tested:

- **Payload Module** (PLM), the full set of Instruments as well as the optical bench, supporting structures and the hardware thermal control.
- **Service Module** (SVM), the part of the Spacecraft that supports the PLM and the Sunshield.
- **Sunshield** (SSH), the part of the Spacecraft that shields the payload from the Sun, as well as generates power via body-mounted solar cells.

The top-level product tree of the PLATO spacecraft resulting from this system architecture and from the definition of the reference Payload is provided in Figure 5.1. Within the PLM, the products under the responsibility of the PLATO Mission Consortium (PMC) will be delivered to the industrial Prime Contractor as customer furnished equipment (CFE) by ESA for their integration in the spacecraft.

5.3 Mission operations

5.3.1 Orbit

PLATO shall orbit the Earth-Sun Lagrange Point 2 (L2). Such operational orbit is defined as a free-insertion, large amplitude, **eclipse-free** libration orbit around L2 and is shown in Figure 5.2.

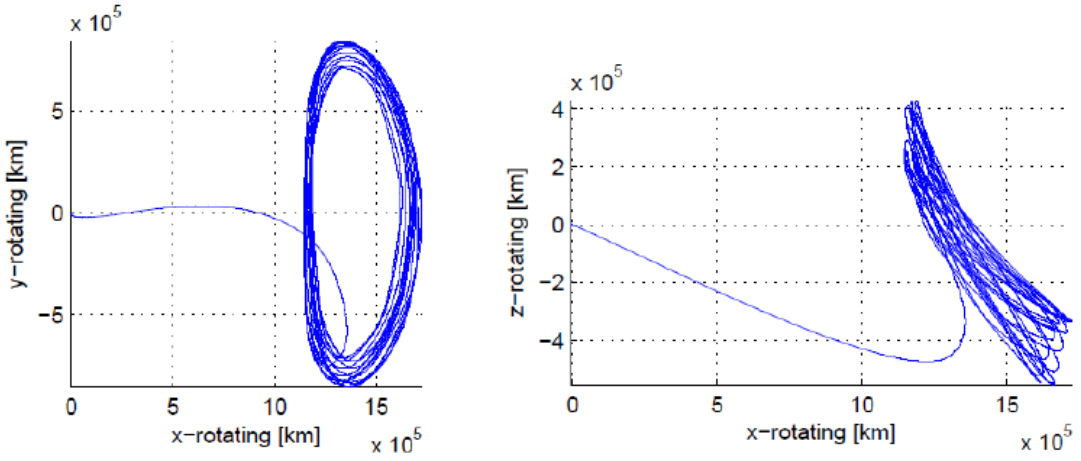

Figure 5.2: PLATO Orbit in L2.

5.3.2 Mission phases

From the duration and composition of the various phases and sub-phases, the overall mission timeline shown in Figure 5.3 has been obtained. From the end of the Transfer Phase to the completion of the Extended Science Operations Phase, PLATO will spend in total 8 years and 2 months around L2. In the same figure, the spacecraft orbits and the ground stations that will ensure the telecommunications coverage during the various phases are also indicated. During LEOP and the first day of the Transfer Phase, the ESA stations at Kourou (15-m), New Norcia (35-m) and Cebreros (35-m) will be used for contact with the spacecraft. After the first day of the Transfer Phase and till the end of the Extended Science Operations Phase, the ESA station at New Norcia (35-m) shall be used for contact with the spacecraft, with Cebreros (35-m) as backup and Kourou (15-m) as backup for critical/contingency operations. During the Nominal and Extended Science Operation Phases a 4 hour communication session per day with the ground station will be available: 0.5 hours allocated to communication setup and ranging and 3.5 hours to data transmission.

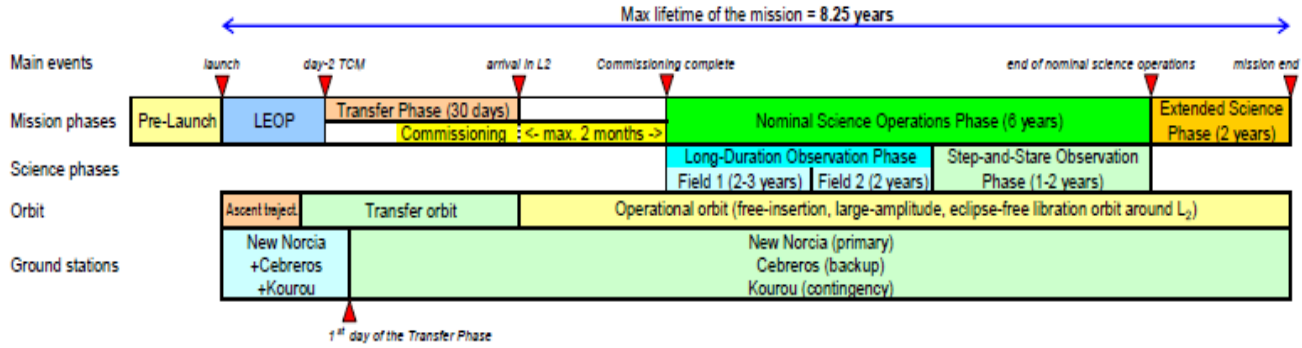

Figure 5.3: PLATO Mission Phases

5.3.3 Observing strategy

PLATO has a flexible observing approach. Two observing strategies, long continuous pointings versus shorter coverage of different fields, complement each other and allow for a wide range of different science cases to be addressed. Long duration pointings will be devoted to surveys for small planets out to the Habitable Zone of solar-like stars. Short pointings will be devoted to shorter-period planet detections and will address a number of different science cases.

In its nominal science operation phase, PLATO's current baseline observing strategy combines:

- Long-duration Observation Phases, consisting of continuous observations for two sky pointings, lasting a minimum of 2 years with a maximum of 3 years for the first pointing, and 2 years coverage for the second pointing.
- Step-and-Stare Operation Phases, consisting of shorter-period observations of several sky fields which will last 1–2 years total, depending on the duration of the long duration phases. Sky fields in this phase will be observed for at least 2 months, up to a maximum of 5 months.

The proposed observing strategy aims at covering a large fraction of the sky (see Figure 5.4), thereby maximising the number of well characterised planets and planetary systems, in combination with wide-angle long pointings that will significantly increase the number of accurately known terrestrial planets at intermediate distances up to 1 au. The latter detection range will be unique to PLATO and is not covered by any other planned transit survey mission nor can it be achieved for a large number of RV detections in any feasible observing time.

In view of the exceptionally fast development of exoplanet science, the order of long and short runs will be re-investigated after mission selection and adapted to the needs of the community by 2022/24, e.g., to investigate earlier in the mission interesting sky regions and targets with a step-and-stare run. The PLATO observing concept offers sufficient flexibility.

Each of the long-duration observations will monitor a separate field in the sky that together will be encompassing a minimum of 20,000 dwarf and sub-giant stars of spectral type later than F5, each sufficiently bright to reach a photometric accuracy $\leq 3.4 \times 10^{-5}$, in one hour. The step-and-stare phase will consist of a series of separate observations each lasting up to 5 months. The rationale is to extend the surveyed area of the sky and to further characterise planetary candidates of specific interest found during the long monitoring phases (e.g., long period candidates that have shown only two transits).

The photometric precision required by the mission puts stringent requirements on the pointing stability and accuracy of the S/C that must reach 0.2 arcsec per $Hz^{1/2}$ (Relative Pointing Error) over time scales of 25 seconds to 14 hours.

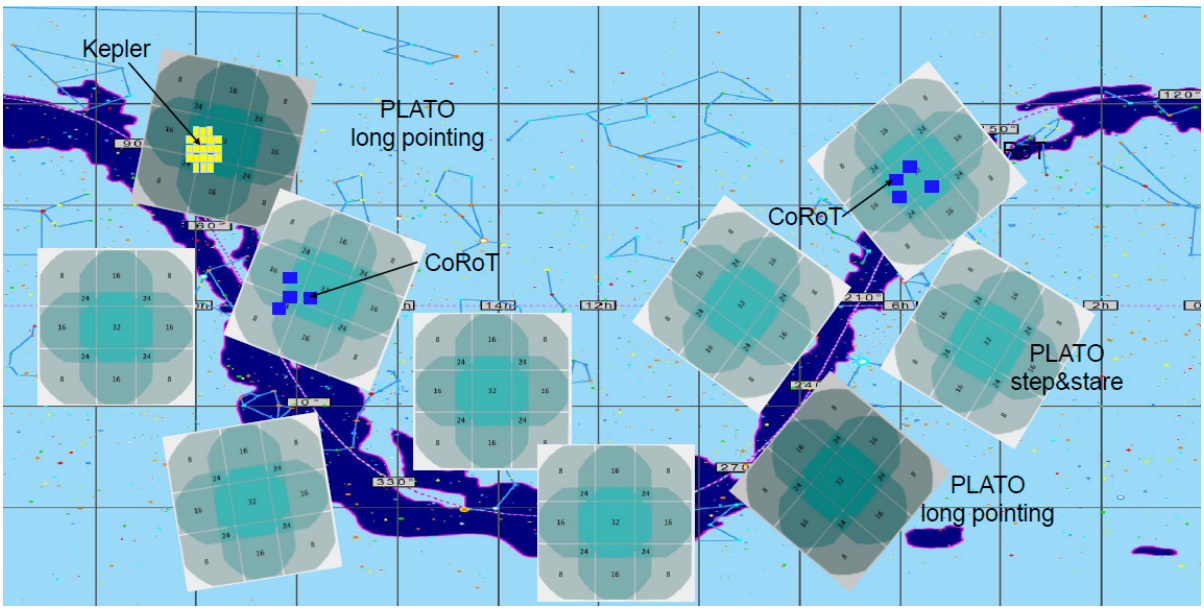

Figure 5.4: Schematic comparison of observing approaches. Blue squares: CoRoT target fields in the galactic centre and anti-centre direction. Upper left corner (yellow): the Kepler target field. Large squares: size of the PLATO field. A combination of short and long (darker) duration pointings is able to cover a very large part of the sky. Note that the final locations of long and step-and-stare fields will be defined after mission selection and are drawn here for illustration only.

During long observations, the Spacecraft must maintain the same line-of-sight (LoS) towards one field for up to several years. However, the Spacecraft must be periodically re-pointed in order to ensure the solar arrays are pointed towards the Sun. This is achieved by rotating the Spacecraft around the LoS by 90° roughly every 3 months, as shown in Figure 5.5.

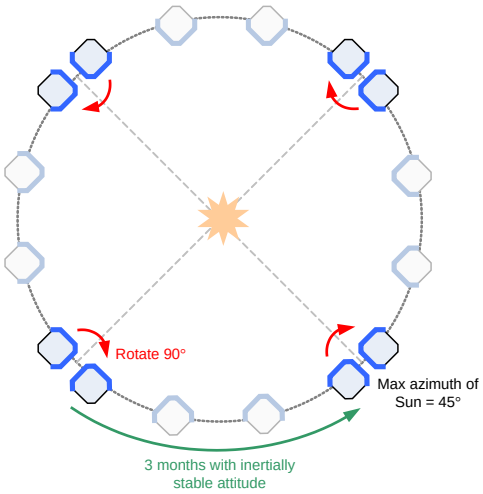

Figure 5.5: Spacecraft Rotation around Payload LOS during one Orbit

These mission requirements have led to the definition of two candidate design concepts for the PLATO spacecraft developed by the respective Industrial contractors, Astrium/EADS, and Thales Alenia Space (TAS).

5.4 Astrium design of the PLATO spacecraft

5.4.1 Overall configuration

The spacecraft is based on a prism-shaped structure with equilateral triangle basis (see Figure 5.6 and Figure 5.7). Three main vertical panels of 2 m×5 m constitute the all-CFRP main structure, together with closing panels and stiffening struts. The 34 instruments that constitute PLATO's payload are installed horizontally on one of the 3 vertical panels.

This vertical accommodation offers the best area for accommodation of the payload, while the load of the significant payload mass is directly carried by the main structure. In consequence, the central main structure constitutes the optical bench, and together with cameras and electronics, they constitute the Payload Module (PLM). Cameras are attached through an individual camera support structure, and are installed in 34 holes on that panel. This design allows preserving a reasonable centring of the spacecraft Centre of Mass, and separates the Front-End Electronics from the main panel of the optical bench, offering a natural filtering of FEE dissipation noise onto Optical Bench thermo-elastic performances.

Furthermore the cameras are accommodated on the optical bench so that they fit both the organisation in "subgroups" – with 8 cameras belonging to a given subgroup (see Chapter 4) – and organised in "batches", connected to the same electronics boxes, which allow keeping the electronics directly facing their related cameras, and minimise payload harness mass.

In order to minimise disturbances towards PLM, in particular thermal and thermo-elastic disturbances, the SVM is made of several suspended backpacks. Up to 7 backpack panels are defined, each carrying a consistent set of equipment corresponding to each main functional chain of the Service Module (3 panels for PLM electronics, 1 panel for TT&C, 1 panel for Power, 1 panel for avionics, 1 panel for Reaction Control System, i.e. RCS or Propulsion). Each of them is simple in its design, with a simple plate, isostatically mounted on the main structure and as much as possible thermally isolated from the main structure.

The Propulsion panel is nested within the main structure at the bottom of the satellite, while the 6 other backpacks are installed on one other of the 3 main structural panels, permanently facing the cold space.

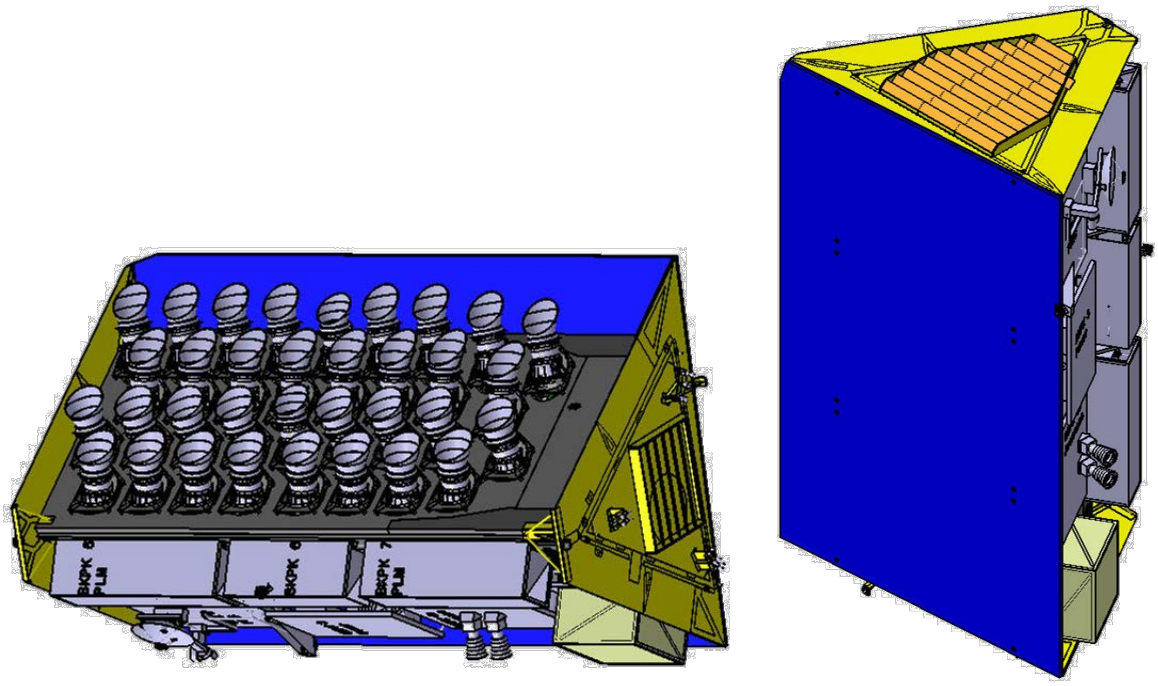

Figure 5.6: Astrium concept - General view showing the PLM side(left) of the spacecraft and the sunshield (right).

The Sunshield is the last major element of the spacecraft. It has a double role: It shall protect payload and electronics from direct illumination by the Sun, and also serves as Solar Array for power generation. It is mainly based on a main flat panel of 3×5 m^2 covered of solar cells facing the third structural panel, plus additional MLI on the top and bottom sides of the satellite. The design is therefore based on an inversion of the classical separation of SVM and PLM, while the PLM constitutes the main satellite bus, and the SVM is mounted isostatically on it.

The triangular shape of the spacecraft allows both the payload side and the SVM side to be permanently in the shade, once shielded by the Sunshield, for any ecliptic latitude of observation higher than 60° (in Northern or Southern hemisphere), as specified for the design-driving long-duration observation phase. The main panel of the sunshield provides 15 m² of surface potentially covered with solar cells, with a solar incidence that never falls below 51°, i.e., providing comfortable margins with respect to the spacecraft power needs.

The mass of the PLATO spacecraft is about 2,000 kg at launch, and uses about 1,6 kW of power in normal operations, all margins included. This allows us to have a growth margin of nearly 5% in mass with respect to the Soyuz capacity, and a similar growth margin around 5% with respect to the maximum available area for the Solar Array.

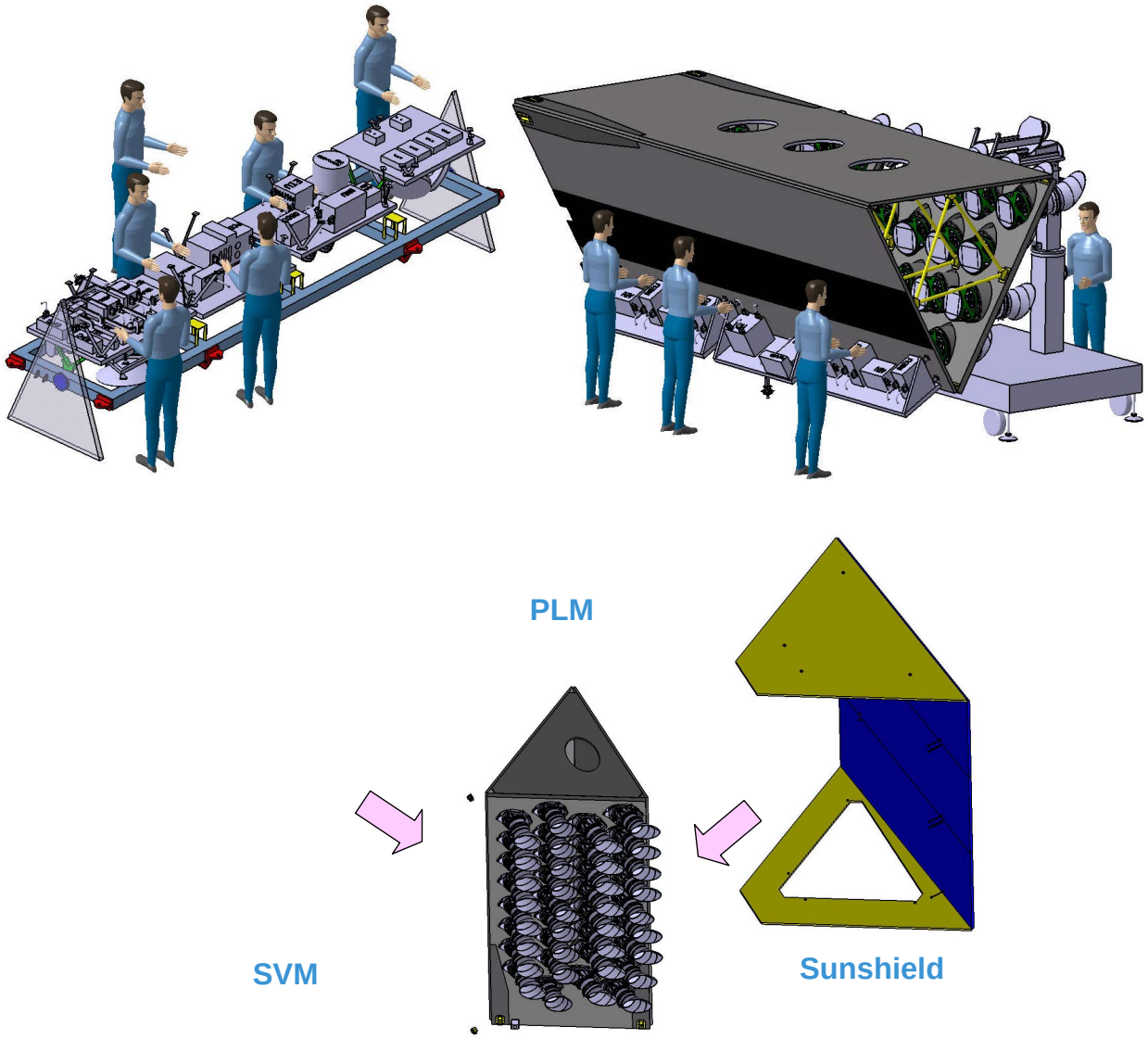

Figure 5.7: Astrium concept - The spacecraft is organised in 3 main parts, i.e,. the payload module (PLM), the service module (SVM) and the sunshield. The SVM (left) and the PLM (right) can be integrated in parallel.

5.4.2 Avionic architecture

The main functional chains are:

- the payload functional chain made of the cameras and their electronics;
- the On-Board Computer (OBC), Mass-Memory Unit (MMU), and Remote Interface Unit (RIU);
- the Power System, in charge of providing electrical power to all spacecraft equipment, thanks to the Solar Array (formally falling into the "Sunshield" Subsystem), Power Control and Distribution Units, and battery. The entire spacecraft harness also falls into the perimeter of the power subsystem;
- the AOCS, based on Star Trackers and gyroscopes as sensors (with Sun sensors for safe mode), and 4 reaction wheels as actuators;
- the Reaction Control System, which is a mono-propellant propulsion system (hydrazine), with 2 redundant branches of 7 thrusters, spread on 4 separate pods;
- the Telemetry, Tracking and Command subsystem (TT&C), which is based on a X-band only, with 2 LGA for LEOP and contingency situations and a 2-axis-steerable High Gain Antenna of 50 cm of diameter for nominal communications;
- the Thermal Control System, composed of passive thermal items (MLI, radiators), and active control (thermistors and heaters);
- the structure system, made of primary and secondary structure parts. Structure and thermal are grouped into a single subsystem.

The spacecraft functional architecture matches well with the electrical architecture.

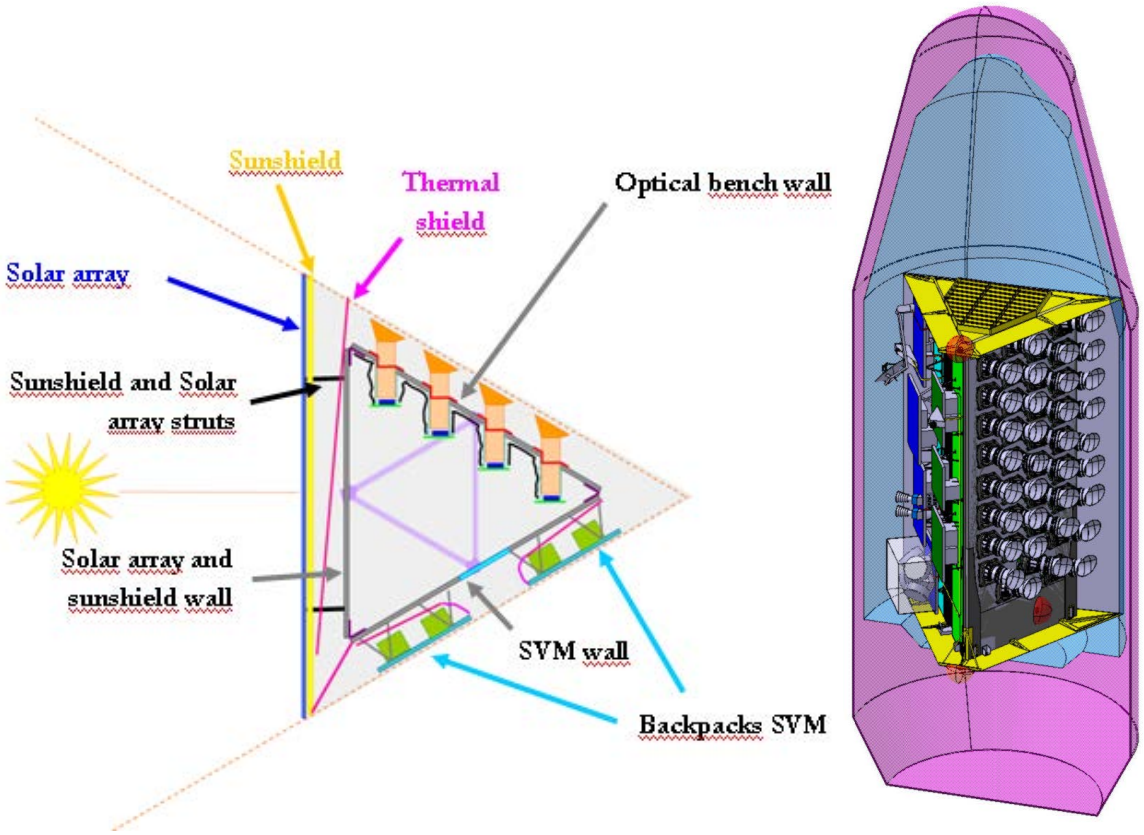

Figure 5.8: Astrium concept - PLATO general architecture with respect to Sun illumination (left) and within the spacecraft fairing (right).

5.5 TAS design of the PLATO spacecraft

5.5.1 Overall configuration

The PLATO spacecraft is composed by three main modules that can be individually integrated and tested (Figure 5.9):

- **Payload Module** (PLM), that functionally includes the entire Payload (i.e., the items supplied as CFE), the Optical Bench (OB), the supporting and interface structures, the thermal control hardware and the harness interconnecting the P/L units among them and with the SVM.
- **Service Module** (SVM), that provides the spacecraft subsystems supporting the P/L functioning and operation, and provides the structural interfaces to the PLM, the Sunshield, and the launch vehicle. The SVM hosts also the P/L electronics boxes (MEU, FEU, N-AEU, F-AEU, ICU), which functionally belongs to the PLM.
- **Sunshield** (SSH), that shields the P/L instruments installed on the OB from the solar radiation and supports the Photovoltaic Assembly (PVA) that supplies electrical power to the whole spacecraft.

The SVM is octagonal-base prism built around a central cone that provides the interfaces with the launcher and with the Optical Bench of the PLM and hosts the propellant tanks. The lateral panels of the SVM accommodate the S/C equipments and the P/L electronics boxes.

The external lateral panels of the SVM accommodate the radiators and the insulators for the thermal control of the internal equipments. The following equipments are also installed outside the SVM:

- Two star trackers, placed on the upper platform, $-X_{SC}$ side, a position very close to the PLM optical bench.
- Four clusters of 4 thrusters each, utilised for the spacecraft attitude control, placed on the lower platform and protruding from the 45° tilted sides.
- Two clusters of 2 thrusters each, utilised for the orbital manoeuvres, placed on the lower and upper platforms and protruding from the $+X_{SC}$ and $-X_{SC}$ sides respectively.
- Two low-gain antennas (LGA), placed on the lower platform, $+X_{SC}$ and $-X_{SC}$ sides respectively.
- A high-gain antenna (HGA) with its deployment and pointing mechanism, placed under the lower platform so that it is deployed towards the $+X_{SC}$ side.

A cluster of 4 Fine Sun Sensors is accommodated on top of the $+X_{SC}$ side of the Sunshield.

In its deployed position, the HGA beam (cone with 5° half-angle at 20 dBi gain) is free to span the whole working range necessary to point the Earth in any S/C position on its libration orbit around L2 and in any nominal attitude assumed during the Long-Duration Observation Phase: azimuth = ±85°, elevation = ±55°. The equipments inside the SVM are mounted on the lateral panels grouped per subsystems (Figure 5.10):

- TT&C subsystem equipments mounted on the $+X_{SC}+Y_{SC}$ panel.
- AOCS equipments mounted on the $+X_{SC}-Y_{SC}$ panel, with the exception of the ICU of the gyroscope, installed alone on the $-Y_{SC}$ panel for a better insulation and a more stable thermal environment.
- CDMU mounted on the $+Y_{SC}$ panel.
- EPS equipments mounted on the on the $-X_{SC}$ panel.
- P/L electronics boxes distributed on the $-X_{SC}+Y_{SC}$ and $-X_{SC}+Y_{SC}$ panels respectively.

Each lateral panel can be individually dismounted to facilitate the equipment integration. In particular, the P/L electronics panels can be installed on a suitable MGSE in proximity of the Optical Bench during the integration and functional verification of the PLM.

The Optical Bench is a step-based structure (each step bears a set of cameras) connected by an isostatic mount (formed by three bipods) to brackets installed on the upper edge of the central cone.

The Sunshield surrounds the Optical Bench following the octagonal shape of the SVM. The Sunshield has been designed to keep the Optical Bench in shadow under Sun aspect angles that exceeds the values defined by the nominal sky observation strategy during the Long-Duration Observation Phase. The shading effect of the Sunshield is shown in Figure 5.11 for different values of the Sun azimuth and elevation angles, The Sunshield and the Optical Bench are designed also to avoid any vignetting of the camera UFOV (Figure 5.12).

The spacecraft dimensions are compatible with the Soyuz fairing envelope, considering a ST type fairing (Figure 5.13). The interface between the spacecraft and the launcher is implemented by a Standard 1666-SF type separation system.

5.5.2 Avionic Architecture

The services provided by the spacecraft avionics for the proper mission operation accomplishment are:

- power conditioning and distribution to the spacecraft and payload units under a 28V regulated and protected form;
- spacecraft data handling tasks;
- reception via the X-Band receivers of ground telecommands;
- collection and storage of science data and satellite housekeeping data for the 72 hours specified functional autonomy duration;
- capability to store on board up to 72 hours Mission Timeline;
- downlink of stored and real-time data using the X-Band transmitter;
- spacecraft accurate time maintenance and distribution to instruments and AOCS;
- radiofrequency signal reception and demodulation for the uplink, modulation and transmission for the downlink;
- thermal control of the spacecraft and FPA via temperature sensors-heaters loops;
- spacecraft attitude and orbit control, including AOCS sensors acquisition and processing, actuators and thrusters commanding;
- spacecraft failure detection isolation and recovery to satisfy fault protection and autonomy requirements.

The above functions are implemented with the following main units:

- Centralised On-Board Computer (CDMU) providing science data storage, spacecraft and AOCS Command, Control and Data processing, It is based on modular unit including core standard boards, mass memory boards and dedicated I/O boards to interface AOCS and S/C unit/devices. It interfaces Instrument Control Unit with SpaceWire serial links and the other units by Mil-Std-1553 bus, serial lines, analogue and discrete interfaces.
- PCDU providing: Solar Array regulation, bus regulation, power outlet protection and distribution. The regulated 28Vdc power bus will be distributed by independent outlets protected by LCLs/FCLs. The PCDU interfaces with the panels and the battery used to supply the Spacecraft during the LEOP phases, in case of attitude loss or whenever Solar Array power is not sufficient. The PCDU interfaces with CDMU for command and control via 1553 MIL bus.
- X-Band Transponders to handle the telemetry downlink, ranging operations and TC uplink based on X-band communication capability. The Transponders are controlled by CDMU through 1553 bus.
- AOCS sensor and actuators for attitude commanding and control. All the AOCS items are interfaced with CDMU by 1553 Mil bus interfaces or by dedicated serial or discrete interfaces.

- Thermal Control. The thermal control is performed through acquisition of temperature sensors and actuation of heater lines. Thermal control maintains units within their proper operative temperature range and guarantees the necessary stability.
- Propulsion based on Hydrazine thrusters.

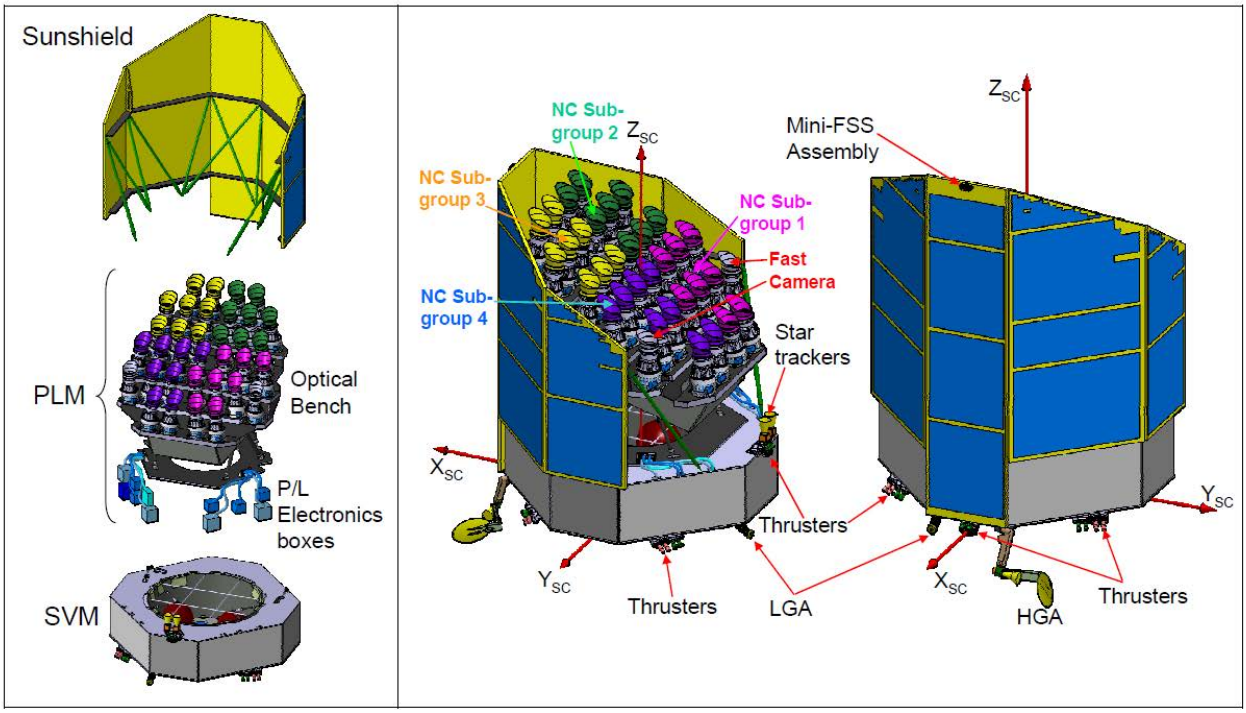

Figure 5.9: TAS concept - PLATO spacecraft configuration and external equipment layout (X_{SC}, Y_{SC}, Z_{SC} = Spacecraft Reference Frame - SRF).

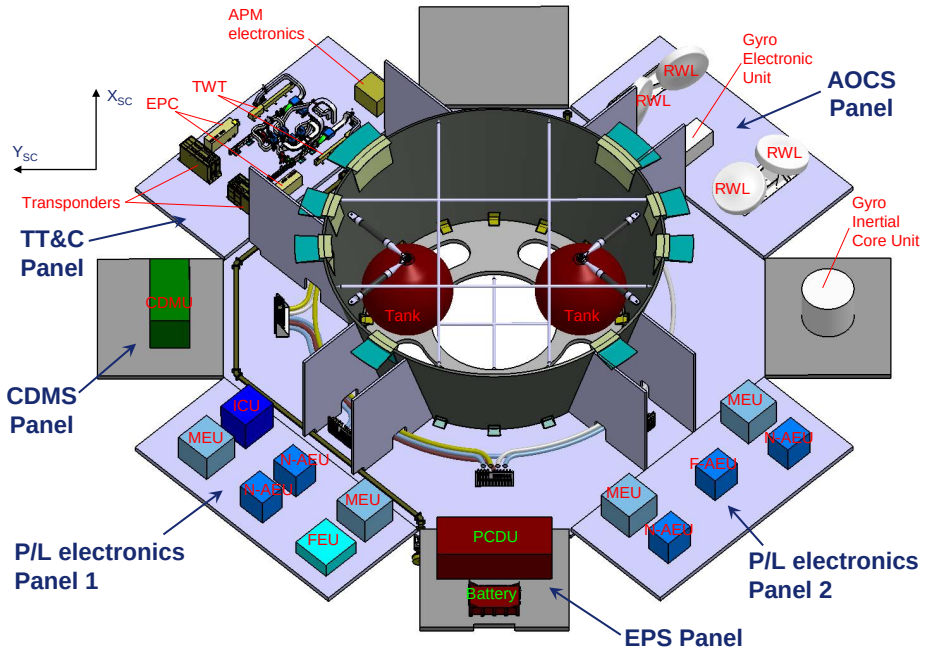

Figure 5.10: TAS concept - Internal view of the SVM showing the equipment accommodation (the lateral panels have been rotated outwards by 90°).

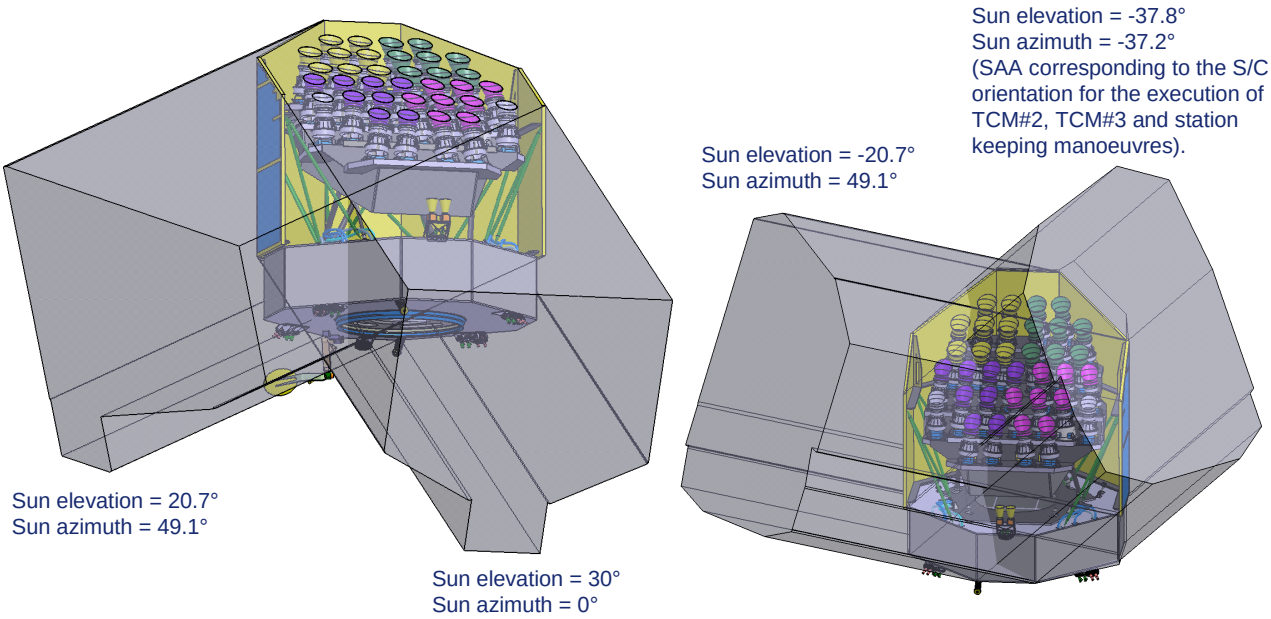

Figure 5.11: TAS concept - Shading effect of the Sunshield for the limit values of the azimuth-elevation angles of the S/C-Sun vector in the SRF.

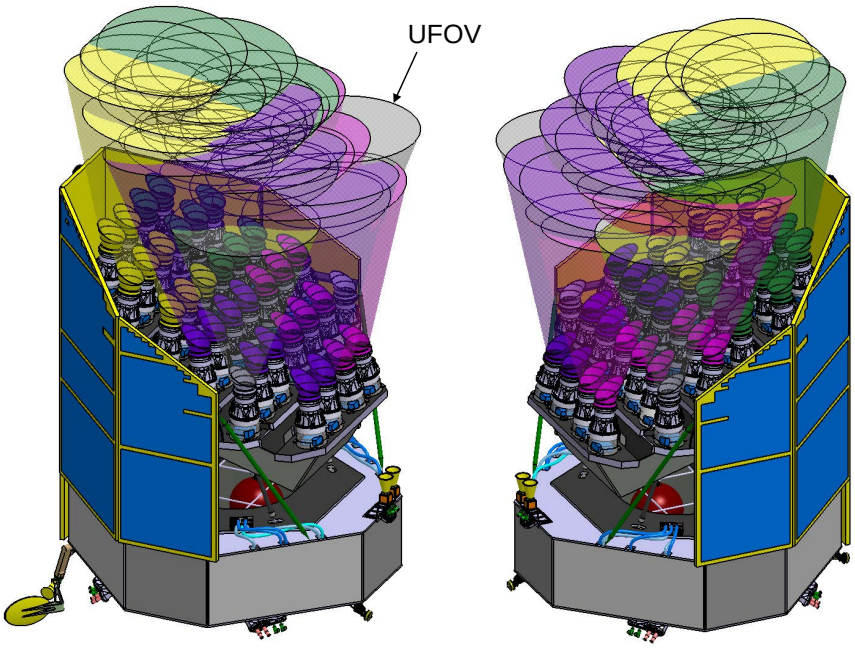

Figure 5.12: TAS concept - Spacing between the cameras UFOV and the Sunshield.

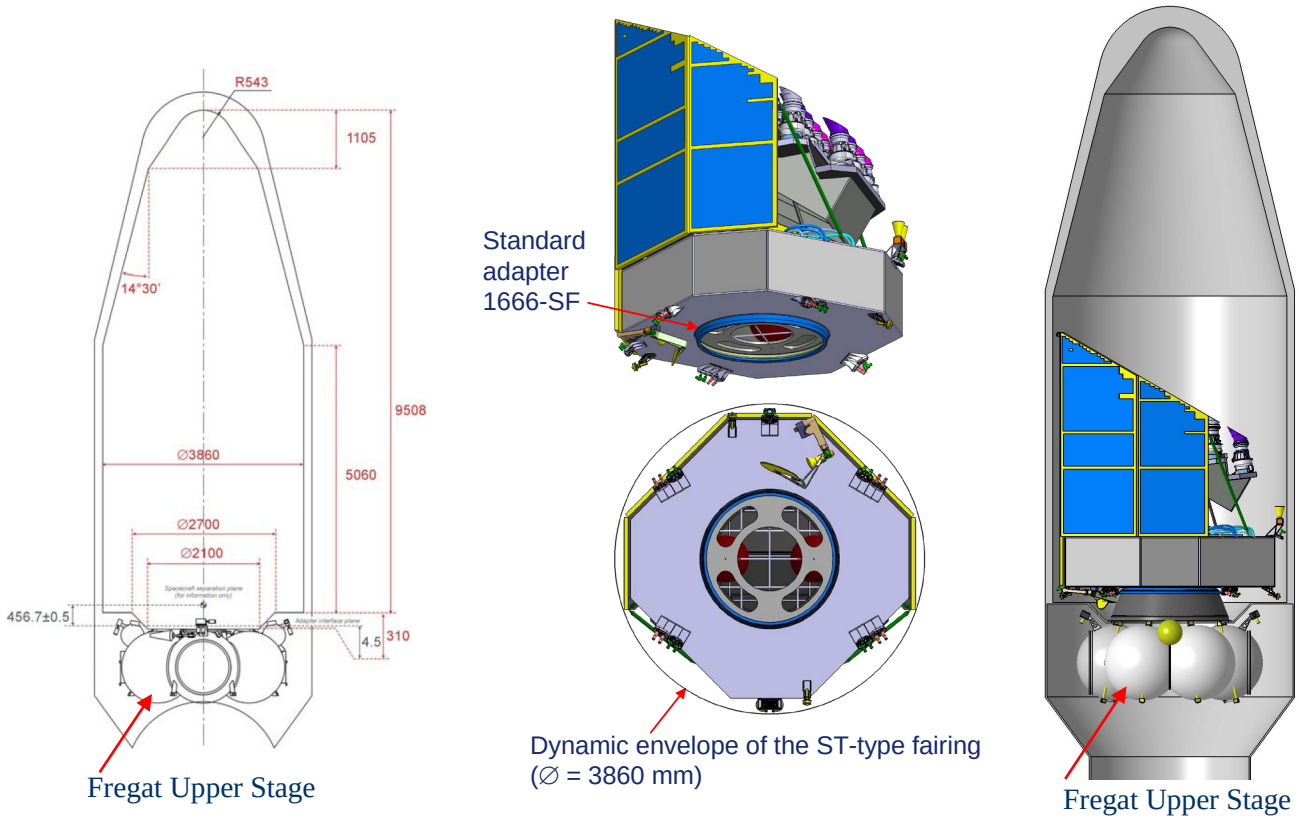

Figure 5.13: TAS concept - Spacecraft launch configuration under the Soyuz ST-type fairing.

The spacecraft has a total dry mass of 1732.1 kg, without system margin. Including the propellant (80.8 kg) and an allocation of 5 kg for balancing mass, the launcher limit of 2100 kg is met with a system margin of 16.3% (282 kg).

The largest power consumption (1645 W, including 20% system margin) occurs in the P/L Observation Mode during the 4-hour daily telecommunication period for the transmission of the collected data to the ground station.

The battery (777 W capacity) supplies power to the load or complements the contribution of the solar array from pre Lift-off to fist Sun acquisition, during the orbital manoeuvres in which the S/C deviates significantly from the nominal attitude, and in case of loss of the nominal pointing following a failure.

The on-board mass memory (capacity = 512 Gbit) can store up to 3 days of science data collected by the P/L and 7 days of housekeeping data collected by the P/L and by the S/C subsystems, with a margin > 50%.

The X-band telecommunication system has a throughput of 8.718 Mbps in downlink, sufficient to transmit to the ground station in 3.5 hours all the science and housekeeping (P/L plus S/C) data stored in the previous 24 hours, plus the housekeeping data collected in real time during the telecommunication period.

5.6 Technological readiness of the PLATO spacecraft

The Service Module and Sunshield of the proposed PLATO spacecraft are heavily based on current technology and heritage from other missions. The AOCS and propulsion subsystems can use off-the-shelf equipment with no development required. Data handling and communications equipment can be performed with current technology, and proposals from industrial contractors are based on modifications of units used in current missions.

The SVM and Sunshield structures will use either qualified- or soon-to-be-qualified materials. There is one mechanism on the spacecraft (2-DOF high-gain antenna pointing mechanism), which at most will require a

minor modification to accommodate the large azimuth and elevation range of the Earth as seen by the Spacecraft. All platform units TRL is 5 and above.

In the payload design there are no show stoppers. Critical aspects exists (e.g., the CCD quantum efficiency, the telescope focusing via thermal control, the complexity of the overall data processing architecture) but all is in reach of the available technology, and the areas requiring development attention are identified. Demonstration of TRL 5 and above is planned in the frame of the Phase B1.

6 Ground Segment

6.1 Overview

The ultimate goal of the PLATO Ground Segment is to deliver a list of confirmed planetary systems, which will be fully characterised by combining information from the planetary transits, the seismology of the planet-host stars, and the follow-up observations. The major part of the PLATO data will become publicly available as soon as it is reduced.

The PLATO Ground Segment consists of two main parts. The PLATO Operations Ground Segment and the PLATO Science Ground Segment.

The PLATO Operations Ground Segment consists of the ESA provided Ground Station Facilities and the Mission Operations Centre (MOC), which operates the spacecraft and creates the telemetry and flight dynamics products.

The PLATO Science Ground Segment consists of the ESA provided PLATO SOC and the PLATO Mission Consortium provided science ground segment components. The Science Ground Segment is responsible for mission planning and the end-to-end handling of the PLATO data and production of the PLATO Mission Products. The PMC part of the SGS consists of a Plato Data Centre (PDC) and the PLATO Science Preparatory Management (PSPM) group.

The SOC and the PDC/PSPM are jointly responsible for preparing and carrying out the science operation phases as regards use of the instrument to achieve the science objectives defined in the Science Management Plan. This will involve provision of the input catalogue to the MOC for uplink to the spacecraft, processing of the dumped data from the instrument, performing quality control of the dumped data and generating level 0, 1 and 2 products to be placed into the PLATO Archive at SOC for access (according to the expiry of the relevant proprietary periods) by the scientific community.

The PDC will provide support for the validation, calibration, and processing of the PLATO observations in order to deliver the PLATO Science Data Products. The PSPM will provide the scientific specification of the high-level scientific algorithms implemented in the PDC, coordinate the ground-based follow-up and scientific community activities, and evaluate the scientific performance of the PLATO data chain.

The PLATO Ground Segment covers the in-flight operations of the satellite, such that the mission objectives can be met.

The roles and responsibilities of the PDC and PSPM are distinct and complementary. During the development phase, they are organised according to the following guidelines: 1) PSPM provides the scientific specifications of the software, 2) PDC translates the scientific specifications into technical specifications, 3) PDC implements the technical specifications, 4) PSPM checks that the PDC software is consistent with the initial scientific specifications; this validation by PSPM occurs within the PDC – a normal part of the development quality assurance process.

Apart from the SOC, the instrument operations dependent section of the Science Ground Segment is composed of the PMC Instrument team who are responsible for contribution to end-to-end testing, maintenance of the instruments, payload monitoring and control specifications, instrument trend analysis, instrument calibration, second-level quality control (on calibrated data). This team will be set-up during the pre-launch phase taking advantage of the experience gathered in previous missions and during the development of PLATO instruments and GSEs.

6.2 PLATO science data products

The baseline science telemetry budget yields a daily uncompressed data volume of 109 Gb. Over a nominal 6 year mission the total science telemetry down-linked will therefore be around 30 TB uncompressed data. The raw telemetry will be reformatted into a standard self-describing format in common use by the astronomical community (FITS).

The three data product levels to be generated from the PLATO mission are as follows:

Level 0

- The validated light curves and centroid curves for all individual telescopes. These are all the downloaded light curves (one each from each star and from each telescope) as well as the centroid curves and validated by assessing the quality and integrity of the data.
- Housekeeping data
- Auxiliary data, e.g., pointing

Level 1

- The calibrated light curves and centroid curves for each star and corrected for instrumental effects e.g., jitter. For all stars, the L1 calibrated data is the basic science-ready PLATO data. For the normal telescopes and for each star, the L1 light curves and centroid curves are (suitably) averaged, and an associated error is provided. The stars for which imagettes are available undergo a specific treatment.
- Auxiliary data, e.g., pointing, time correlation
- Associated calibration data

Level 2

- The planetary transit candidates and their parameters with formal uncertainties.
- The asteroseismic mode parameters with formal uncertainties.
- The stellar rotation periods and stellar activity models inferred from activity-related periodicities in the light curves, with formal uncertainties.
- The seismically-determined stellar masses and ages of stars, (and their formal errors), obtained from stellar model fits to the frequencies of oscillations
- The list of confirmed planetary systems, which will be fully characterised by combining information from the planetary transits, the seismology of the planet-host stars, and the follow-up observations. This represents the most important PLATO (the final and highest level PLATO science) deliverable. The parameters of the confirmed planets will be the orbital parameters, planet size, mass, and age (from the seismology of central stars). Any additional characterisation of the properties of the planetary systems from the long duration PLATO light curves (e.g., secondary transits) and from specific ground-based observations (e.g., planetary atmospheres, imaging, etc) will also be included.

Within the PMC, these three data processing levels are thus organised according to specific PLATO Data Products, from DP0 to DP6, with DP0 and DP1 corresponding to Level 0 and Level 1 data respectively. The Level 2 data comprise DP2 to DP6, listed in Table 6.1 below.

Table 6.1: PLATO Science Data Products

Calibrated light curves and centroid curves	**DP1**	**L1**
Planetary candidate transits and their parameters	**DP2**	**L2**
Asteroseismic mode parameters	**DP3**	**L2**
Stellar rotation and activity	**DP4**	**L2**
Stellar masses and ages	**DP5**	**L2**
Confirmed planetary systems and their characteristics	**DP6**	**L2**

All Level 2 sublevel products will be delivered for ingestion into the archive within 3 months of reception of the data at the PDC. These will be identified as proprietary data. The final Level 2 product, DP6, will take significantly more time to be delivered to the SOC for ingestion into the PLATO Archive due to the links

such product generation has in follow-up observations etc. Upon ingestion of the DP6 products into the archive, the full level 2 product data set will be made public.

6.3 Mission operations

ESA is responsible for the readiness of the ground station facilities. The ESA Deep Space station at Cebreros is baselined as the primary ground station for PLATO operations and is equipped with K (26 GHz) and X band facilities.

MOC is responsible for the availability and operations during the operations phase. Data transfer and supporting infrastructure within the operations ground segment is managed by MOC. The MOC is in charge of the following tasks:

- Monitoring spacecraft health and safety.
- Monitoring the payload safety and reacting to contingencies and anomalies according to procedures provided by the PLATO consortium.
- Alerting the SGS of all significant anomalies or deviations from nominal behaviour of the satellite.
- Executing predetermined procedures to safeguard the spacecraft and payload, and preserve data integrity.
- The uplink of the satellite and payload telecommands.
- The maintenance of the satellite's on-board software.
- The uplink of payload on-board SW executables as generated, validated and delivered by the PDC via the SOC.
- The flight dynamics support including determination and control of the satellite's orbit and attitude.
- Handling and provision of the telemetry to the SOC.
- Production and provision of auxiliary data to the SOC (e.g., orbit files, pointing information).

MOC will keep an archive of the housekeeping telemetry, the telecommand history and other auxiliary mission operations data for up to 6 months from the end of mission (depending on the volume of science data, only short term storage of science data may be provided with long term storage at the SOC) and will keep on hard copy an off-line archive in a secure location for up to 5 years after the end of the operations.

6.4 Science operations and data handling/archiving (SOC)

6.4.1 SOC responsibilities

The ESA Project Manager delegates to the Science Operations Department of the Science and Robotic Exploration Directorate based at the European Space Astronomy Centre (ESAC) the design, development, validation, and operation of the SOC. The SOC is the only interface to the MOC during routine operations. Within the overall ESA responsibility for the PLATO SGS, the SOC coordinates the overall design, implementation and operation of the PLATO Science Ground Segment with the PMC. It is specifically responsible for:

- Acquisition and distribution of spacecraft telemetry from MOC.
- Acting as interface between the PDC and the MOC for payload operations and for all files and procedures required for optimising the quality of the data and safeguarding of the payload.
- The SOC is responsible for the planning, co-ordination & support of a number of calls for proposals, including one taking place 2 years before launch.
- Scientific mission planning based on input from the PDC after endorsement by the PST. In particular, Provision to the MOC of all parameters for each sequence of observations: at each rotation of the satellite (every 3 months), and at each field re-pointing (every 2 or 3 years for the

long sequences, every few months for the step-and-stare phase), the full list of targets with their expected location on the focal planes, and the full list of parameters for each star (essentially photometric mask parameters).

- Quality control: Monitoring of data integrity and quality.
- Fine tuning of on-board software, parameters and payload configuration, based on quick look data.
- Ground support for onboard processing. The SOC issues payload configuration change requests to the MOC as appropriate to optimise the quality of the PLATO data. In particular, the SOC provides support to the on-board processing through parallel running on-board algorithms on the down-linked imagettes and provision of updated optimised parameters to the MOC for uplink.
- Lead the development, with support from the PDC, in the design, development, testing and maintenance of the modules in the data analysis system required for the quick-look assessment, decompression and statistical tools related to the validation of L0 data.
- Support the PDC in the design, development, testing and maintenance of the data analysis modules required for the generation of the L1 data. Of these data analysis modules, SOC shall lead the development of the light & centroid curve averaging with support provided by PDC to that task.
- Archiving of all PLATO data products, HK data, Auxiliary data and Science ancillary data.
- Distribution of the data products to the scientific community.
- Providing support to the general scientific community, including helpdesk support – especially in the context of the calls for proposals.
- Post-operations activities. The SOC will remain active until three years after the end of operations to continue data processing, the product validation, and the ingestion of the final L2 data products into the archive.

In addition to the above, the SOC will also provide support in the coordination of payload health and maintenance activities which will be done in conjunction with the PMC instrument team based on the regular instrument health reports and quality check during the L1 processing.

6.4.2 SOC operational activities – Uplink, downlink & interface to the community

The planning of science operations will be performed at the SOC based upon input from the PDC endorsed by the PLATO Science Team. These will be checked at the SOC and then forwarded to the MOC where they are to be uplinked and executed on board.

Every 24 hours during the 4 hour daily telecommunication period, the data will be acquired via the ground station and delivered to the MOC. The SOC shall retrieve this Level 0 data and perform a quick look assessment and validate this data through the running of quality control. The data will be placed in the SOC archive after which the standard pipeline generation process will be executed, whereby the Level 0 data will pass through a pipeline thus generating Level 1 products, again being placed into the archive. Further quality control checks will be performed by the SOC of this data set to confirm correct integrity and scientific merit before it is made public in the archive.

The SOC will be the main interface point between the PDC and the MOC as regards payload operations in particular relating to safeguarding the payload and optimising the quality of the data set. Such interactions will also include the fine tuning of on-board software, parameters and payload configuration as a result of the quick look data checks of the L0 products.

The PDC data base will access the archive and retrieve L0, L1 and other data sets at which point it will make it available to the centres within the PLATO Consortium to produce the L2 data set. Upon generation of the L2 data set, these will be provided back to the SOC and ingested into the archive.

6.4.3 Calibration activities

6.4.3.1 On-ground calibration operations (Payload)

The PMC shall support the SOC in the production of the L1 data by performing the task of calibration of scientific data. This includes the definition of a calibration plan, the specification of observations or payload configurations required to gather calibration data, the derivation of the calibration parameters and their delivery to the SOC for implementation into the L1 processing pipeline.

Specific calibration data will be collected during the development phase on sub-system to instrument levels, either as initial estimates for the commissioning and operational phases or to aid calibration model development.

All calibration data collected on-ground as well as in-orbit shall be stored in the Mission Archive for use in the L1 processing.

6.4.3.2 In-Orbit calibration operations

In-orbit calibrations will be carried out i) during in-flight commissioning and performance verification; ii) during normal operations, using the science & HK data; iii) by observing specific calibration fields, generally combined with the on-going long observation campaign.

The in-orbit calibration procedures will be performed throughout the mission, with certain activities specifically tailored to the performance verification phase, and also carried out on normal science data throughout the operations phase, with SGS tasks oriented to identifying calibration sources and extracting the calibration parameters. Note that most of the procedures permit several calibrations to be carried out.

During the Development & Operation phases, the PDC will deliver to the SOC the calibration data and instrument parameter data sets to support quick look assessment and real time analysis of data. In addition, calibration data to support processing of Level 0 and Level 1 data sets shall also be provided for importing into the Archive. Finally, calibration algorithms and procedures shall be delivered to SOC.

6.5 PLATO Data Centre (PDC)

6.5.1 PDC responsibilities

The PLATO Data Centre is under the responsibility of the PLATO Mission Consortium. The PDC supports the SOC in the production of the L1 data by carrying out the following tasks:

- Calibration of the scientific data, based on the calibration procedure and calibration data provided by the instrument team, for implementation into the L1 processing pipeline.
- Definition of algorithms and support to the implementation of modules to monitor the scientific integrity and health of the observations.
- Definition of algorithms and support to the implementation of modules in the data analysis system for the removal of instrumental effects and generation of L1 data.
- Provision of input to the scientific quality control software and procedures.
- Provision of the necessary algorithms and tools for the optimisation of the onboard processing.
- Provision of tools and support to simulate, test and validate the L0 to L1 processing pipeline.

The PDC implements, tests and maintains the data analysis tools needed to generate the Level 2 data and higher level scientific products, which include catalogues, list of planets, their parameters and additional characterisation information.

The PDC supports the spacecraft operations by providing input to the procedures needed for payload operation and for scientific mission planning.

The PDC is responsible for the development and maintenance of all systems required to process the final PLATO mission products and for the computing infrastructure required to deliver the PLATO Level 2 scientific data products. Specifically:

- The PDC technically designs, implements, tests and maintains the data analysis tools needed to generate the (exoplanet and stellar) Level 2 data and higher level scientific products, which include catalogues, list of planets, their parameters and additional characterisation information. The scientific validation of the data analysis tools will occur within the PDC based upon PSPM specifications and with PSPM involvement.
- The PDC shall develop and maintain a main PDC Data Base (PDC-DB) which will acquire, from the SOC, the L0 and L1 data, and other data. The PDC-DB shall make the data available to the PDC Data Processing Centres (PDPCs) to produce the L2 data products. The validated L2 data products, will then be provided back to the SOC. The PDC-DB shall be a central hub for the exchange and maintenance of data within the PDC.
- The PDC provides the PLATO Input Catalogue to the SOC for the scientific mission planning.
- The PDC is responsible for the management of the database that assembles all follow-up observations on PLATO targets, plus ancillary data extracted from various existing catalogues and databases, and places them in the PDC Data Base at the disposal of the PLATO Mission Consortium.
- Provision of data analysis support tools to assist the science team to inspect and to scientifically validate the PLATO data products within the PDC. In particular, these tools will assist the PST & the PSPM to update the ranking of planetary candidates and to confirm planetary systems.

6.5.2 PDC development

The software and hardware technologies available today would suffice to build a successful PDC. The complexity of the PDC lies mostly in the management, integration, and validation of its many hardware and software components.

The PDC will adopt a well defined cyclical development schedule (6 month cycles). Software developed in the PDC will be released at the end of each cycle, with this being integrated into an end-of-cycle system. Over the development lifetime, there will always be a working system, with this working system increasing in functionality over time, such that by the system readiness review prior to launch, the processing system has fully met the requirements.

This approach ensures that work developed over many sites is integrated on a frequent timescale – ensuring that any interface issues are resolved at an early stage. It enables end-to-end testing to commence at an early stage – thus facilitating the 'smooth transition' of a system handling test data to one handling real instrument data (from the lab during development) to one handling real data from the S/C during flight operations.

A key part of the development process will be access to simulation data, required to test all software components. This data will simulate the PLATO telemetry stream, PLATO pixel level data and PLATO catalogue level data. Simulation data will be released ahead of each cycle to allow for testing of the following cycle release. The simulation data is provided to the PDC-DB and is then available through the PDC-DB interface to all PDPCs.

The PDC shall remain operational for at least three years after the end of the PLATO space operations phase to enable the confirmation of planets with periods of up to three years.

6.5.3 PDC facilities

The PDC will encompass several facilities in Europe. The PDC-DB at MPSSR (Germany) will hold the PLATO scientific data products, the input catalogue, and all the ancillary data on the PLATO targets that are required for the processing of the L2 data products, in particular specifically acquired ground-based follow-up observations. Computing resources will be distributed among five Data Processing Centres: PDPC-C at IoA-Cambridge (UK) for the Exoplanet Analysis System, PDPC-I at IAS (France) for the Stellar Analysis System, PDPC-A at ASI (Italy) for the Input Catalogue, PDPC-L at LAM (France) for the Ancillary Data

Management, and PDPC-M at MPSSR (Germany) for the running of the data analysis support tools. The PDC activities through all phases of the mission will be funded through institutional and national agencies.

6.6 PLATO Science Preparation Management (PSPM)

6.6.1 PSPM responsibilities

The PLATO Science Preparatory Management Group (PSPM) is under the responsibility of the PLATO Mission Consortium. In particular, the PSPM has the following responsibilities :

- The PSPM is responsible for carrying out preparatory activities ensuring the scientific results of the mission. It provides the PDC with the specifications and inputs required to implement optimised methods and tools for PLATO data exploitation.
- The PSPM is responsible for the overall coordination of the Scientific preparation, for coordinating the scientific community activities and for PMC public relations and outreach.
- The PSPM is responsible for the scientific specification of the required elements for the detection of exoplanetary transits and the determination of exo-planetary parameters that are the main product of the PLATO mission.
- Likewise, the PSPM is responsible for the scientific specification of the required elements for carrying out the stellar physics part of the mission. Specifically as what concerns the detection of oscillation modes, stellar evolution models and the determination of fundamental stellar parameters.
- For both elements, the PSPM will provide the resulting scientific specifications to the PDC.
- The PSPM is also responsible for the target/field characterisation and thus the preparation of the PLATO input catalogue and the preparation of Target/Field selection.
- The PSPM is also responsible for the organisation, of the required (ground- and space-based) follow-up observations.
- The PSPM is responsible for the development and implementation of the End-to-End Simulator (PLATO Data Simulator).
- Finally the PSPM is also responsible for the preparation of the complementary science program.
- In the operation and exploitation phase the PSPM (then PSM) is responsible for providing input and support to the PDC and scientifically validate the L2 data products.
- In the operation and exploitation phase the PSM is responsible to coordinate planet detection, ranking, rejection, and the required follow-up observations.
- In the operation and post-operation phases the PSM is responsible to evaluate the scientific performance of the PLATO data chain and specify upgrades of scientific algorithms and tools.
- In the operation and post-operation phases the PSM is responsible to continue Target/Field selection and characterisation and update the PIC.
- The PSM is also responsible to continue coordination of the Scientific preparation, for coordinating the scientific community activities and for PMC public relations and outreach until end of the post-operation phase.

6.6.2 PSPM facilities and resources

The PSPM consists of sub-groups totalling more than 100, mainly European, experts who provide the needed state-of-the art scientific know-how, including in particular expertise from previous space missions like CoRoT and Kepler and expertise in ground-based follow-up observations for planet confirmation. This expertise is specially required to set-up an efficient scheme for planet detection, ranking and organisation of resource efficient follow-up observations. This is a lessons-learned from the on-going transit search space missions. The PSPM also provides the expertise for target field selection and characterisation and the specification of the PLATO Input Catalogue. Experts in the PSPM will provide updated stellar models to

optimise the determination of stellar parameters. The CCD Simulator will make realistic simulated data available. The additional (complementary) science task in the PSPM includes experts from various scientific fields, but mainly on different aspects of stellar science not covered in the core program. These experts will help maximising the scientific return of the mission by expanding its science exploitation. The PSPM will fund its activities through all phases of the mission by institutional and agency funding, depending on the national and institutional environments of the participants.

6.7 Level 2 data processing

With Level 0 and Level 1 data products existing in the PLATO Archive, the PDC can retrieve them. The current envisaged mechanism is for the PDC to retrieve the FITS format products from the archive via the Bulk Product Transfer Mechanism. This will be running at the PDC on an automatic basis and will retrieve products from the archive that have been updated or changed since its last retrieval.

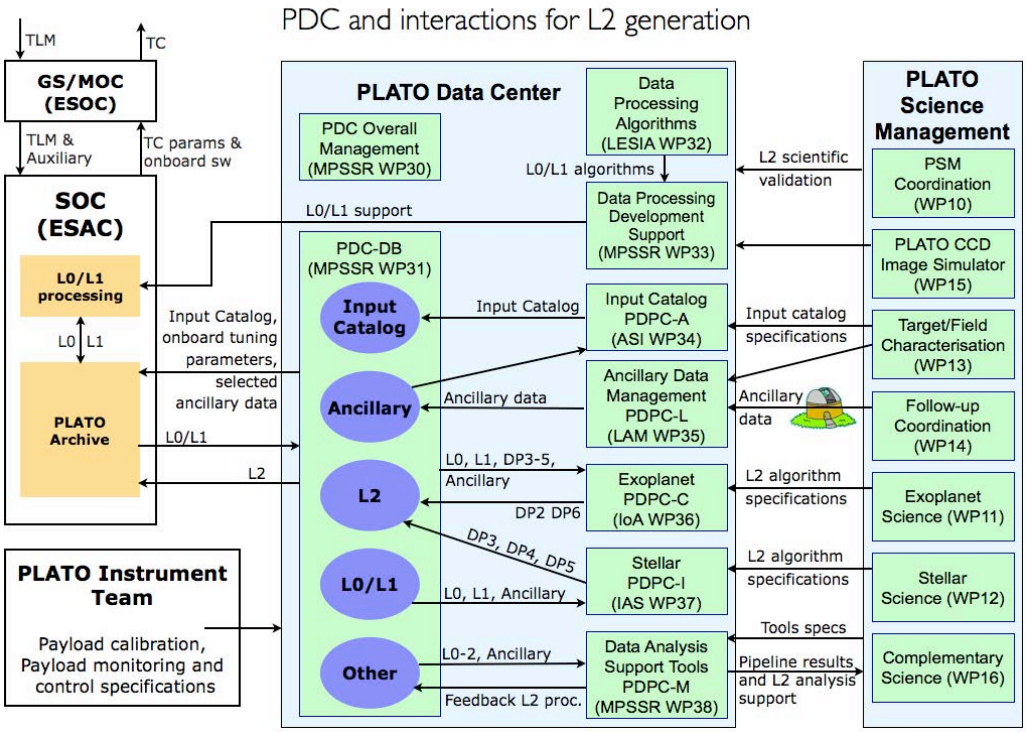

Figure 6.1: PLATO Data Centre with its main elements and main interactions with the SOC, Payload Team and PSM for L2 generation during operations. The PDC includes the PDC Data Base (PDC-DB) and five PLATO Data Processing Centres (PDPCs).

The products (including associated auxiliary products) will be placed into the PDC main database (PDC-DB), as can be seen in Figure 6.1. Access to the PDC-DB is possible by all the sub-centres of the PDC to allow the Level 2 generation process to be started. After acquisition of the L1 data from the PDC-DB by the stellar PDPC, the PLATO light curves are Fourier transformed and power spectra are analysed to provide the oscillation mode parameters DP3. In parallel, analyses of the light curves provide the stellar rotation and activity information DP4. Finally, DP3 and DP4 are used together with the science ancillary and catalogue data, which are stored and managed in the PDC, for producing the DP5. The exoplanet PDPC processing of the L1 data, for the production of the L2 products, is based on a ca. two week cycle. This cycle will allow an update of DP2 providing a ranked list of candidate planet systems. False positive modelling is undertaken to refine the estimate of probable planet systems, using follow up information when available. The ca. two weekly cycle allows for triggering of the ground based follow-up of objects which pass a certain threshold of interest and enables triggering of imagettes of planet candidates. Successive updates are applied over a three-month main processing cycle, corresponding to the period between PLATO satellite field rotations. At the

close of the three month period, a full update of the L2 parameters for the objects observed by PLATO will be made to the PDC-DB.

The PSPM group will access the L2 pipeline products, and Level 0 and 1 data as needed, via the data analysis support tools in the PDC. The PSPM will in particular evaluate the planet ranking and organise the required ground-based follow-up campaigns, including confirmation of planet candidates by radial-velocity follow-up. The PSPM will scientifically validate L2 data to finally obtain DP6 level products.

The PSPM group will furthermore evaluate the scientific performance of the L2 pipeline on real data in the operation phase and provide updated scientific specifications to the PDC data processing as needed.

The PDC shall deliver L2 data, corresponding to DP2-DP5 data levels, for each target to the SOC (for eventual incorporation into the PLATO Archive) within 3 months of reception of the L1 data of that target at the PDC. This data will be given a proprietary status in the archive.

The PDC shall deliver the final scientifically validated L2 data (corresponding to level DP6) for each target to the SOC (for eventual incorporation into the PLATO Archive) not later than at the time of the first publication of that target.

Upon delivery to the SOC, the Level 2 (DP6) data products will be placed into the archive and shall then be made public to the scientific community.

Large external datasets (science ancillary data, including follow up data) will be generated around each of the target level 2 data sets and these will be also fed back to the SOC and the PLATO Archive.

7 Management

7.1 Project management

After the M1/M2 selection of Solar Orbiter and Euclid, the SPC offered the PLATO Mission Consortium the opportunity to enter the competition for the M3 mission selection. Since the M1/M2 selection, the leadership of the PLATO Management was transferred to Germany, which resulted in a revised payload consortium. An outline of the new management structure was submitted to ESA in June 2012. The first issue of this PLATO Management Plan was successfully reviewed by ESA in January 2013, whereupon PLATO was announced as an official M3 Mission candidate. Here, we describe the ESA and consolidated new payload consortium structure.

7.1.1 Responsibilities

The overarching responsibility for all aspects of the PLATO mission rests with the ESA Directorate of Science and Robotic Exploration and its Director. The overall project of PLATO envisages three major organisations: ESA, the PLATO Mission Consortium (PMC) and the Industrial Contractor, with responsibilities in the Implementation Phase defined as follows:

- ESA has the overall responsibility for the PLATO mission design and implementation. ESA is also responsible for the development and procurement of the Charge Coupled Devices (CCDs).
- The Industrial Contractor is responsible for the development, procurement, manufacturing, assembly, integration, test, verification and timely delivery of a fully integrated spacecraft capable of accommodating the defined payload elements, fulfilling the established mission requirements and achieving the mission objectives.
- The PMC develops, procures and timely delivers the full set of payload (cameras and warm electronic units) fully verified and calibrated for later integration into the PLATO spacecraft by industry through the delivery via ESA of related units and sub-assemblies.
- The PLATO Mission Consortium Science Ground Segment (PMC SGS) is in charge of processing all data beyond Level 1 and transferring them to the ESA SOC for archival and distribution. The PMC also provides the organisation and leadership of associated ground based observations required by the mission.

The Contractor and the Consortium report individually to ESA via related management. In addition, ESA would be responsible for:

- Spacecraft Launcher procurement and launch (Soyuz operated by Arianespace);
- Spacecraft Operations (ESOC and ESAC);
- Acquisition and distribution of data to the Payload Data Centre (ESOC and ESAC).

7.1.2 PLATO Mission Consortium (PMC) proposed structure

The overall structure of the PMC is shown in the diagram in Figure 7.1 and briefly described in the following text.

The PMC is placed under the overall responsibility of a PMC Lead (PCL). The PCL constitutes the formal interface of the consortium to ESA. The PCL ensures that the performances of the mission meet the science requirements set by the PLATO Science Team (PST). The PCL also constitutes the main scientific interface of all consortium sub-structures with ESA and the PST. The PCL is one of the members of the Science Team nominated by the PMC and appointed by ESA.

A Steering Committee established through a Multi-Lateral Agreement between ESA and the national agencies supporting the partners of the PMC, provides an overall supervision of the PMC and monitors potential future evolutions of the Consortium structure, e.g., the introduction of new partners.

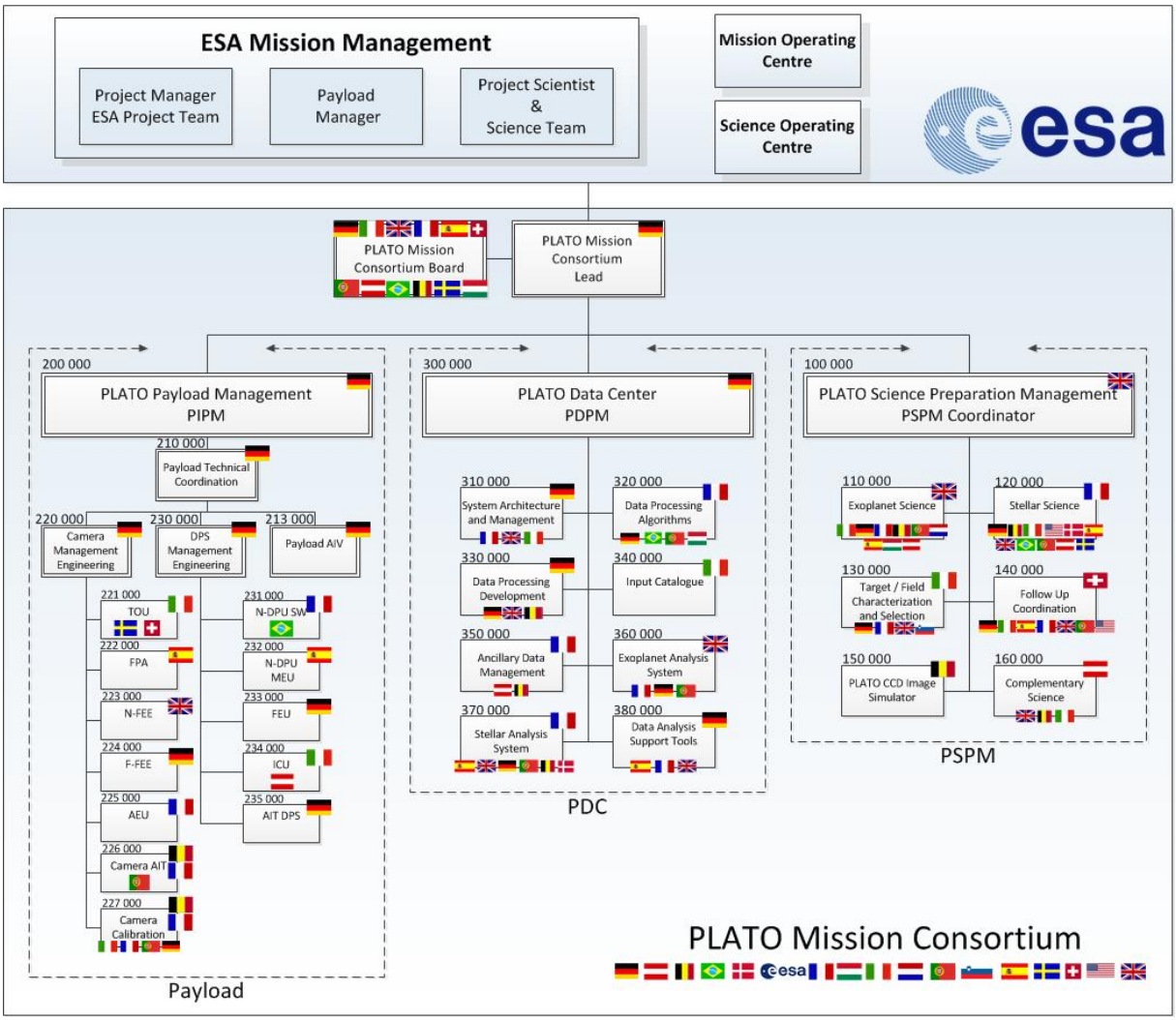

Figure 7.1: Organisation of the mission and structure of the PLATO Mission Consortium (PMC) with key elements and proposed national responsibilities of main work packages.

All consortium activities will be monitored by the PMC Board, which will serve as interface between the consortium on one hand, and the national agencies and institutes involved in the consortium on the other hand. The PMC Board addresses problems concerning the procurement of the PMC elements of the mission, either payload, ground segment or science preparation activities, before they eventually reach the Steering Committee level. The PMC Board is chaired by the PCL, and is constituted by members of the Consortium. The PMC Board includes two representatives of each one of the main countries involved in the mission (France, Italy, Germany, Spain, UK and Switzerland) and one representative of all other contributors (Belgium, Portugal, Brazil, Austria, Sweden, Denmark, Hungary). The PIPM (see below) is invited to all Board meetings. The PCM Board meets at least once a year. The chair is responsible for the organisation of these meetings. The PCL may decide to hold additional meetings, as needed.

The PLATO Instrument Project Manager (PIPM) acts as a support to the PCL on all technical and managerial aspects of the payload development. The hierarchical structure is shown in Figure 7.1. The PLATO Consortium Payload Management is commissioned to a German industrial partner, who appoints the PIPM. The PIPM acts as a support for the PMC Lead on all technical and managerial aspects of the payload development. The PIPM takes responsibility for the overall management of the payload development, including all schedule, financial and quality aspects. The PLATO Data Centre (PDC) is the PMC contribution to the Science Ground Segment, which also includes the Science Operation Centre (SOC) under ESA responsibility. The PDC is led by the PLATO Data Processing Manager. Science Preparation Activities will be carried out under responsibility of a specific substructure of the Consortium, called

PLATO Science Preparation Management (PSPM). They will result in the definition of specific tools for an optimised exploitation of the PLATO data, which will be implemented under PDC responsibility.

7.2 Procurement philosophy

This section gives an overview of the procurement philosophy for PLATO.

7.2.1 Procurement of spacecraft, industrial contractors and organisation

After a possible down-selection of the PLATO mission in February 2014, two parallel definition studies (Phase B1) of the PLATO mission will be conducted by Industry under ESA contract.

Subject to adoption of the PLATO mission by the ESA Science Program Committee (SPC) in February-March 2016, an Invitation to Tender (ITT) for the Implementation Phase (B2/C/D/E1) will be released in mid-early 2016. The scope of this contract would be to implement all industrial activities leading to a launch and commissioning of PLATO in the requested timeframe. The successful bidder will be appointed as Prime Contractor in charge, amongst other items, of system engineering and management of the sub-contractors.

The final industrial organisation will be completed only in Phase B2, mostly through a process of competitive selection and according to the ESA Best Practices for subcontractor selection, by taking into account geographical distribution requirements.

It is currently foreseen that the industrial prime contractor would design, manufacture and test the Service Module. The industrial prime contractor would also be in charge of the global assembly, integration and testing of the whole PLATO spacecraft (SVM and PLM).

Industrial contracts would be funded and placed by ESA. The responsibility for control and monitoring of the contracts and provision for liaison between partners, contractors and outside scientists would be with the ESA project team. ESA would be responsible:

- The overall mission design and provision of Service Module (through industrial contract);
- Global Assembly/Integration/Testing and Verification of SVM and PLM (through industrial contract);
- Spacecraft launch and operations, acquisition and distribution of data to the Science Data Centre.

7.2.2 Payload procurement

The PLATO payload (PLM) is provided by the PLATO Mission Consortium which is financed by the national agencies.

7.3 Schedule

The PLATO payload (PLM) is provided by the PLATO Mission Consortium which is financed by the national agencies. The PMC has planned its activities until the M3 mission selection based on the Reference Schedule for the M3 Mission Candidates, published by ESA. This Reference Schedule defines a primary launch date in 2024. Further, the project schedule shall be compatible with an alternative launch in 2022.

The PLATO payload development is based on the development plan made during the M1/M2 mission selection process. Since the general technical design of the PLATO mission has not changed from the M1/M2 selection round, the payload development follows the same approach, but adapted to the M3 Reference Schedule and the prioritised launch date in 2024 (see Figure 7.2).

The M3 Mission Reference Schedule calls for a launch date flexibility, to realise a launch date in 2022. It is anticipated that the launch date will be defined following the JUICE mission adoption, possibly at the end of 2014. The PLATO project planning offers several options to meet an earlier launch date in 2022. Due to the extensive design work which was already done for PLATO during the M1/M2 selection process, it is possible to reduce the duration of Phase B1, as outlined in the PLATO development plan.

7.4 Science management

7.4.1 ESA Project Scientist (PS)

The PLATO Project Scientist (PS) is the ESA interface to the PMC and to the general scientific community for scientific matters related to the mission. The PS chairs the PLATO Science Team and coordinates its activities.

7.4.2 PLATO Science Team (PST)

The PLATO Science Team (PST) supports the PS in monitoring the correct implementation of the scientific objectives of the mission and maximising its scientific return. The PST is formed with the selection by ESA of the PMC and remains in place until the end of the active archive phase.

7.4.3 Data policy

The general data policy is to make the PLATO L1 data publicly available as soon as they are validated by the SOC, following a procedure defined by the PST (based on current best knowledge this time ranges from approximately a few months in the early phases of the mission to days later on).

The L2 data, which depend on additional observations, will be made publicly available in a timely manner, and no later than the acceptance for publication of the first refereed papers based on them.

However, among the several hundreds of thousands of targets, the data from a certain number (not exceeding 2,000 in total, the exact number will be defined and agreed by the PST), are exclusively available to the PLATO-involved scientists for a period of one year after the corresponding L1 data have been validated and made available to them by the SOC. In this context, PLATO-involved scientists are considered to be members of the PMC, members of the PST, as well as ESA scientists involved in the mission. The distribution of reserved targets (or an equivalent metrics agreed by the PST) is such that 5% is assigned to the ESA scientists.

The list of proprietary targets is established at least 6 months prior to each phase of the mission (one phase being defined as one long run or the step-and-stare phase), as the outcome of a call for proposals aimed at PLATO-involved scientists. In response to such a call, PLATO-involved scientists will submit proposals for a limited number of identified targets, specifying the scientific use they propose to make of these proprietary data, as well as the preparation work that they have performed or intend to perform, detailing the organisation of their teams toward these goals. The PST will review the proposals and come up with a final selection of proprietary targets that will then be distributed among PLATO-involved scientists. All L1 data distributed under this procedure will become public after one year of proprietary period.

A call for proposals directed at the general scientific community is to be issued before launch and after the outcome of the call for proprietary data. More open calls may be issued during the mission to the discretion of ESA, following the advice from the PST. The open calls will ask for complementary science programmes not covered by the PLATO core science objectives. Complementary science programmes will focus on additional objects found within the field of view of each core programme pointing. They will not require re-pointing of the spacecraft or exclusively dedicated observing time. Proposers will be requested to describe the science objectives, specify the requirements on PLATO data acquisition and calibration to achieve the science goals, and provide a plan for the associated data processing. The proposals will be selected by a committee of experts formed under the supervision of the ESA. The SOC will provide dedicated support to the successful proposers. When an open call programme contains targets that are part of the proprietary target list, access to the associated data may be granted also to this programme, with the condition that the observations are exclusively used in relation with the science objectives of the proposal, and the same proprietary period will apply. For the remaining targets in the programme, no proprietary period will be assigned and the L1 data will be publicly available as soon as they are validated by the SOC.

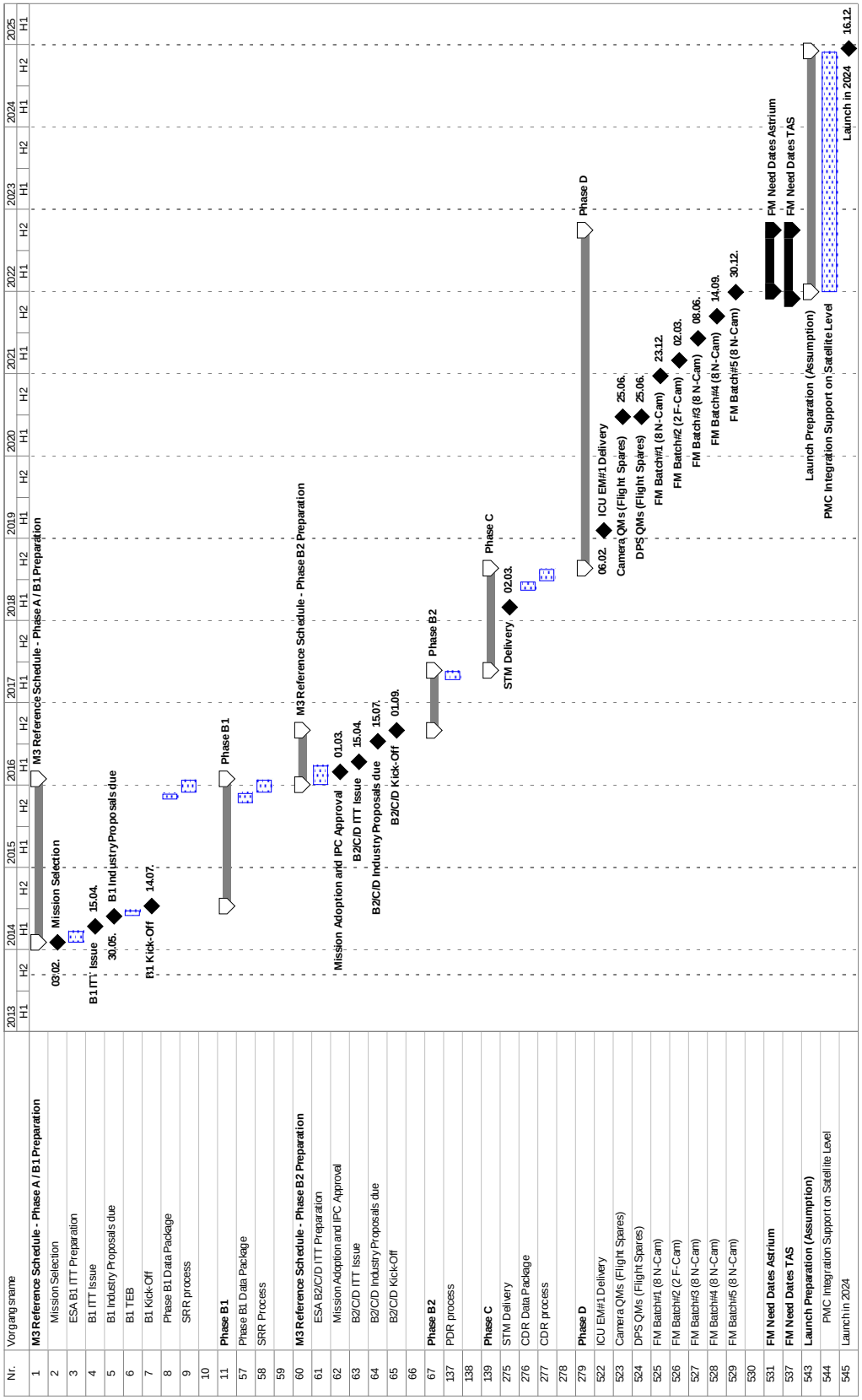

Figure 7.2: Overall schedule of the PLATO mission for a launch in 2024.

8 Communications and Outreach

The existence of planets around other stars, and their potential as habitats for life, fascinates people. PLATO addresses a fundamental question of human existence: Are we alone in the Universe? It is vital that we capitalise on this unique opportunity to promote public scientific literacy and reinvigorate astronomy education. We have assembled an international team comprised of professional astronomers with extensive communication skills and experience. Our team will produce engaging, attractive, concise and accurate materials prepared for media professionals, members of the public, and educators.

8.1 Education and public outreach strategy

Our primary task is to ensure high visibility, acceptance and identification with PLATO and its goals in the general public with a focus on young people. The consortium will deliver resources to enable effective media feeding via ESA's outreach and communication teams.

An ambitious and creative web portal: The consortium already maintains a web portal, which is used to document the progress of the mission project. Our aim is to maintain a state-of-the-art portal which includes technical information in concise, easy-to-digest text and graphics, and entertaining interactive content designed for interested members of the public, including resources targeted specifically at young people. The web portal will host an archive of mission press releases and associated image data, graphics and video content [1].

Visuals: We will commission professionally produced space-art, and still still-graphics and animations to inspire and communicate key mission findings.

Interactive and video assets: We will deliver audio podcasts and video sequences for the education tool iTunes U and YouTube on exoplanets, their detection via transits, and the scientific impact of the PLATO mission. We will develop interactive learning objects, which will be delivered by the PLATO Mission Consortium via the web portal and will be freely available for educators in schools, universities, museums and science organisations to disseminate.

Printed Materials: We will produce resource packs for school teachers in the languages of ESA member countries. Three sets will be made, aimed at kids of younger, and intermediate age, and older children teenagers, respectively. We will consult with school teachers to ensure we meet their needs. We will prepare brochures, stickers, posters and T-shirts promoting the mission.

Social Media: We will communicate key milestones via social media, amplifying the reach of ESA press releases and refreshing awareness of the assets held on the web portal. The precise tools are likely to evolve on the timescale of the mission, and we will adapt to changing public usage patterns. We already tweet under @PLATOMissionCon and will use blogs, social network pages, smart-phone apps and emerging tools as appropriate.

Exhibitions: We will develop a modular multi-lingual mobile exhibition system in ESA's corporate design to promote PLATO's science at appropriate high footfall public events held at science festivals, conferences, musea, etc. We have experience in designing, building and running a similar exhibit: "Is there anybody out there? Looking for New Worlds", which was show-cased at the 2008 Royal Society Summer Exhibition in London and subsequently at several other locations in Europe and Asia.

8.2 EPO Team and Credentials

EPO activities are an essential part of the PLATO Mission Consortium. An "Education and Public Outreach (EPO) Coordination Office (EPOCO)" is established (coordinator: U. Koehler, DLR). This office reports to the PCL and ESA Science Team.

The proposed structure of EPOCO has three sub-units:

1. Web-page maintenance
Coordinator: I. Pagano, INAF – Catania Astrophysical Observatory

Dr. Pagano oversees the team which maintains the PLATO website and develops content for these websites. We will provide top-nudge web content that underlines that ESA is at the leading edge of space-based astronomy.

2. Editorial Office
Coordinator: U. Köhler, DLR

Mr. Köhler, a planetary scientist, has a long experience in EPO from his involvement in the ESA solar-system missions (MEx, VEx, Rosetta), coordinating media contents with DLR's and ESA's communication department. He is also coordinating press and image releases between DLR, NASA and JAXA for the DLR science participations in deep-space missions. Through DLR's participation in the CNES/ESA space telescope CoRoT, he became involved in EPO activities with exoplanet astronomy for German media. He is a fluent writer in German and English and an author of popular science books dealing with the Moon and Mars, as well as school text-books on planetary science and astronomy.

3. Visuals, writing and learning object design
Coordinators: C.A. Haswell & A.J. Norton, The Open University

The Open University (OU) is a world-leader in open-access, supported distance learning, and has public engagement at the heart of its mission. Its high profile TV offering often features astronomy, exemplified by "Stargazing Live" [2] and "Bang Goes the Theory" [3], typically reaching 300 million programme-views per year. This is complemented by our presence on iTunesU [4] comprising >3500 tracks with >64 million downloads by 9 million unique visitors to date, including >1 million subscriptions via the iTunes app; and four YouTube channels [5] containing >1600 videos, with >18 million views and >84,000 subscribers (more than any other European educational institution). Recently we made 14 episodes of "60 Second Adventures in Astronomy" [6] which might serve as a model for PLATO science communication videos. We also produced the first undergraduate textbook dealing with PLATO's science: "Transiting Exoplanets", Haswell, CUP, ISBN-10: 0521139384, and an exoplanet storybook for children: "Oogle Flip and the Planet Adventure", Norton, Magic World Media, ISBN-10: 0982114168.

8.3 Wider Context

The PLATO mission has an unrivalled opportunity to inspire and educate future scientists and citizens. The most significant problems of the 21st century, climate change and overpopulation, can only be solved with scientific and technological innovation. The mission and its EPO strategy thus have an importance that reaches far beyond the immediate science goals, despite the enormous intrinsic value of those goals.

URLs of our existing web resources:

[1] http://www.oact.inaf.it/plato/PPLC/Home.html
[2] http://www.bbc.co.uk/programmes/b019h4g8
[3] http://www.bbc.co.uk/programmes/b00lwxj1
[4] http://open.edu/itunes/
[5] http://www.youtube.com/user/TheOpenUniversity
[6] http://www.youtube.com/playlist?list=PLhQpDGfX5e7CSp3rm5SDv7D_idfkRzje-

9 References

Agol, E., ApJ, 731, 31 (2011)
Alibert, Y., et al., A&A, 417, 25 (2004)
Alibert, Y., et al., A&A, 434, 343 (2005)
Almenara, J. M., et al., SF2A-2012, Proceedings of the Annual meeting of the French Society of Astronomy and Astrophysics (2012)
Alonso, R., et al., A&A, 506, 353-358 (2009a)
Alonso, R., et al., A&A, 501, L23-L26 (2009b)
Ammons, S. M., et al., ApJ, 638, 1004-1017, (2006)
Baglin, A., et al., 36th COSPAR Scientific Assembly, 36, 3749 (2006)
Ballot, J., et al., A&A 530, A97 (2011)
Barclay, T., et al., Nature, 494, 452-454 (2013)
Barnes, J. W. & Fortney, J. J., ApJ, 616, 1193 (2004)
Barnes, S. A., ApJ, 669, 1167-1189 (2007)
Basu, R., et al., ApJ, 728, id. 157, 10 (2011)
Batalha, N. M., et al., ApJ, 729, 27 (2011)
Batygin, K., et al., ApJ, 738, 1-11 (2011)
Bean, J. L., et al., Nature, 468, 669-672 (2010)
Beck, P.G., et al., Science, 332, 205 (2011)
Beck, P.G., et al., Nature, 481, 55-57 (2012)
Bedding, T. R., et al., ApJ, 713, L176-L181, (2010)
Bedding, T. R., et al., Nature, 471, 608-611 (2011)
Belikov, A.N, & Roeser, S., A&A, 489, 1107, (2008)
Ben-Jaffel, L., ApJ, 671, L61-L64 (2007)
Ben-Jaffel, L. & Sona Hosseini, S., ApJ, 709, 1284(2010)
Benneke, B. & Seager, S., ApJ, 753, 100 (2012)
Bergemann, M., et al., MNRAS, 427, 27-49 (2012)
Berta, Z. K., et al., ApJ, 747, 35 (2012)
Bilir, S., et al., AN, 327, 72, (2006)
Bodenheimer, P., et al., ApJ, 592, 555-563 (2003)
Boley, A. C., et al., Icarus, 207, 509-516 (2010)
Bonfils, X., et al., A&A, 474, 293, (2007)
Bonfils, X., et al., A&A, 549, A109 (2013)
Borucki, W. J., Icarus, 58, 121B (1984)
Borucki, W. J., et al., Science, 325, 709 (2009)
Borucki W.J., et al., ApJ, 728, 117B (2011)
Borucki, W. J., et al., Science, 340, 587 (2013)
Boss, A., Science 267, 360, (1995)
Boss, A.P., ApJ, 503, 923-937 (1998)
Broeg, C., et al., EPJWC, 47, 3005 (2013)
Bryson, S., et al., ApJ, submitted (2011)
Cabrera, J., PhD thesis, (2008)
Cabrera, J., et al., A&A, 506, 501, (2009)
Cabrera, J., et al., A&A, 522, A110, 10 (2010a)
Cabrera, J., EAS Publications Series, 42, 109(2010b)
Carter, J. A., et al., Science, 337, 556 (2012)
Casertano, S., et al., A&A, 482, 699 (2008)
Casewell, S. L., et al., ApJ, 759, L34 (2012)
Cassan, A., et al., Nature, 481, 167-169 (2012)
Chambers, J. E. & Cassen, P., M&PS, 37, 1523 (2002)
Chaplin, W. J., et al., ApJ, 766, 101 (2013)
Charbonneau, D., et al., Protostars and Planets V, 701 (2007)
Charbonneau, D., et al., Nature, 462, 7275, 891 (2009)

Charpinet, S., et al., Natur, 461, 501 (2009)
Charpinet, S., et al., A&A, 516, 6 (2010)
Charpinet, S., et al., Nature, 480, 496 (2011)
Chiappini, C., et al., A&A, 449, L27-L30 (2006)
Cooper, C. S. & Showman, A. P., ApJL, 629, L45 (2005)
Corsaro, E., et al., ApJ, 757, id. 190, 13 (2012)
Cowan, N.B. & Agol, E., ApJL, 678, L129 (2008)
Cowan, N.B. & Agol, E., ApJ, 726, 82 (2011)
Crossfield, I. J. M., A&A, 545, A97 (2012)
Csizmadia, S., et al., A&A, 417, 745-750 (2004)
Czesla, S., et al., A&A, 505, 1277-1282 (2009)
Deeg, H. J., et al., A&A, 338, 479 (1998)
Deeg, H. J. & Doyle, L. R., EPJWC, 11, id.05005 (2011)
Deheuvels, S., et al., A&A, 515, A87, (2010)
Deheuvels, S., et al., ApJ, 756, 19 (2012)
De Mooij, E. J. W. et al., A&A, 538, A46 (2012)
Demory, B.-O., et al., ApJL, 735, L12 (2011a)
Demory, B.-O., et al., ApJS, 197, 12 (2011b)
Demory, B.-O., et al., ApJL, 751, L28 (2012)
De Ridder, J., et al., Nature, 459, 398 (2009)
Diaz, R. F., et al., submitted to MNRAS (2013)
Dodson-Robinson, S. E. & Bodenheimer, P., Icarus, 207, 491-498, (2010)
Doyle, L. R., et al., Science, 333, 1602 (2011)
Dravins, D., A&A, 228, 218, (1990)
Dumusque, X., et al., A&A, 525, 140, (2011a)
Dumusque, X., et al., A&A, 527, A82, (2011b)
Dvorak, R., et al., A&A, 226, 335 (1989)
Dziembowski, W. A. & Pamyatnykh, A. A., MRNAS, 385, 2061-2068 (2008)
Dzigan, Y. & Zucker, S., ApJL, 753, L1 (2012)
Eggenberger, P., et al., A&A, 519, A116 (2010)
Eggenberger, P., et al., A&A, 544, L4 (2012)
Eggleton, P. P., JASS, 29, 145-149 (2012)
Ehrenreich, D., et al., A&A, 547, A18 (2012)
Ekenbäck, A., et al., ApJ, 709, 670-67 (2010)
Elkins-Tanton, L. & Seager, S., ApJ, 685, 1237 (2008)
ESA/SRE(2011)13, PLATO Definition Study Report during M1/M2 candidate application (2011)
Escobar, M. E.., et al., A&A 543, A96 (2012)
Fabrycky, D. C., et al., ApJ, 750, A114 (2012)
Faedi, F., et al., MNRAS, 410, 899 (2011)
Faigler, S., et al., ApJ, 771, 26 (2013)
Figueira, P., et al., A&A, 493, 671 (2009)
Fontaine, G., et al., PASP, 113, 409 (2001)
Fontaine, G. & Brassard, P., PASP, 120, 1043 (2008)
Ford, E. B., et al., ApJ, 750, 113-131 (2012)
Fortier, A., et al., A&A, 473, 311-322 (2007)
Fortier, A., et al., A&A, 549, 44 (2013)
Fortney, J. J., et al., ApJ, 659, 1661-1672 (2007)
Fortney, J. J. & Nettelmann, N., SSRv, 152, 423 (2010)
Fossati, L., et al., ApJ, 714, L222-L227 (2010)
Fressin, F., et al., ApJ, 745, 81 (2012a)
Fressin, F., et al., Nature, 482, 195-198 (2012b)
Fressin, F., et al., ApJ, 766, 81 (2013)
García Hernández, A., et al., A&A, 506, 79-83 (2009)
Giammichele, N., et al., ASPC, 469, 49 (2013)
Gilliland, R. L., et al., ApJS, 197, 6 (2011)

Gilliland, R. L., et al., ApJ, 766, 40 (2013)
Gillon, M., et al., A&A., 520, A97-A105 (2010)
Girardi, L., et al., A&A, 436, 895-915 (2005)
Gizon, L. & Solanki, S., ApJ, 589, 1009-1019 (2003)
Gizon, L., et al., PNAS, 213, 110, 13267 (2013)
Goldreich, P. & Soter, S., Icarus, 5, 375 (1966)
Gómez de Castro, A. I., et al., Ap&SS, 335, 283 (2011)
Grasset, O., et al., ApJ, 693, 722-733 (2009)
Griest, K., et al., arXiv1307.5798G (2013)
Guilera, O. M., et al., A&A, 532, 142 (2011)
Guillot, T., et al., ApJL, 459, L35-L38 (1996)
Guillot, T., et al., A&A, 453, L21-L24 (2006)
Guillot, T. & Havel, M., A&A, 527, A20-A35 (2011)
Heber, U., ARA&A, 47, 211 (2009)
Hekker, S., et al., MNRAS, 414, 2594-2601 (2011)
Hekker, S., et al., Astron. Nachr., 333, 1022 (2012)
Helled, R. & Schubert, G., Icarus, 198, 156-162 (2008)
Helled, R., et al., ApJ, 726, 15-22 (2011)
Helled, R. & Bodenheimer, P., Icarus, 211, 939 (2011)
Helled, R. & Guillot, T., ApJ, 767, 113 (2013)
Heller, R. & Barnes, R., arXiv:1210.5172 (2012)
Heng, K., et al., MNRAS, 413, 2380-2402 (2011)
Hogan, E., et al., MNRAS, 396, 2074 (2009)
Holmberg, J., A&A, 501, 941H, (2009)
Holmström, M., et al., Nature, 451, 970-972 (2008)
Hori, Y. & Ikoma, M., MNRAS, 416, 1419-1429 (2011)
Howard, A. W., et al., ApJS, 201, 15 (2012)
Huber, D., et al., ApJ, 760, 32 (2012)
Huber, D., et al., ApJ, 767, 127 (2013)
Hubickyj, O., et al., Icarus, 179, 415-431 (2005)
Ida, S. & Lin, D. N. C., ApJ, 604, 388-413 (2004)
Ikoma, M., et al., ApJ, 537, 1013-1025 (2000)
Kasting, J. F., et al., Icarus, 101, 108-128 (1993)
Kipping, D. M., MNRAS, 396, 1797-1804 (2009)
Kipping, D. M., et al., MNRAS, 400, 398-405 (2009)
Kipping, D. M., et al., ApJ, 750, 115 (2012)
Kipping, D. M., et al., MNRAS, arXiv: 1306.3221 (2013)
Kjeldsen, H., et al., ApJ, 635, 1281, (2005)
Knutson, H. A., et al., Nature, 447, 183-186 (2007)
Knutson, H. A., et al., ApJ, 690, 822-836 (2009)
Knutson, H. A., et al., ApJ, 735, 27 (2011)
Koch, D. G., et al., ApJL, 713, L79-L86 (2010)
Koskinen, T. T., et al., arXiv:1210.1536 (2012)
Kovacs, G., et al., ApJ, 724, 866-877 (2010)
Kroupa, P., ASPC, 228, 187, (2001)
Lallement, R., et al., A&A, 411, 447, (2003)
Lammer, H., et al., Ap&SS, 335, 9-23 (2011a)
Lammer, H., et al., Ap&SS, 335, 39-50 (2011b)
Lammer, H., et al., EP&S, 64, 179-199 (2012)
Lattanzi, M.G. & Sozzetti, A., ASPC, 430, 253, (2010)
Lebreton, Y. & Goupil, M., A&A 544, 13 (2012)
Lecavelier des Etangs, A., et al., A&ASS, 140, 15 (1999)
Lecavelier des Etangs, A., et al., A&A, 543, 4 (2012)
Lefever, K., et al., A&A, 463, 1093-1109 (2007)
Liebert, J., et al., ApJ, 769, 7 (2013)

Linsky, J. L., et al., ApJ, 717, 1291-1299 (2010)
Llama, J., et al., MNRAS, 416, L41-L44 (2011)
Loeb, A. & Maoz, D., MNRAS, 432, 11 (2013)
Lovis, C., et al., Nature, 441, 305, (2006)
Lovis, C., et al., A&A, 528, 112, (2011)
Madhusudhan, N. & Seager, S., ApJ, 707, 24-39 (2009)
Maeder, A., Physics, Formation and Evolution of Rotating Stars, Springer Eds., (2009)
Magic, Z., et al., A&A, accepted, arXiv:1302.2621 (2013)
Marley, M. S., et al., JGR, 100, 23349-23354 (1995)
Marshall, D.J., et al., A&A, 453, 635, (2006)
Mathur, S., et al., ApJ, 749, 152 (2012)
Mayer, L., et al, Science, 298, 1756, (2002)
Mayer, L., et al., MNRAS, 363, 641-648 (2005)
Mayor, M., et al., A&A, 493, 639, (2009)
Mayor, M., et al., arXiv:1109.2497 (2011)
Metcalfe, T. S., et al., ApJ, 699, 373-382 (2009)
Metcalfe, T. S., et al., ApJ, 723, 1583-1598 (2010)
Metcalfe, T. S., et al., ApJ, 748, 10 (2012)
Michel, E., et al., Science, 322, 558, (2008)
Miglio, A., et al., arXiv:1108.4406 (2011)
Miglio, A., in "Red Giants as Probes of the Structure and Evolution of the Milky Way", Eds. Miglio, Montalban & Noels, Springer (2012a)
Miglio, A., et al., EPJWC, 19, 5012 (2012b)
Miglio, A., et al., MNRAS, 429, 423-428 (2013)
Militzer, B., et al., ApJL, 688, L45-L48 (2008)
Miller, N. & Fortney, J. J., ApJL, 736, L29-L34 (2011)
Moravveji, E., et al., ApJ, 749, 74, (2012a)
Montalban, J., et al., ApJ, 766, 118 (2013)
Mordasini, C., et al., A&A, 501, 1161-184 (2009)
Mordasini, C., et al., A&A, 541, A97 (2012a)
Mordasini, C., et al., A&A, 547, id.A111, 23 (2012b)
Morton, T.D., Johnson, J.A., ApJ, 738, 12 (2011)
Mosser, B., et al., A&A, 532, A86 (2011)
Mosser, B., et al., A&A, 540, A143 (2012)
Moutou, C., et al., A&A, 498, L5, (2009)
Moutou, C., et al., submitted to A&A (2013)
Neckel, Th., Klare, G., A&AS, 42, 251, (1980)
Nettelmann, N., et al., ApJ, 683, 1217-1228 (2008)
Noack, L., et al., P&SS, submitted (2013)
Nordhaus, J. & Spiegel, D. S., MNRAS, 432, 500 (2013)
Noyes, R., et al., ApJ, 279, 763, (1984)
Ofek, E.O., PASP, 120, 1128, (2008)
Ohta, Y., et al., ApJ, 690, 1-12 (2009)
Østensen, R. H., et al., MNRAS, 409, 1470 (2010)
Palle, P.L., et al., ApJ, 441, 952, (1995)
Pepe, F. & Lovis, C., Physica Scripta, Vol 30, p. 14007, (2008)
Pepe, F., et al., A&A, 534, 58, (2011)
Pickles, A., Depagne, E., PASP, 122, 1437, (2010)
Pierens, A., Nelson, R.P., A&A, 472, 993 (2007)
Podolak, M., et al., P&SS, 43, 1517-1522 (1995)
Pollack, J.B., Icarus, 124, 62, (1996)
Pont, F., et al., MNRAS, 432, 2917-2944 (2013)
Queloz, D., et al., A&A, 379, 279, (2001)
Rafert, J. B. & Twigg, L. W., MNRAS, 193, 7 (1980)
Rauer, H. & Catala, C., IAUS, 276, 354-358 (2011)

Rauer, H., et al., in: 'Habitability of Other Planets and Satellites ', Ed. deVera (2013)
Robin, A. C., et al., A&A, 409, 523-540 (2003)
Saar S.H., Donahue R., ApJ, 485, 319, (1997)
Saar S.H., et al., ApJ, 498, 153, (1998)
Saio, H., et al., ApJ, 650, 1111-1118 (2006)
Samus, N.N., et al., Fifty years of Cosmic Era: Real and Virtual Studies of the Sky. Conference of Young Scientists of CIS Countries, Ed. Mickaelian, A.M. et al., 39-47 (2012)
Sanchís-Ojeda, R., et al., Nature, 487, 449-453 (2012)
Santerne, A., et al., arXiv:1310.2133 (2013)
Sartoretti, P. & Schneider, J., A&AS, 134, 553-560 (1999)
Saumon, D. & Guillot, T., ApJ, 609, 1170-1180 (2004)
Schneider, J., et al., A&A, 532, 79 (2011)
Seager, S., et al., ApJ, 669, 1279-1297 (2007)
Showman, A. P. & Guillot, T., A&A, 385, 166-180 (2002)
Showman, A. P., et al., ApJ, 699, 564 (2009)
Shustov, B., et al., Ap&SS, 320, 187-190 (2009)
Shustov, B., et al., Ap&SS, 335, 273-282 (2011)
Siebert, A., et al., AJ, 141, 187, (2011)
Simon, A.E., et al., MNRAS, 419, 164-171 (2012)
Silva Aguirre, V., et al., ApJ, 757, 99 (2012)
Silva-Valio, A. & Lanza, A. F., A&A, 529, A36 (2011)
Silvotti, R., et al., Nature, 449, 189 (2007)
Silvotti, R., et al., A&A, submitted (2013)
Snellen, I. A. G., et al., Nature, 459, 543-545 (2009)
Snellen, I. A. G., et al., A&A, 513, A76 (2010)
Sohl, F. & Schubert, G., In: Treatise on Geophysics (Editor-in-Chief G. Schubert), Volume 10, Planets and Moons, Ed. T. Spohn, p. 27-68, Elsevier (2007)
Sotin, C., et al., Icarus, 191, 337-351 (2007)
Stahn, T., 2011, PhD Dissertation, University of Goettingen
Stello, D., et al., ApJ, 700, 739, id. 13, 13 (2011)
Suárez, J. C., et al., A&A, 449, 673-685 (2006)
Suárez, J, C., et al., ApJ, 690, 1401 (2009)
Swift, D. C., et al., ApJ, 744, 595 (2012)
Szabó, R., et al., MNRAS, 413, 2709, (2011)
Torres, G., et al., ApJ, 727, 24 (2011)
Tran, K., et al., arXiv.org:1305.4639 (2013)
Udry, S. & Santos, N. C., ARA&A, 45, 397-439 (2007)
Valencia, D., et al., Icarus, 181, 545-554 (2006)
Valencia, D., et al., ApJ, 665, 1413-1420 (2007)
Van Grootel, V., et al., A&A, 553, 97 (2013)
Vazan, A. & Helled, R., ApJ, 756, 90 (2012)
Vergely, J. -L., et al., A&A, 518, A31, (2010)
Vidal-Madjar, A., et al., Nature, 422, 143-146 (2003)
Vidal-Madjar, A., et al., ApJ, 604, 69-72 (2004)
Wagner, F. W., et al., Icarus, 214, 366-376 (2011)
Wagner, F. W., et al., A&A, 541, A103-A116 (2012)
Welsh, W. F., et al., ApJL, 713, L145-L149 (2010)
Welsh, W. F., et al., Nature, 481, 475-479 (2012)
Wright, J., et al., ApJS, 152, 261, (2004)
Zahn, J.-P., A&A, 265, 115 (1992)
Zwintz, K., et al., A&A, 550, A121 (2013)

10 List of Acronyms

1D	one dimensional
3D	three dimensional
AEU	Ancillary Electronics Units
AFE	Analogue Front End
AGB	Asymptotic Giant Branch
AIT	Assembly, Integration and Testing
AO	Announcement of Opportunity
AOCS	Attitude and Orbit Control System
APASS	AAVSO Photometric All-Sky Survey
APOGEE	APO Galactic Evolution Experiment
ASI	Agenzia Spaziale Italiana
ASW	Application SoftWare
BEB	Blended Eclipsing Binary
BGEB	Background Eclipsing Binaries
CCD	Charge Coupled Device
CCSDS	Consultative Committee for Space Data Systems
CDMU	Central Data Management Unit
CBP	CircumBinary Planet
CCF	Cross Correlation Function
CFE	Customer Furnished Equipment
CFHT	Canada France Hawaii Telescope
CFRP	Carbon-Fibre Reinforced Plastic
CHEOPS	CHaracterising ExoPlanet Satellite
CNES	Centre National d'Etudes Espatiales
CODEX	COsmic Dynamics and EXo-earth experiment
CoRoT	COnvection ROtation and planetary Transits
CPU	Control Processing Unit
CV	Cosmic Vision
CU	Coordination Unit
DAC	Digital to Analogue Converter
DB	DataBase
DC	Direct Current
DLR	Deutsches Zentrum für Luft- und Raumfahrt
DoF	Degrees of Freedom
DP	Data Product (DP1-DP6)
DPAC	Gaia Data Processing & Analysis Consortium
DPS	Data Processing System
DPU	(Telescope) Data Processing Unit
EADS	European Aeronautic Defense and Space Company
EKF	Extended Kalman Filter
ELT	Extremely Large Telescope
EM	Electrical Model
EOS	Equation of State
EPO	Education and Public Outreach
EPOCO	Education and Public Outreach Coordination Office
EPS	Electrical Power Subsystem
ESA	European Space Agency
ESAC	European Space Astronomy Centre
ESO	European Southern Observatory
ESOC	European Space Operations Centre
ESPRESSO	Echelle SPectrograph for Rocky Exoplanet and Stable Spectroscopic Observations
EUV	Extreme UltraViolet
F-AEU	Fast Ancillary Electronics Units
FCL	Foldback Current Limiter
FEE	Front End Electronics
FEROS	Fiber-fed Extended Range Optical Spectrograph
FEU	Fast Electronics Unit
FF	Full Frame
FGS	Fine Guidance Sensor
FITS	Flexible Image Transport System
FM	Flight Model
FoV	Field of View
FPA	Focal Plane Assembly
FPGA	Field-Programmable Gate Array
FPI	Focal Plane Instrument
FT	Full Transfer
GEB	Grazing Eclipsing Binaries
GFRP	Glass-Fibre Reinforced Plastic
GMSK	Gaussian Minimum Shift Key
GS	Ground station
GSE	Ground Support Equipment
HARPS	High Accuracy Radial Velocity Planet Searcher
HAT	Hungarian-made Automated Telescope
HGA	High Gain Antenna
HK	House Keeping data
HST	Hubble Space Telescope
HZ	Habitable Zone
IAS	Institut d'Astrophysique Spatiale
ICU	Instrument Control Unit
IR	InfraRed
ITT	Invitation To Tender
JAXA	Japan Aerospace Exploration Agency
JUICE	JUpiter ICy moons Explorer
JWST	James Webb Space Telescope
LAM	Laboratoire d'Astrophysique de Marseille
LCL	Latching Current Limiter
LEOP	Launch and Early Orbit Phase
LGA	Low Gain Antenna

LOS	Line Of Sight
MEG	M dwarfs or brown dwarfs Eclipsing Giant stars
MEU	Main Electronics Unit
MG	Gaia Magnitude
MGSE	Mechanical Ground Segment Equipment
MLI	Multi-Layer Insulation
MMU	Mass Memory Unit
MOC	Mission operations Centre
MOST	Microvariability and Oscillations of STars telescope
MPSRR	Max Planck Institute for Solar System Research
MW	Milky Way
N-AEU	Normal Ancillary Electronics Units
NASA	National Aeronautics and Space Administration
N-DPU	Normal Data Processing Unit
NGTS	Next Generation Transit Survey
OB	Optical Bench
OBC	On-Board Computer
OHP	Haute-Provence Observatory
P/L	Payload
PASTIS	Planetary Analysis and Small Transit Investigation Software
PCDU	Power Conditioning & Distribution Unit
PCL	PLATO Consortium Lead
PDC	PLATO Data Centre
PDPC	PLATO Data Processing Centre
PI	Principal Investigator
PIC	PLATO Input Catalogue
PIPM	PLATO Instrument Project Manager
PLATO	PLAnetary Transits and Oscillations of stars
PLM	Payload Module
PMC	PLATO Mission Consortium
PPLC	Plato PayLoad Consortium
ppm	part per million
PSF	Point Spread Function
PSM	PLATO Science Management
PSPM	PLATO Science Preparation Management
PST	PLATO Science Team
PSU	Power Supply Unit
PVA	Photovoltaic Assembly
RAVE	RAdial Velocity Experiment
RCS	Reaction Control System
RGB	Red Giant Branch
RIU	Remote Interface Unit
RMAP	Remote Memory Access Protocol
rms	Root mean square
RPM	Reduced Proper Motion
RV	Radial Velocity
S/C	Spacecraft
S/N	Signal to Noise ratio
SB2	double line Spectroscopic Binary
sdB	subdwarf B
SDRAM	Synchronous Dynamic Random Access Memory
SEGUE	Sloan Extension for Galactic Understanding and Exploration
SGS	Science Ground Segment
SOC	Science Operations Centre
SPC	Science Programme Committee
SRF	Spacecraft Reference Frame
SSH	Sunshield
SST	Science Study Team
SVM	Service Module
SW	SoftWare
TAS	Thales Alenia Space
TBC	To Be Confirmed
TC	Telecommand
TDV	Transit Duration Variations
TESS	Transiting Exoplanet Survey Satellite
TM	Telemetry
TNG	Telescopio Nazionale Galileo
TOU	Telescope Optical Unit
TRL	Technology Readiness Level
TRP	Temperature Reference Point
TTV	Transit Time Variations
TT&C	Telemetry, Tracking and Command
UFOV	Useful Field Of View
VLT	Very Large Telescope
WD	White Dwarf
XRB	X-Ray Binaries

Annex: Assessment Study Contributors

Contributions to this Assessment Study have been made by the PLATO Team, and part of its text has been submitted to Experimental Astronomy (arXiv:1310.0696). Contributors to these activities are:

Australia: Martin Asplund (ANU/MPA), P. Cally (Monash Univ.), L. Casagrande (Mt. Stromlo Obs.), D. Stello (Univ. Sydney), R. Mardling (Monash Univ.); **Austria:** J. Alves (Univ. Vienna), R. Dvorak (Univ. Vienna), M. Guedel (Univ. Vienna), Th. Kallinger (Univ. Vienna), F. Kerschbaum (Univ. Vienna), M. Khodachenko (OEAW), K.G. Kislyakova (OEAW), F. Kupka (Univ. Vienna), R. (Univ. Vienna), H. Lammer (SSI Graz), Th. Lüftinger (Univ. Vienna), M. Netopil (Univ. Vienna), R. Ottensamer (Univ. Vienna), E. Paunzen (Univ. Vienna), E. Pilat-Lohinger (Univ. Vienna), W. Weiss (Univ. Vienna); **Belgium:** C. Aerts (KU Leuven), P.M. Arenal (KU Leuven), P. Beck (KU Leuven), St. Bloemen (KU Leuven), R. Blomme (Royal Observatory Belgium), M. Briquet (Univ. of Liège), L. Carone (KU Leuven), A. Chiavassa (Univ. of. Bruxelles), K. Clémer (KU Leuven), J. Cuypers (Royal Obs. Belgium), P. De Cat (Royal Obs. Belgium), K. De Munck (IMEC), J. De Ridder (KU Leuven), J. Debosscher (KU Leuven), L. Decin (KU Leuven), P. Degroote (KU Leuven), P. Demoor (IMEC), R. Drummond (BIRA-IASB), M.-A. Dupret (Univ. Liège), Y. Fremat (Royal Obs. Belgium), M. Gillon (Univ. Liège), E. Gosset (Univ. Liège), M. Grosjean (Univ. Liège), L. Hermans (CMOSIS), E. Huygen (KU Leuven), P. Lampens (Royal Obs. Belgium), A. Lemaitre (Univ. Namur), G. Lepage (CMOSIS), A.-S. Libert (Univ. Namur), P. Magain (Univ. Liège), J. Montalban (Univ. Liège), E. Moravveji (KU Leuven), Th. Morel (Univ. of Liège), L. Noack (Royal Obs, Belgium), A. Noels (Univ. Liège), R. Oestensen (KU Leuven), P. Papics (KU Leuven), P.R. Ramachandra (IMEC), G. Raskin (KU Leuven), G. Rauw (Univ. Liège), D. Reese (Univ. Liège), S. Regibo (KU Leuven), E. Renotte (CSL), P. Rochus (CSL), P. Royer (KU Leuven), S. Salmon (Univ. Liège), S. Scaringi (KU Leuven), R. Scuflaire (Univ. Liège), A. Thoul (Univ. Liège), A. Tkachenko (KU Leuven), S. Vanaverbeke (KU Leuven – KULAK), A.C. Vandaele (BIRA-IASB), B. Vandenbussche (KU Leuven), Bram Vandoren (KU Leuven), V. Van Grootel (Univ. Liège), K. Zwintz (KU Leuven); **Brazil:** E. Janot-Pacheco (Univ. Sao Paulo), J.-D. do Nascimento (UFRN), J. Melendez (Univ. São Paulo), V. Parro (Mauna Inst. of Technology), A. Silva-Valio (Univ. Mackenzie); **Canada:** M. Bonavita (Univ. Toronto), S. Talon (Quebec Univ.); Diana Valencia (Univ. Toronto); **Chile:** S. Sale (Valparaiso Univ.); **Czech Republic:** J. Krticka (Masaryk Univ.), J. Liška (Masaryk Univ.), M. Skarka (Masaryk Univ.), M. Svanda (AUUK), M. Zejda (Masaryk Univ.); **Denmark:** L. Buchhave (Niels Bohr Institute), J. Christensen-Dalsgaard (Aarhus Univ.), F. Grundahl (Aarhus Univ.), G. Houdek (Aarhus Univ.), Ch. Karoff (Aarhus Univ.), H. Kjeldsen (Aarhus Univ.); **France:** G. Alecian (LUTH)**,** F. Allard (CRAL), J.M. Almenara (OAMP), L. Alvan (CEA), Th. Appourchaux (IAS), K. Baillie (CEA), J. Ballot (IRAP), C. Barban (OBSPM), F. Baudin (IAS), K. Belkacem (LESIA), L. Bigot (OCA), Th. Böhm (LATT), X. Bonfils (IPAG), F. Bouchy (IAP), P. Boumier (IAS), J.-C. Bouret (OAMP), A. Brahic (CEA), A.S. Brun (CEA), C. Catala (OBSPM), T. Cellier (CEA), G. Chabrier (CRAL), M. Chadid (Univ. Nice), S. Charnoz (CEA), St. Charpinet (LATT), A. Chiavassa (OCA), O. Creevey (IAS), P. de Laverny (OCA), C. Damiani (LAM), F. De Oliveira Fialho (LESIA), M. Deleuil (LAM), X. Delfosse (IPAG), P.-A. Desrotour (IMCCE/CEA)B. Dintrans (Univ. Toulouse), J.-F. Dinati (LATT), D. Ehrenreich (IPAG), Th. Fenouillet (LAM), Th. Forveille (IPAG), S. Fromang (CEA), R.A. Garcia (CEA), M.-J. Goupil (LESIA), M. Guenel (CEA), T. Guillot (Univ. Nice), G. Hebrard (IAP), L. Jouve (Univ. Toulouse), P. Kervella (OCA), A.-M. Lagrange (IPAG), J. Laskar (IMCCE), V. Lainey (IMCCE). Y. Lebreton (OBSPM), A. Lecavelier des Etangs (IAP), A. Leger (IAS), J.-F. Lestrade (LERMA), C. Leponcin (SYRTHE), P. Levacher (OCA), R. Ligi (OCA), F. Lignières (Univ. Toulouse), D. Marshall (CESR), L. Marheut (CEA), St. Mathis (CEA), J.-C. Meunier (OAMP), N. Meunier (IPAG), E. Michel (LESIA), C. Moreau (LAM), K. Morel (CEA), B. Mosser (LESIA), D. Mourard (OCA), C. Moutou (LAM), C. Neiner (LESIA), R.-M. Ouazzani (OBSPM), N. Nardetto (OCA), A. Palacios (Univ. Montpellier), G. Perrin (LESIA), P. Petit (OMP), B. Pichon (OCA), P. Plasson (LESIA), B. Plez (Univ. Montpellier), N. Rambaux (IMCCE), A. Recio-Blanco (OCA), D. Reese (OBSPM), F. Remus (IMCCE), V. Reville (CEA), M. Rieutord (LATT), D. Rouan (LESIA), C. Reyle (Obs. Becancon), D. Salabert (OCA), P. Robutel (IMCCE), R. Samadi (LESIA), J. Schneider (OBSPM), F. Selsis (Univ. Bordeaux), E. Taillefet (CEA), C. Soubiran (Univ. Bordeaux), P. Stee (OCA), F. Thevenin (Univ. Nice), S. Turck-Chieze (CEA), S. Vauclair (LATT), J.-P. Zahn (LUTH); **Germany:** P. Amaro-Seoane (AEI) , M. Ammler von Eiff (TLS), W. Ball

(Univ. Göttingen), S. Barnes (AIP), J. Bartus (AIP), S. Berdyugina (KIS), M. Bergemann (MPA), A. Birch (MPSSR), G. Bihain (AIP), D. Breuer (DLR), M. Bruns (MPSSR), R. Burston (MPSSR), J. Cabrera (DLR), C. Chiappini (AIP), R. Collet (MPA), Sz. Csizmadia (DLR), I. Di Varano (AIP), St. Dreizler (Univ. Göttingen), C. Dreyer (DLR), P. Eigmüller (DLR), A. Erikson (DLR), K.-P. Förster (KT), M. Fridlund (DLR), L. Gizon (MPSSR), M. Godolt (DLR), Th. Granzer (AIP), L. Grenfell (DLR), D. Griessbach (DLR), S. Grziwa (Univ. Cologne), E. Guenther (TLS), R. Haarmann (KT), A. Hatzes (TLS), P. Hauschildt (Univ. Hamburg), S. Hekker (MPSSR), F. v. Hessmann (Univ. Göttingen), H. Hussmann (DLR), W. Kley (Univ. Tübingen), U. Koehler (DLR), K. Lind (MPA), H.-G. Ludwig (Univ. Heidelberg), Z. Magic (MPA), J. Marques (Univ. Göttingen), H. Michaelis (DLR), H. Michels (MPSSR), H. Moradi (Monash/MPSSR), Ch. Mordasini (MPIA), J. Morin (Univ. Göttingen), R. Müller (MPSSR), M.B. Nielsen (Univ. Göttingen), A. Ofir (Univ. Göttingen), I. Pardowitz (MPSSR), M. Pätzold (Univ. Cologne), G. Peter (DLR), R. Redmer (Univ. Rostock), A. Quirrenbach (Univ. Heidelberg), H. Rauer (DLR), S. Reffert (Univ. Heidelberg), J. Schou (MPSSR), S. Schuh (Univ. Göttingen), H. Schunker (MPSSR), M. Sobol (MPSSR), F. Sohl (DLR), T. Spohn (DLR), K. Strassmeier (AIP), F.W. Wagner (DLR), J. Weingrill (AIP), R. Titz-Weider (DLR), S. Wolf (Univ. Kiel), G. Wuchterl (TLS); **Hungary:** A. Derekas (Konkoly Obs.), M. Hareter (Konkoly Obs.), L. Kiss (Konkoly Obs.), L. Molnár (Konkoly Obs.), E. Plachy (Konkoly Obs.), A.E. Simon (Konkoly Obs.), L. Szabados (Konkoly Obs.), G. Szabo (GAO, Konkoly Obs.), R. Szabo (Konkoly Obs.), A. Szing (Konkoly Obs.); **Israel:** R. Helled (Tel Aviv Univ.), T. Mazeh (Tel Aviv Univ.); **Italy:** E. Antonello (INAF-OAB), L. Affer (INAF-OAPA), M. Barbieri (Univ. Padova), St. Basso (INAF-OAB), L. Bedin (INAF-OAPD), A. Bellini (Univ. Padova), M. Bergomi (INAF-OAPD), I. Boisse (OAMP), A. Bonanno (INAF-OACT), F. Borsa (INAF-OAB), R. Bonito (Univ. Palermo), G. Bono (INFN), A.S. Bonomo (INAF-OATO), L. Borsato (Univ. Padova), E. Brocato (INAF-OAR), A. Bressan (INAF-OAPD), A. Brunelli (INAF-OAPD), R. Buonanno (INAF-OACTe, INFN), D. Cardini (INAF-IAPS), E. Carolo (INAF-OAPD), S. Cassisi (INAF-OACTe), M. Castellani (INAF-OAR), R. Cerulli (INAF-IAPS), R. Claudi (INAF-OAPD), R. Cosentino (INAF-OACT, FGG), G. Cutispoto (INAF-OACT), M. Damasso (Univ. Padova, INAF-OATO), M. Rosaria D'Antonio (ASDC), D. De Martino (INAF-OAC), S. Desidera (INAF-OAPD), S. Di Franco (Univ. Florence), M. Dima (INAF-OAPD), A.M. Di Giorgio (INAF-IAPS), M.P. Di Mauro (INAF-IAPS), J. Farinato (INAF-OAPD), E. Flaccomio (INAF-OAPA), M. Focardi (Univ. Florence), P. Giommi (ASDC), L. Girardi (INAF-OAPD), G. Giuffrida (ASDC), M. Ghigo (INAF-OAB), V. Granata (Univ. Padova), A.F. Lanza (INAF-OACT), M.G. Lattanzi (INAF-OATO), G. Leto (INAF-OACT), D. Magrin (INAF-OAPD), L. Malavolta (Univ. Padova), M. Marconi (INAF-OAC), G. Marcucci (Univ. Florence), P. Marigo (Univ. Padova), P.M. Marrese (ASDC), F. Marzari (Univ. Padova), D. Mesa (INAF-OAPD), S. Messina (INAF-OACT), M. Munari (INAF-OACT), U. Munari (INAF-OAPD), V. Nascimbeni (OAPD-INAF), R. Orfei (INAF-IAPS), S. Ortolani (Univ. Padova), E. Pace (Univ. Florence), I. Pagano (INAF-OACT), F. Palla (INAF-OAA), M. Pancrazzi (Univ. Florence), St. Pezzuto (INAF-IAPS), G. Picogna (Univ. Padova), A. Pietrinferni (INAF–OACTe), G. Piotto (Univ. Padova), E. Poretti (INAF-OAB), L. Prisinzano (INAF-OAPA), R. Ragazzoni (INAF-OAPD), G. Raimondo (INAF – OACTe), M. Rainer (INAF-OAB), V. Ripepi (INAF-OAC), G. Scandariato (INAF-OACT), S. Scuderi (INAF-OACT), R. Silvotti (INAF-OATO), R. Smart (INAF–OATO), A. Sozzetti (INAF-OATO), D. Spiga (INAF-OAB), P. Ventura (INAF-OAR), V. Viotto (INAF-OAPD); **Netherlands:** I. Snellen (Univ. Leiden); **Norway:** St. Werner (Univ. of Oslo); **Poland:** W. Dziembowski (Warsaw Univ.), G. Handler (CAMK), A. Niedzielski (Univ. Torun); **Portugal:** V. Adibekyan (CAUP), M. Bazot (CAUP), I.M. Brandão (CAUP), A. Cabral (CAAUL), A. Correia (Aveiro University), M. Cunha (CAUP), P. Figueira (CAUP), J. Gomes da Silva (CAUP), J. Martins (CAUP), M. Montalto (CAUP), M. Monteiro (CAUP), A. Mortier (CAUP), M. Oshagh (CAUP), J. Rebordão (CAAUL), B. Rojas-Ayala (CAUP), A. Santerne (CAUP), N. Santos (CAUP), S. Sousa (CAUP); **Romania:** D. Pricopi (Romanian Academy), M.D. Suran (Romanian Academy); **Slovenia:** T. Zwitter (Univ. Ljubljana); **Spain:** C. Allende (IAC), P. J. Amado (IAA-CSIC), R. Alonso (IAC), A. Claret (IAA), H. Deeg (IAC), A. Garcia Hernández (IAA-CSIC), R. Garrido (IAA-CSIC), J.I. Gonzáles-Hernández (IAC), P. Klagyivik (IAC), S. Meszaros (IAC), M. Mas-Hesse (CAB-INTA), A. Moya (CAB), R.U. O'Callaghan (CAB-INTA), A. Serenelli (ICE), I. Skillen (Isaac Newton Group), E. Solano (INTA), J. Carlos Suarez (IAA-CSIC), H. Voss (DAM); **Sweden:** A. Brandeker (Stockholm Univ.), R.P. Church (Lund Obs.), M.B. Davies (Lund Obs.), S. Feltzing (Lund Obs.), A. Johansen (Lund Obs.), O. Kochukhov (Univ. Uppsala), G. Olofsson (Stockholm Univ.); **Switzerland:** Y. Alibert (Univ. Bern), W. Benz (Univ. Bern), C. Charbonnel (Obs. Geneva), R. Diaz (Univ. Geneva), P. Eggenberger (Univ. Geneva), D. Ehrenreich (Univ. Geneva), W. Hayek (AF-Consult Baden), K. Heng (Univ. Bern), Ch. Lovis (Univ. Geneva), D. Naef (Univ. Geneva), F. Pepe (Univ. Geneva),

D. Segransan (Univ. Geneva), St. Udry (Obs. Geneva); **UK:** S. Aigrain (Univ. Oxford), M. Burleigh (Univ. Leicester), W. Chaplin (Univ. Birmingham), A. Collier Cameron (Univ, St Andrews), Y. Elsworth (Univ. Birmingham), D.W. Evans (Univ. Cambridge), F. Faedi (Univ. Warwick), R. Fares (Univ. of St Andrews), R. Farmer (Open Univ.), Y. Gomez (Warwick University), E. Gonzalez-Solares (Univ. Cambridge), C. Haswell (Open Univ.), S. Hodgkin (Univ. Cambridge), M. Irwin (Univ. Cambridge), U. Kolb (Open Univ.), A. Miglio (Univ. of Birmingham), R. Nelson (Univ. London), M. Niederste-Ostholt (Univ. Cambridge), A. Norton (Open Univ.), D. Pollacco (Univ. Warwick), I.W. Roxburgh (Univ. London), G. Rixon (Univ. Cambridge), M. Salaris (Univ. Liverpool), J. Southworth (Keele Univ.), A. Smith (University College London), M. Thompson (Univ. Sheffield), Y. Unruh (Imperial College London), D. Walton (University College London), N. Walton (Univ. Cambridge), C. Watson (Univ. Belfast), R. West (Univ. Warwick), P. Wheatley (Univ. Warwick); **USA:** S. Basu (Yale Univ.), A. Bhagatwala (Stanford Univ.), E. Depagne (Las Cumbres Obs.), J. Fortney (Univ. Santa Cruz), S. Hanasoge (Princeton Univ.), M. Havel (ORAU), J. Jenkins (SETI Inst.), D. Latham (Harvard Univ.), J. Linsky (Colorado Univ.), S. Mathur (SSI), N. Nettelmann (Univ. of Santa Cruz), M. Pinsonneault (Ohio State Univ.), I. Ramirez (Univ. Texas), Ch. Sotin (JPL), R. Trampedach (Univ. Colorado), Amaury Triaud (MIT).